Designing microcapsules based on protein fibrils and protein – polysaccharide complexes

Hứa Kiều Nam Phương (K.N.P. Hua)

Thesis committee

Thesis supervisor

Prof. dr. E. van der Linden

Professor of Physics and Physical Chemistry of Foods

Wageningen University

Thesis co – supervisor

Dr. L.M.C. Sagis

Associate Professor, Physics and Physical Chemistry of Foods,

Wageningen University

Other members

Prof , dr. M.A. Cohen Stuart, Wageningen University

Prof. dr. A. Fery, University of Bayreuth, Germany

Prof. dr. A.-M. Hermansson, Chalmers University of Technology, Sweden

Prof. J. Vermant, K.U. Leuven, Belgium

Designing microcapsules based on protein fibrils and protein – polysaccharide complexes

Hứa Kiều Nam Phương (K.N.P. Hua)

Table of contents

List of abbreviations

CLSM   Confocal Laser Scanning Microscopy

CPD   Critical Point Drying

DEMG   Doi-Edwards-Marrucci-Grizutti

FITC   Fluorescein isothiocyanate isomer

HMP   High methoxyl pectin

LbL   Layer-by-layer

Lys   Lysozyme

LysFib   Lysozyme fibrils

LysHMP   Lysozyme – high methoxyl pectin complex

Ova   Ovalbumin

OvaFib   Ovalbumin fibrils

OvaHMP   Ovalbumin – high methoxyl pectin complex

SEM   Scanning Electron Microscopy

TEM   Transmission electron microscopy

ThT   Thioflavin T

CHAPTER 1
INTRODUCTION

Developing novel core-shell microencapsulation systems from commonly used food-grade materials requires insight in the relation between the properties of these materials (such as size, persistence length, or charge), and the structure and mechanical properties of the shells formed by these materials. In this thesis, we investigate the suitability of several food-grade materials (protein fibrils, polysaccharides, and polysaccharide – protein complexes) for the production of core-shell microcapsules, and characterize the mechanical and release properties of these novel encapsulation systems.

ENCAPSULATION

Microencapsulation was first introduced in the 1950s by Green and Schleicher.[1] Since then, encapsulation technology has developed significantly and is applied in various fields such as pharmaceuticals, cosmetics, and food.[2] In food, encapsulation of functional ingredients, such as aromas, vitamins, minerals, colorants, antioxidants, probiotics and enzymes,[2–5] is used either to improve or enhance nutritional value, or for preservation purposes. Since food products cover a wide pH, temperature, and compositional range, simple and flexible methods are needed to produce capsules for a specific application. The common methods of producing capsules to date include physical chemical techniques (such as interfacial polymerization, solidification, coacervation, molecular inclusion, gelation, or evaporation) and mechanical techniques (such as spray-drying, spray chilling/cooling, extrusion, or fluidized bed coating).[2,6,7]

LAYER-BY- LAYER (LBL) ADSORPTION TECHNIQUE

In 1991, Decher *et al.* introduced a new adsorption technique for forming multilayer films based on electrostatic interactions between oppositely charged components.[8,9] This technique is called layer-by-layer (LbL) assembly or adsorption. Because of its ability to create highly tailored capsule shells using a simple, inexpensive and easily controllable adsorption process,[10] it has become a popular technique for preparing polyelectrolyte capsules of various sizes, ranging from the nanometer to micrometer scale,[11,12] with well-defined barrier properties.[12]

In this technique, assembly is driven by the electrostatic attraction of oppositely charged materials (polycations and polyanions) to form polyelectrolyte shells.[13–15] After each adsorption step, the excess of materials in the solution is removed by centrifuging and/or washing. When the required number of layers is obtained, the inner phase (the core) can be removed to obtain hollow capsules.[10,11,16] The materials for assembly can be small organic molecules, inorganic compounds, macromolecules,

bio-macromolecules or colloids.[14,17–25] Polyelectrolyte microcapsules made by this technique have many potential applications including controlled release of materials.[23,26]

The structure of the polyion layered capsule shell is determined mainly by the electrostatic interactions between the polyions used.[10] The fundamentals of multilayer formation with pH-sensitive charged components has got considerable attention[17,20,21,24,26] since the average charge of the shell can easily be tuned by the acidity of the continuous phase, thus offering the possibility to control the interactions between the charged materials. The mechanical strength and permeability of the capsules can be controlled by varying the number of layers or by changing the characteristics of the encapsulating materials.[12]

ENCAPSULATING MATERIALS

The most common encapsulating materials in food products are biomolecules from various sources such as plants (polysaccharides such as starch, or proteins such as gluten), marine life (polysaccharides such as alginate, carrageenan, or chitosan), bacteria (polysaccharides such as xanthan), or animal sources (proteins from milk, or eggs). These materials have a wide range of structures that vary from compact globular structures to linear or branched flexible coils, and have charges that vary from neutral to high values.

The main challenges in encapsulation are to select suitable techniques and encapsulating materials that produce encapsulation systems suitable for a specific application. In this thesis, we will investigate the suitability of egg proteins (ovabumin – Ova, and lysozyme – Lys) in fibril form, and complexes of these globular proteins with polysaccharides (high methoxyl pectin – HMP) as encapsulating materials.

Protein fibrils

Protein-based fibril assembly has the potential of broadening the functional properties of the proteins.[27] β-lactoglobulin fibrils have been reported to be effective stabilizers at air – water and oil – water interfaces[28,29] and to be able to form films at the interfaces with a high interfacial modulus.[30] Their charge can be adjusted by changing the pH of the solvent, which makes them excellent candidates for encapsulation based on electrostatic LbL self-assembly.[12]

In general, the formation of fibrils occurs in a narrow pH and ionic strength range. It can be induced by increasing the temperature of the protein solution, to a temperature close to the protein denaturation temperature,[31–33] and/or adding co-solvents like alcohols, salts or metal ions, which destabilize the native conformation of

the protein.[34] The formation of fibrils from protein solutions can be characterized by a lag time, a nucleation event and finally a period of growth.[35]

Ovalbumin fibrils

Ova fibrils can be prepared by heating Ova solutions at pH 2 at 80 °C for 10h.[33] At these conditions, Ova monomers assemble irreversibly into semi-flexible fibrils with a contour length of a few hundred nanometer and effective diameters of a few nanometer.

Lysozyme fibrils

There are several methods to prepare Lys amyloid fibrils. From independent studies, it appears that the mechanism of Lys fibril formation does not have a specific path but depends on the conditions inducing fibril formation.[36–41] The morphology of Lys fibrils formed from different conditions and initial states of Lys (native or reduced) is also diverse. Even a small change in the inducing conditions produces fibrils that vary from short to long, and from stiff to flexible. In a study of Arnaudov *et al.,*[36] the authors found that fibrils obtained by heating Lys solutions at pH 2 at 57 °C or 80 °C were long, thin and semi-flexible. When increasing the pH of the solution to pH 3, more flexible fibrils were formed.

Several studies have found that stirring, shaking, applying mechanical agitation or shear flow can influence the rate of fibril formation.[27,42,43] Akkermans *et al.* found that the length of β-lactoglobulin fibrils can be influenced only to a minor extent by shear flow: shear flow results in slightly shorter fibrils.[43] The effects of flow on Lys fibril formation have, however, remained unexamined.

In order to investigate the effect of flow on the formation of Lys fibrils, Lys fibrils were prepared by heating Lys solutions at pH 2 at 57 °C[36] with either shear or turbulent flows (*chapter 2*).

Protein – polysaccharide complexes

Proteins can act as emulsion stabilizers by adsorbing to the oil – water interface, forming a complex viscoelastic (multi)layer.[44–49] Polysaccharides, on the other hand, can stabilize oil-in-water emulsions using their thickening and gelling properties to form a macromolecular barrier in the aqueous medium between the dispersed droplets. Combining proteins and polysaccharides at various conditions (such as different mixing ratios, pH, and ionic strength) will result in three different states:[50–52]

   (i)   Phase separation: the components repel each other forming 2 phases – a protein-rich phase and a polysaccharide-rich phase.

(ii)   Co-solubility: the components are well mixed forming a stable single phase solution.

(iii)   Associative phase separation or complex coacervation: strong binding between proteins and polysaccharides forms a protein – polysaccharide-rich phase and a dilute phase.

The protein – polysaccharide complexes of our interest are in a co-soluble state. They have been used more and more as emulsifiers and stabilizers because they have the combined advantages of both components. In theory, soluble protein – polysaccharide complexes can be ideal steric stabilizers because they can attach firmly to an interface like a protein, and they are able to form a gel-like charged film of significant thickness, with polymer chains extending extensively from the interface.[47,52] The mechanical strength of the adsorbed layer, together with the electrostatic repulsion and steric effects are the most important factors affecting the kinetic stability of oil in water emulsions.[13]

We have mixed proteins (Ova and Lys) and HMP at various ratios, and the optimum ratio to obtain stable complexes was determined by visual observation, light scattering and ζ-potential distribution measurements. In order to avoid the effect of charge screening on the formation of complexes,[51,52] no extra salts were added to the polymer solutions.

DILATATIONAL ELASTIC MODULI AND SHEAR COMPLEX MODULI OF OIL – WATER INTERFACES STABILIZED BY THE ENCAPSULATING MATERIALS

Emulsions have been used by various industries as delivery vehicles for either aqueous- or oil-based functional ingredients.[53] While water-in-oil emulsions can be used for controlling water-soluble-materials, oil-in-water emulsions can be used for controlling oil-soluble-materials such as aroma, dietary fats, antioxidants, or vitamins.

The emulsion structure, stability, and rheology as well as the crystallization behavior of the dispersed phase and the kinetics of mass transport between droplets are influenced by the composition, thickness and viscoelasticity of the (multi)layer, either formed by proteins or protein – polysaccharide complexes, at the oil – water interface.[54–56]

In order to establish the relationship between interfacial stress and the resultant deformation of the interface, the interfacial rheological properties of the (multi)layer at the interface are investigated by exposing it to mechanical stresses.[55] Two common surface rheology measurements are dilation and shear rheology.[46] Information related to stabilizing interfaces during making emulsions or foams can be

obtained from dilation measurements.[57] Interfacial dilatational rheology is sensitive to the relaxation of molecules under compression and/or expansion and kinetics of exchange of material between interface and bulk phase.[56,58] Information about the interfacial composition, the structural state and the interactions between adsorbed species, on the other hand, can be obtained from interfacial shear measurements.[55,58–60] Since the deformations in droplet collision are a combination of shear and dilation, it is most likely that both dilatational and shear properties have an influence on emulsion stability.[56]

The mesoscopic structure of the interfacial layer containing proteins and polysaccharides depends not only on factors like pH and ionic strength but also on the procedure used to make the emulsion.[61] There are two methods to prepare emulsions with protein and polysaccharides, resulting in two types of emulsions: mixed-layer emulsions and bilayer emulsion. To create a mixed-layer emulsion, protein – polysaccharide complexes are first prepared and then used as emulsifiers during droplet formation. Previous studies have confirmed that the formation of a strong soluble protein – polysaccharide complex improves the emulsion stability without changing the emulsifying capacity significantly.[47,54,62–64] To create a bilayer emulsion, protein is first used as emulsifier, and then the washed emulsion is dispersed in a polysaccharide solution. The polysaccharide will adsorb onto the protein layer as a complexing secondary layer.[58,61,65–67] The interfacial compositions and structures of the emulsion droplets and the stability against creaming or flocculation of these two emulsions are different.[67]

AIM AND OUTLINE OF THIS THESIS

The aim of this thesis is to design core-shell microencapsulation systems for the controlled release of oil-soluble functional ingredients, and to relate the structure and mechanical properties of the shells to the properties of the encapsulating materials. The encapsulating materials are food-grade protein fibrils, polysaccharides, and complexes of proteins and polysaccharides.

First, in *chapter 2*, we explore the possibilities to tune the morphology and flexibility of the protein fibrils. Then, the surface activity and rheological properties of the encapsulating materials are investigated (*chapter 3*). Finally, we develop and study the assembled layers of these encapsulating materials at interfaces (oil – water) to create microcapsules (*chapters 4* and *chapter 5*). The controlled release of the encapsulated materials can be achieved by controlling the permeability of the multiple barriers.

In *chapter 2*, the effects of simple shear flow and turbulent flow during heating on the conversion and morphology of Lys fibrils are presented. Different than in the case of β-lactoglobulin, the length of the Lys fibrils, as well as the amount of fibrils obtained, is strongly affected by flow.

In *chapter 3*, we study the rheological properties of adsorbed films at the oil – water interface, formed by proteins, their fibrillar aggregates, and their complexes with high methoxyl pectin (HMP), using both interfacial shear and dilatation rheology. For investigating the interfacial dilatational behavior, an automated drop tensiometer was used. The interfacial shear rheological properties of these interfaces were characterized by a stress controlled rheometer with biconical disk geometry. Results show that complexation of proteins with high methoxyl pectin improved the interfacial moduli of the oil – water interfaces they stabilized. At most of the experimental conditions, fibrils form films at the oil – water interface with the highest interfacial moduli.
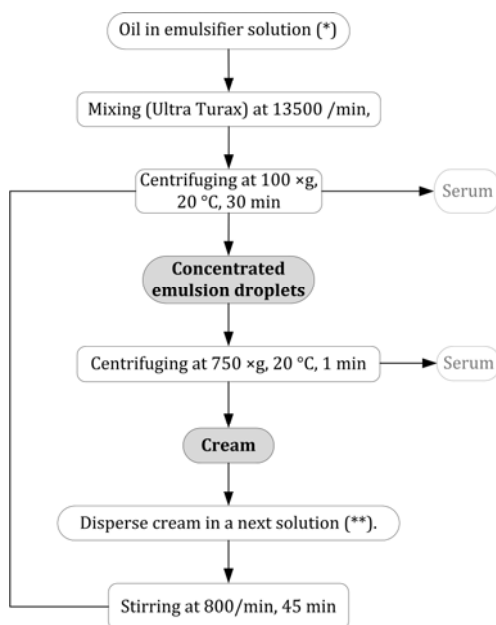
Figure 1.1 Scheme showing the process of making capsules. (*): emulsifiers can either be Ova fibrils or protein:HMP complexes. (**): next solution contains oppositely charged polyelectrolytes

To design microcapsules, we used the LbL assembly technique using oil in water emulsion droplets as a template (*chapter 4* and *chapter 5*). Surface-active food-grade

protein fibrils, or complexes of proteins and HMP, were used as the emulsifier of the template emulsion. These materials were also used to add additional layers to the shell. After preparing the emulsion droplet templates, alternating layers of HMP or fibrillar protein aggregates were adsorbed to build the even-number layers of the microcapsule. By using emulsion droplets as a liquid-core template, we were able to control the size distribution by adjusting the energy input and the concentration of the stabilizer.[12] We used simple and standard operations in order to increase the potential for scaling up to industrial production volumes (**Figure 1.1**).

From various protein complexes and fibrillar aggregates, three encapsulation systems were developed (**Table 1.1)**. In *chapter 4*, microcapsules from Ova fibrils and HMP are presented. These microcapsules were prepared at pH 3.5. Ova fibrils were the emulsifier and odd-layer material (positively charged) and HMP (negatively charged) was the even-layer material. For this system, the release of an aroma compound (limonene) is investigated. The results show that by varying the number of layers, the release of limonene can be controlled – increasing the number of layers of the shell from 4 to 8 decreases the release rate by a factor 6.

In *chapter 5*, we design microcapsules from protein – polysaccharide complexes and protein fibrils. System 1 was composed of OvaHMP complexes and Ova fibrils. Microcapsules of this system were also prepared at pH 3.5. At this pH, OvaHMP complexes have a negative net charge while Ova fibrils are positively charged. In this system, the complexes were the emulsifier.

System 2 was composed of LysHMP complexes and two types of Lys fibrils (short rod-like and long semi-flexible). LysHMP complexes were adsorbed on the template at pH 7 – negatively charged – and Lys fibrils were adsorbed at pH 5, and hence positively charged. Using a range of fibrils (short and semi-flexible Ova, short and rod-like Lys, long and semi-flexible Lys) allowed us to investigate the effect of fibril properties on mechanical stability of the multilayer capsules. The results show that by varying the flexibility of the protein fibrils, mechanical properties of this type of capsule can be tuned: the stiffer Lys fibrils produce capsules with a hard but more brittle shell, whereas the semi-flexible Ova fibrils produce capsules with a softer but more stretchable shell.

Table 1.1. An overview of various microcapsule systems

System	*OvaFib + HMP*	*OvaHMP + OvaFib*	*LysHMP + LysFib*
Material 1 → odd layer	Ova fibrils, pH 3.5	Ova:HMP 2:1, pH 3.5	Lys:HMP 4:1, pH 7
Material 2 → even layer	HMP, pH 3.5	Ova fibrils, pH 3.5	Lys fibrils, pH 5

In *chapter 6*, the results of previous chapters are used to give a general discussion of the link between mesoscopic properties of protein fibrils and complexes of proteins with HMP, and the structure, mechanical properties, and release properties of microencapsulation systems produced with these materials. In this chapter we also present some speculative outlooks on further research and applications of these materials in emulsion stabilization and encapsulation, based on the newly achieved insights.

REFERENCES

1   Green, B. K. & Schleicher, L. Pressure Responsive Record Materials. 2730456, 2730457 (1956).

2   Madene, A., Jacquot, M., Scher, J. & Desobry, S. Flavour Encapsulation and Controlled Release: A Review. *Int J Food Sci Tech* **41**, 1 – 21 (2006).

3   Jackson, L. S. & Lee, K. Microencapsulation and The Food Industry. *Lebensm Wiss Technol* **24**, 289 – 297 (1991).

4   Schrooyen, P. M. M., Meer, R. V. D. & Kruif, C. G. D. Microencapsulation: Its Application In Nutrition. *P Nutr Soc* **60**, 475 – 479 (2001).

5   Dziezak, J. D. Microencapsulation and Encapsulated Ingredients. *Food Technol.* **42**, 136 – 151 (1988).

6   Rosenberg, M. & Sheu, T. Y. Microencapsulation of Volatiles By Spray-Drying In Whey Protein-Based Wall Systems. *Int Dairy J* **6**, 273 – 284 (1996).

7   Dewettinck, K. & Huyghebaert, A. Fluidized Bed Coating In Food Technology. *Trends Food Sci Tech* **10**, 163 – 168 (1999).

8   Decher, G., Hong, J. D. & Schmitt, J. Buildup of Ultrathin Multilayer Films By A Self-Assembly Process: Iii. Consecutively Alternating Adsorption of Anionic and Cationic Polyelectrolytes On Charged Surfaces. *Thin Solid Films* **210 – 211**, 831 – 835 (1992).

9   Decher, G. & Hong, J. D. Buildup of Ultrathin Multilayer Films By A Self-Assembly Process: I. Consecutive Adsorption of Anionic and Cationic Bipolar Amphiphiles. *Makromol. Chem., Macromol. Symp.* **46**, 321 – 327 (1991).

10   Peyratout, C. S. & Dähne, L. Tailor-Made Polyelectrolyte Microcapsules: From Multilayers To Smart Containers. *Angew Chem Int Edit* **43**, 3762 – 3783 (2004).

11   Yow, H. N. & Routh, A. F. Formation of Liquid Core-Polymer Shell Microcapsules *Soft Matter* **2**, 940 – 949 (2006).

12   Sagis, L. M. C. *et al.* Polymer Microcapsules With A Fiber-Reinforced Nanocomposite Shell. *Langmuir* **24**, 1608 – 1612 (2008).

13   McClements, D. J. Theoretical Analysis of Factors Affecting The Formation and Stability of Multilayered Colloidal Dispersions. *Langmuir* **21**, 9777 – 9785 (2005).

14   Decher, G. (Eds Gero Decher & Joseph B. Schlenoff) 1 – 46 (Wiley – Vch, 2003).

15   Ai, H., Jones, S. A. & Lvov, Y. M. Biomedical Applications of Electrostatic Layer-By-Layer Nano-Assembly of Polymers, Enzymes, and Nanoparticles *Cell Biochem Biophys* **39**, 23 – 43, (2003).

16   Schönhoff, M. Layered Polyelectrolyte Complexes: Physics of Formation and Molecular Properties. *J Phys – Condens Mat*, **15**, R1781 – 1808 (2003).

17   Sukhorukov, G. B., Antipov, A. A., Voigt, A., Donath, E. & Möhwald, H. pH-Controlled Macromolecule Encapsulation In and Release From Polyelectrolyte Multilayer Nanocapsules. *Macromol Rapid Comm* **22**, 44 – 46 (2001).

18   Rmaile, H. H. & Schlenoff, J. B. "Internal Pka's" In Polyelectrolyte Multilayers: Coupling Protons and Salt. *Langmuir* **18**, 8263 – 8265 (2002).

19   Richert, L. *et al.* Layer By Layer Buildup of Polysaccharide Films: Physical Chemistry and Cellular Adhesion Aspects. *Langmuir* **20**, 448 – 458 (2003).

20   Déjugnat, C. & Sukhorukov, G. B. pH-Responsive Properties of Hollow Polyelectrolyte Microcapsules Templated On Various Cores. *Langmuir* **20**, 7265 – 7269 (2004).

21   Tong, W., Gao, C. & Möhwald, H. Stable Weak Polyelectrolyte Microcapsules With pH-Responsive Permeability. *Macromolecules* **39**, 335 – 340 (2005).

22   Schneider, G. & Decher, G. Functional Core/Shell Nanoparticles Via Layer-By-Layer Assembly. Investigation of The Experimental Parameters For Controlling Particle Aggregation and For Enhancing Dispersion Stability. *Langmuir* **24**, 1778 – 1789 (2008).

23   Wang, C. *et al.* Microcapsules For Controlled Release Fabricated Via Layer-By-Layer Self-Assembly of Polyelectrolytes. *J Exp Nanosci* **3**, 133 – 145 (2008).

24   Kietzmann, D., Béduneau, A., Pellequer, Y. & Lamprecht, A. pH-Sensitive Microparticles Prepared By An Oil/Water Emulsification Method Using N-Butanol. *Int J Pharm* **375**, 61 – 66 (2009).

25   Kim, J.-H., Hwang, J.-H. & Lim, T.-Y. A Layer-By-Layer Self-Assembly Method For Organic – Inorganic Hybrid Multilayer Thin Films. *J Ceram Process Res* **10**, 770 – 773 (2009).

26   Mauser, T., Déjugnat, C. & Sukhorukov, G. B. Balance of Hydrophobic and Electrostatic Forces In The pH Response of Weak Polyelectrolyte Capsules. *J Phys Chem B* **110**, 20246 – 20253 (2006).

27   Akkermans, C. *et al.* Shear Pulses Nucleate Fibril Aggregation. *Food Biophys* **1**, 144 – 150 (2006).

28   Isa, L., Jung, J.-M. & Mezzenga, R. Unravelling Adsorption and Alignment of Amyloid Fibrils At Interfaces By Probe Particle Tracking. *Soft Matter* **7**, 8127 – 8134 (2011).

29   Jung, J.-M. & Mezzenga, R. Liquid Crystalline Phase Behavior of Protein Fibers In Water: Experiments Versus Theory. *Langmuir* **26**, 504 – 514 (2009).

30   Jung, J.-M., Gunes, D. Z. & Mezzenga, R. Interfacial Activity and Interfacial Shear Rheology of Native β-Lactoglobulin Monomers and Their Heat-Induced Fibers. *Langmuir* **26**, 15366 – 15375 (2010).

31   Sagis, L. M. C., Veerman, C. & van der Linden, E. Mesoscopic Properties of Semiflexible Amyloid Fibrils. *Langmuir* **20**, 924 – 927 (2004).

32   Veerman, C., Ruis, H. G. M., Sagis, L. M. C. & van der Linden, E. Effect of Electrostatic Interactions On The Percolation Concentration of Fibrillar Beta-Lactoglobulin Gels. *Biomacromolecules* **3**, 869 – 873 (2002).

33   Veerman, C., De Schiffart, G., Sagis, L. M. C. & van der Linden, E. Irreversible Self-Assembly of Ovalbumin Into Fibrils and The Resulting Network Rheology. *Int J Biol Macromol* **33**, 121 – 127 (2003).

34   Schmittschmitt, J. P. & Scholtz, J. M. The Role of Protein Stability, Solubility, and Net Charge In Amyloid Fibril Formation. *Protein Sci* **12**, 2374 – 2378 (2003).

35   Rochet, J.-C. & Lansbury, P. T. Amyloid Fibrillogenesis: Themes and Variations. *Curr Opin Struc Biol* **10**, 60 – 68 (2000).

36   Arnaudov, L. N. & De Vries, R. Thermally Induced Fibrillar Aggregation of Hen Egg White Lysozyme. *Biophys. J.* **88**, 515 – 526 (2005).

37   Cao, A., Hu, D. & Lai, L. Formation of Amyloid Fibrils From Fully Reduced Hen Egg White Lysozyme. *Protein Sci* **13**, 319 – 324 (2004).

38   Goda, S. *et al.* Amyloid Protofilament Formation of Hen Egg Lysozyme In Highly Concentrated Ethanol Solution. *Protein Sci* **9**, 369 – 375 (2000).

39   Krebs, M. R. H., Devlin, G. L. & Donald, A. M. Protein Particulates: Another Generic Form of Protein Aggregation? *Biophys J* **92**, 1336 – 1342 (2007).

40   Krebs, M. R. H. *et al.* Formation and Seeding of Amyloid Fibrils From Wild-Type Hen Lysozyme and A Peptide Fragment From The α-Domain. *J Mol Biol* **300**, 541 – 549 (2000).

41   Mishra, R. *et al.* Lysozyme Amyloidogenesis Is Accelerated By Specific Nicking and Fragmentation But Decelerated By Intact Protein Binding and Conversion. *J Mol Biol* **366**, 1029 – 1044 (2007).

42   Hill, E. K., Krebs, B., Goodall, D. G., Howlett, G. J. & Dunstan, D. E. Shear Flow Induces Amyloid Fibril Formation. *Biomacromolecules* **7**, 10 – 13 (2006).

43   Akkermans, C., van der Goot, A. J., Venema, P., van der Linden, E. & Boom, R. M. Formation of Fibrillar Whey Protein Aggregates: Influence of Heat and Shear Treatment, and Resulting Rheology. *Food Hydrocolloid* **22**, 1315 – 1325 (2008).

44   Cases, E., Rampini, C. & Cayot, P. Interfacial Properties of Acidified Skim Milk. *J Colloid Interf Sci* **282**, 133 – 141 (2005).

45   Alahverdjieva, V. S. *et al.* Adsorption Behaviour of Hen Egg-White Lysozyme At The Air/Water Interface. *Colloid Surface A* **323**, 167 – 174 (2008).

46   Baldursdottir, S. G., Fullerton, M. S., Nielsen, S. H. & Jorgensen, L. Adsorption of Proteins At The Oil/Water Interface – Observation of Protein Adsorption By Interfacial Shear Stress Measurements. *Colloid Surface B* **79**, 41 – 46 (2010).

47   Dickinson, E. & Galazka, V. B. Emulsion Stabilization By Ionic and Covalent Complexes of β-Lactoglobulin With Polysaccharides. *Food Hydrocolloid* **5**, 281 – 296 (1991).

48   Dickinson, E. Faraday Research Article. Structure and Composition of Adsorbed Protein Layers and The Relationship To Emulsion Stability. *J Chem Soc Faraday T* **88**, 2973 – 2983 (1992).

49   Erni, P., Windhab, E. J. & Fischer, P. Emulsion Drops With Complex Interfaces: Globular Versus Flexible Proteins. *Macromol Mater Eng* **296**, 249 – 262 (2011).

50   Ganzevles, R. A. *Protein/Polysaccharide Complexes At Air/Water Interfaces*, Wageningen University, (2007).

51   Weinbreck, F., De Vries, R., Schrooyen, P. & De Kruif, C. G. Complex Coacervation of Whey Proteins and Gum Arabic. *Biomacromolecules* **4**, 293 – 303 (2003).

52   Ye, A. Complexation Between Milk Proteins and Polysaccharides Via Electrostatic Interaction: Principles and Applications – A Review. *Int J Food Sci Tech* **43**, 406 – 415 (2008).

53   Appelqvist, I. A. M., Golding, M., Vreeker, R. & Zuidam, N. J. In *Encapsulation and Controlled Release Technologies In Food Systems* 41 – 81 (Blackwell Publishing, 2007).

54   Dickinson, E. Interfacial Interactions and The Stability of Oil-In-Water Emulsions. *Pure Appl Chem* **64**, 1721 – 1724 (1992).

55   Murray, B. S. Interfacial Rheology of Food Emulsifiers and Proteins. *Current Curr Opin Colloid In* **7**, 426 – 431 (2002).

56   Freer, E. M., Yim, K. S., Fuller, G. G. & Radke, C. J. Shear and Dilatational Relaxation Mechanisms of Globular and Flexible Proteins At The Hexadecane/Water Interface. *Langmuir* **20**, 10159 – 10167 (2004).

57   Dickinson, E. Milk Protein Interfacial Layers and The Relationship To Emulsion Stability and Rheology. *Colloid Surface B* **20**, 197 – 210 (2001).

58   Dickinson, E. Mixed Biopolymers At Interfaces: Competitive Adsorption and Multilayer Structures. *Food Hydrocolloid* **25**, 1966 – 1983 (2011).

59   Martin, A. H., Bos, M. A. & Van Vliet, T. Interfacial Rheological Properties and Conformational Aspects of Soy Glycinin At The Air/Water Interface. *Food Hydrocolloid* **16**, 63 – 71 (2002).

60   Hotrum, N. E., Cohen Stuart, M. A., Van Vliet, T. & Van Aken, G. A. Flow and Fracture Phenomena In Adsorbed Protein Layers At The Air/Water Interface In Connectin To Spreading Oil Droplets. *Langmuir* **19**, 10210 – 10216 (2003).

61   Dickinson, E. Interfacial Structure and Stability of Food Emulsions As Affected By Protein – Polysaccharide Interactions. *Soft Matter* **4** (2008).

62   Dickinson, E. Stability and Rheological Implications of Electrostatic Milk Protein – Polysaccharide Interactions. *Trends Food Sci Tech* **9**, 347 – 354 (1998).

63   Schmitt, C., Kolodziejczyk, E. & Leser, M. E. In *Food Colloids* (Ed Eric Dickinson) 284 – 300 (The Royal Society of Chemistry, 2005).

64   Santipanichwong, R., Suphantharika, M., Weiss, J. & McClements, D. J. Core – Shell Biopolymer Nanoparticles Produced By Electrostatic Deposition of Beet Pectin Onto Heat-Denatured Aggregates. *J Food Sci* **73**, N23 – N30 (2008).

65   Dickinson, E. Hydrocolloids As Emulsifiers and Emulsion Stabilizers. *Food Hydrocolloid* **23**, 1473 – 1482 (2009).

66   Jourdain, J., Leser, M. E., Schmitt, C. & Dickinson, E. Stability of Emulsions Containing Sodium Caseinate and Anionic Polysaccharides. *Roy Soc Ch* **14**, 272 – 279 (2008).

67   Turgeon, S. L., Schmitt, C. & Sanchez, C. Protein – Polysaccharide Complexes and Coacervates. *Curr Opin Colloid In* **12**, 166 – 178 (2007)

CHAPTER 2

EFFECTS OF FLOW ON HEN EGG WHITE LYSOZYME FIBRIL FORMATION: LENGTH DISTRIBUTION, FLEXIBILITY, AND KINETICS

ABSTRACT

In this chapter the effect of steady shear and turbulent flow on the formation of amyloid fibrils from hen egg white lysozyme was studied. We determined the conversion and size distribution of fibrils obtained by heating lysozyme solutions at pH 2. The formation of fibrils was quantified using flow-induced birefringence. The size distribution was fitted using decay of birefringence measurements and Transmission Electron Microscopy. The morphology of lysozyme fibrils and kinetics of their formation varied considerably depending on the flow applied. With increasing shear or stirring rate, more rod-like and shorter fibrils were obtained, and the conversion into fibrils was increased. The size distribution and final fibril concentration were significantly different from those obtained in the same heat treatment at rest. The width of the length distribution of fibrils was influenced by the homogeneity of the flow.

INTRODUCTION

The assembly of food-grade proteins, such as β-lactoglobulin, bovine serum albumin, and lysozyme (Lys) from hen egg white, into fibrils[1–4] has recently gained considerable attention, because of the potential for broadening the functional properties of these proteins.[5] In a recent paper, fibrils were used to develop microcapsules with a fibril reinforced nano-composite shell.[6] Fibrils are also suitable for use as efficient thickening or gelling agents.[7–9] For use in encapsulation and other functional applications, a simple but controlled method of preparing fibrils with known final fibril concentrations and length distribution is essential.

As described in *chapter 1*, in general the formation of fibrils occurs in a narrow pH and ionic strength range. It can be induced at temperatures close to the protein denaturation temperature,[7–9] and/or by co-solvents such as alcohols, salts or metal ions, which destabilize the native conformation of the protein.[10] The formation of fibrils from protein solutions can be characterized by a lag time, a nucleation event and finally a period of growth.[11] For Lys, various methods to prepare amyloid fibrils have been reported. The exact mechanism of Lys amyloid fibril formation does not have a specific path but depends on the conditions inducing fibril formation.[1–4,12,13]

When intact Lys is introduced to a very concentrated ethanol environment (90% v/v), the process of amyloid formation has several steps. First, the helical content increases leading to a perturbation of the tertiary structure. Then, the helical structures of Lys are partly destroyed due to the highly concentrated ethanol solution, which is followed by the association into amyloid fibrils.[2] In these conditions, fibrils have an average diameter of 7 nm and are as long as 100 – 200 nm. Cao *et al*.[3] have also used concentrated ethanol (90% v/v) to convert fully reduced Lys to amyloid fibrils at low pH (pH 4 – 5), and the fibrillogenesis showed obvious differences. The flexibility of the peptide chain of the fully reduced Lys (without the four disulfide bond constraint) allowed it to explore a much greater conformational space than the disulfide-intact Lys.[3] Consequently, the fibrils formed have a diameter of 2 – 5 nm and are as long as 1 – 2 μm, much thinner and longer than those formed from the native Lys.[3]

Besides alcohols, adding other denaturants, such as 3–4M guanidine hydrochloride,[13] or 30% 2,2,2-trifluoroethanol at respectively 37 °C and 65 °C, can produce fibrils.[1] Also sonication was found to form amyloid-like aggregates from Lys due to protein destabilization.[14] Nevertheless, the most commonly used fibril formation conditions for Lys (or its peptides) involve low pH (1.6 – 2.0) and elevated temperatures (57 – 100 °C).[1,4,12,15]

One of the first studies of the formation of Lys amyloid fibrils by heat treatment was that of Krebs *et al.* (2000).[1] In that study, fibrils were formed from a 1 mM Lys

solution at pH 2 by incubating at 37 °C, after rapid heating to 100 °C and freezing in liquid nitrogen. Besides from native proteins, fibril formation from peptides (in aqueous solutions at pH 2 and pH 4) was also investigated. The authors found that fibril formation of Lys lead to amyloid fibrils containing full-length Lys (when using intact protein) or fragments (when using peptides). The fibrils from either intact Lys or peptides are, in general, long (over 1 µm), and semi-flexible (the persistence length is of the same order of magnitude as the contour length). Those from intact protein appear to be a bit thinner (7.4 (±0.5) nm) than those from peptides (10 (±3) nm).[1]

The effect of thermal conditions on fibrillar aggregation was extensively studied by Arnaudov *et al.* (2005).[4] These authors explored the effects of increasing the pH (from 2 to 4) and temperature (from 57 to 80 °C), and found that the optimal conditions for Lys fibril formation are at pH 2 and 57 °C. At these conditions, the fibrils obtained are semi-flexible and long (about 5 µm) and the longest fibrils observed were about 16 µm. Their predominant thickness is about 4 nm and they appear to be composed of stiff rod-like subunits with lengths of 124 (± 9) nm and 157 (± 11) nm.[4] These fibrils seem to consist mostly of full-length Lys though some fragments – products of hydrolysis at pH 2 and 57 °C – are probably incorporated into fibrils as well.[4] This morphology is close to that found by Cao *et al.*[3] The Lys fibrils formed at pH 3 and 57 °C are also very long (around 5 µm) with a similar thickness to those obtained at pH 2, but they seem more flexible and no rod-like subunits were observed.[4] The fibrils formed at 80 °C were reported to be very long, thin, and semi-flexible as well.[4]

In a recent study,[12] a mechanism of Lys amyloid fibril formation at low pH and elevated temperature (pH 1.6, 65 °C) was proposed, which incorporates steps of hydrolysis, fragmentation, assembly and conversion into amyloid fibrils. This model suggests that the formation of Lys amyloid fibrils is a multi-order process that is highly complex due to a multitude of interactions, and the involvement of quaternary intermediates. First, Lys unfolds, and then partial acid hydrolysis produces a large amount of nicked Lys and fragments. After the nicked full-length proteins are incorporated into amyloid fibrils, they are further degraded and trimmed down to a core composition – a process referred to as "fibril shaving".[12] In this study, it is verified that at pH 1.6 and 65 °C, Lys fragments completely, either before or after incorporation into amyloid fibrils.[12] Thus, the morphology of Lys fibrils formed from different conditions and initial states of Lys (native or reduced) is diverse. Even a small change in the inducing conditions produces fibrils that vary from short to long and from stiff to flexible.

Although several studies have commented that stirring, shaking, applying mechanical agitation or shear flow influence the rate of fibril formation,[5,16,17] effects of flow on

Lys amyloid fibril formation have remained unexamined. These effects have been studied extensively for β-lactoglobulin by Akkermans *et al.*[5,16,17] and Hill *et al.*[17] Akkermans *et al.*[5,16] have studied the effects of shear flow on the formation of β-lactoglobulin amyloid fibrils in heating conditions. Samples (0.5% wt, pH 2) were heated at 80 °C with pulsed and continuous shear treatment at a shear rate of 200 s^{-1}.[5] Results show that shear flow significantly enhances the formation of β-lactoglobulin fibrils. However, there is no difference in the final fibril concentrations between applying continuous shear flow, giving short shear pulses every hour, or giving only one short shear pulse at the start of the heating process. In other words, the onset of the shear flow is the key parameter for enhancing the fibril growth.[5] The results of samples subjected to different continuous shear treatment with various shear rates, using a shear device with a Couette geometry (pH 2, 90 °C, shear rates varied from 0 to 673 s^{-1}, protein concentrations ranged from 0.5 to 5.2% wt), showed that the use of shear flow results in a higher amount of fibrils.[16] But this effect only started around a protein concentration of 3% wt. The total length concentration increased as a function of shear rate up to a shear rate of 337 s^{-1}. Above that shear rate, it decreases with increasing shear rate. The length of the fibrils obtained can be influenced only to a minor extent, and it appears that shear flow results in slightly shorter fibrils.[16]

In this chapter, we present the effects of simple shear flow (Couette flow) and turbulent flow during heating on the length distribution and the conversion of Lys fibrils. We will show that the length of the Lys fibrils, as well as the amount of fibrils obtained, is strongly affected by flow. The effect of flow on fibril formation is much more significant than in the case of β-lactoglobulin.

MATERIALS AND METHODS

Materials

Lys was obtained from Sigma-Aldrich Co., Missouri, USA (3 × crystallized, lyophilized powder, product no. L6876). All other chemicals used were of analytical grade, unless stated otherwise. All solutions were prepared with Millipore water (Millipore Corporation, Billerica, Massachusetts, USA). Protein solutions contained 200 ppm of NaN_3 to prevent bacterial growth. Samples were diluted to desired concentration (if applicable) with the same buffer or solution used for the primary solutions.

Preparing Lys solutions

Dried powder of Lys was dissolved in 10 mM HCl (pH 2) and extensively dialyzed against 10 mM HCl (pH 2) at 4 °C to remove dissolved salts present in Lys (around 5% wt). The dialyzed protein solution was filtered using 0.2 μm pore filter size (FP 30/0.2 CA-S, Schleicher & Schuell, Germany), and its concentration was determined by

absorbance measurement using a UV spectrometer (Cary 50 Bio, Varian, Inc., Palo Alto, California, USA) and a calibration curve of known Lys concentrations at 280 nm. The protein stock solution was diluted with 10 mM HCl to the desired concentrations. The pH of protein solutions was adjusted using a 6 M HCl solution.

Preparing Lys fibrils

Arnaudov *et al.*[4] reported that the optimal conditions for fibril formation at low pH were at pH 2 and 57 °C. On the basis of these results, our Lys solutions of 2% wt were heated at 57 °C with and without applying continuous turbulent or shear flow. After heating, the sample was immediately quenched by cooling on ice, and subsequently stored at 4 °C for further investigations. Crossed polarizers were used to observe whether the fibril solutions were optically isotropic or birefringent at rest.

Steady Shear experiments

A shearing device with a titanium Couette geometry was used to perform simultaneous heating and shearing with minimum water evaporation.[16] The diameter and length of the inner cylinder were 40 mm and 145.5 mm, accordingly. The diameter of the outer cylinder was 42 mm and the length was 148.5 mm. The top and bottom of this device was designed as a cone-and-plate geometry with an angle of 2.8°, which made the shear rate between the cone and plate comparable to that between the two cylinders. The sample volume of this shearing device was 18 mL. During the shearing experiment, the inner cylinder was rotated by a mechanical stirrer (type 2041, Heidolph Instruments, Schwabach, Germany) and the cell was heated in a water bath (Tamson 2500, Labovisco B.V., Zoetermeer, Netherlands) for 24h.[16]

Turbulent flow experiments

Stirred samples were heated in a heating plate (RT15, IKA Werke, Germany) using magnetic stirring bars (20 mm × 6 mm, VWR International, West Chester, Pennsylvania, USA). Bottles with an inner diameter of 24 mm and containing about 18 ml of sample were used in this experiment. Stirring rates of approximately 290 and 550 rpm were applied. Samples of each stirring rate were investigated at various heating times.

Methods

Centrifugal filtration method

This method was carried out as described in a study of Bolder *et al.*[18] Fibril solutions were diluted to 0.1% wt with a 10 mM HCl solution (pH 2). Diluted samples (3.5 ml) were then brought into centrifugal filter devices (Amicon® Ultra-4, Millipore

Corporation, Billerica, Massachusetts, USA) with 100,000 nominal molecular weight limit and filtered by centrifuging at 5,000 ×g for 20 min (Avanti J-26 XP, Beckman Coulter, Inc., Fullerton, California, USA). The obtained filtrates (containing non-aggregated proteins) were transferred, and the centrifuge tubes were washed and dried for the next step. The retentates in the filter units were washed twice with 10 mM HCl solution (pH 2) by gently mixing and then centrifuged at the same conditions to remove any non-aggregated materials left after the previous filtration step. The protein concentrations in various fractions were determined using a UV spectrometer (Cary 50 Bio, Varian, Inc., Palo Alto, California, USA) at a wavelength of 280 nm. The experiment was performed in duplicate.

Gel electrophoresis (SDS-PAGE)

Polyacrylamide gel electrophoresis (PAGE) was performed using a NuPAGE® Electrophoresis System (Invitrogen Corporation, Carlsbad, California, USA). Samples (non – reduced) were run on 4 – 12% Bis – Tris gels (1.0 mm × 10 well) with MES SDS running buffer and stained with Simply Blue™ SafeStain (Invitrogen Corporation, Carlsbad, California, USA). This method was performed on Lys fibril solutions, filtrates, and retentates from the centrifugal filtration method to examine the presence of proteins, their fragments and aggregates of different molecular weights.

Transmission electron microscopy (TEM)

Lys fibril solutions were examined using TEM by negative staining. Samples were first diluted (the dilution factor varied from 2,000 to 4,000 times depending on the fibril concentration and fibril length). Then, a drop of diluted sample was deposited onto a 5 nm thick carbon support film on a copper grid (400 mesh). Filter paper was used to remove the excess of sample after 15 s, before adding a droplet of staining solution (2% uranyl acetate – Sigma-Aldrich, Steinheim, Germany). After another 15 s, the excess was removed and the sample was left to air-dry. The micrographs were taken using a Philips CM 12 electron microscope operating at 80 kV (Eindhoven, Netherlands).[16,18] From the TEM pictures, fibrils were counted and their length was measured to produce the size distribution of the fibrils. To get reliable statistics between 240 and 380 fibrils were analyzed for each sample.

Rheo-optical measurements

Birefringence measurements of Lys fibril solutions were performed on a strain – controlled ARES rheometer (Rheometrics Scientific, Inc., Piscataway, New Jersey, USA) equipped with a modified optical analyzer module II (OAM II). Glass parallel plates with a diameter of 38 mm and a gap of 1mm were used. The wavelength of the laser beam was 670 nm. In this setup, the apparatus was capable of measuring

birefringence in the range of 10^{-9} to 8.10^{-6} at a sampling frequency of 24 Hz. The measurements were performed in a temperature-controlled room at 20 °C.[16,19,20]

Two types of test were performed: steady shear and cessation of flow experiments. In the steady shear tests a shear rate of 200 s^{-1} was used to completely align the fibrils (a shear sweep was performed to confirm that this shear rate was indeed sufficient to completely align the fibrils). The birefringence measured at total alignment is a measure for the total length concentration of the fibrils.[21–23] By combining the results of these tests with the data for the conversions from the centrifugal centrifugation experiments, a fast assay can be constructed for the conversion into fibrils.[19]

In the cessation of flow tests, the measured decay of birefringence curves were used to determine the length distribution of the fibrils, using a method developed by Rogers *et al*.[21] Conditions were identical to those used by Rogers *et al*.[21]

RESULTS AND DISCUSSIONS

Fibrils were produced either in the steady shear cells at shear rates ranging from 71 to 436 s^{-1} and turbulent flows at two flow rates (290 and 550 rpm). The samples were put between crossed polarizers, and they showed permanent birefringence (see **Figure 2.1**), indicating that a significant amount of fibrils is present in all samples.[19] We see that at concentrations as low as 2% wt the systems are no longer isotropic, and liquid crystal- like domains have formed in the solutions.


Figure 2.1. Samples produced by heating in a steady shear cells at various shear rates placed between crossed polarizers. (A): 71 s^{-1}; (B): 151 s^{-1}; (C): 220 s^{-1}; (D): 332 s^{-1}; and (E): 436 s^{-1}

Conversion experiments

In these experiments the conversion is defined as the weight percentage of aggregated protein material. The conversion of Lys protein at pH 2 as a function of shear rates (varying between 71 and 436 s^{-1}) was determined for protein solutions of 2% wt, heated at 57 °C for 24h, using the centrifugal filtration method. The results of the centrifugal filtration experiments of sheared samples are presented in **Figure 2.2A**,

and show a significant increase in conversion with increasing shear rate, up to shear rates of 200 s^{-1}. At higher shear rates no further increase in conversion is observed.
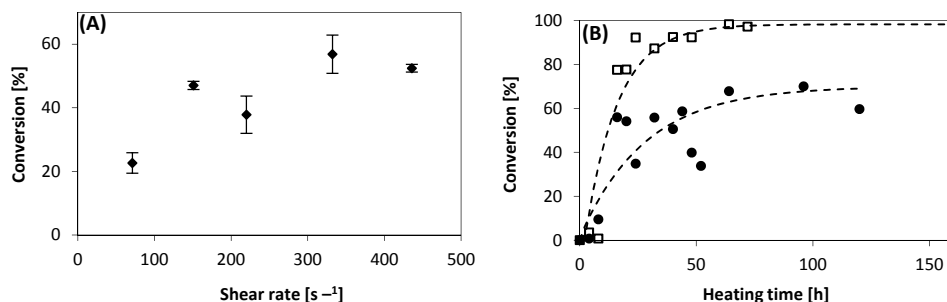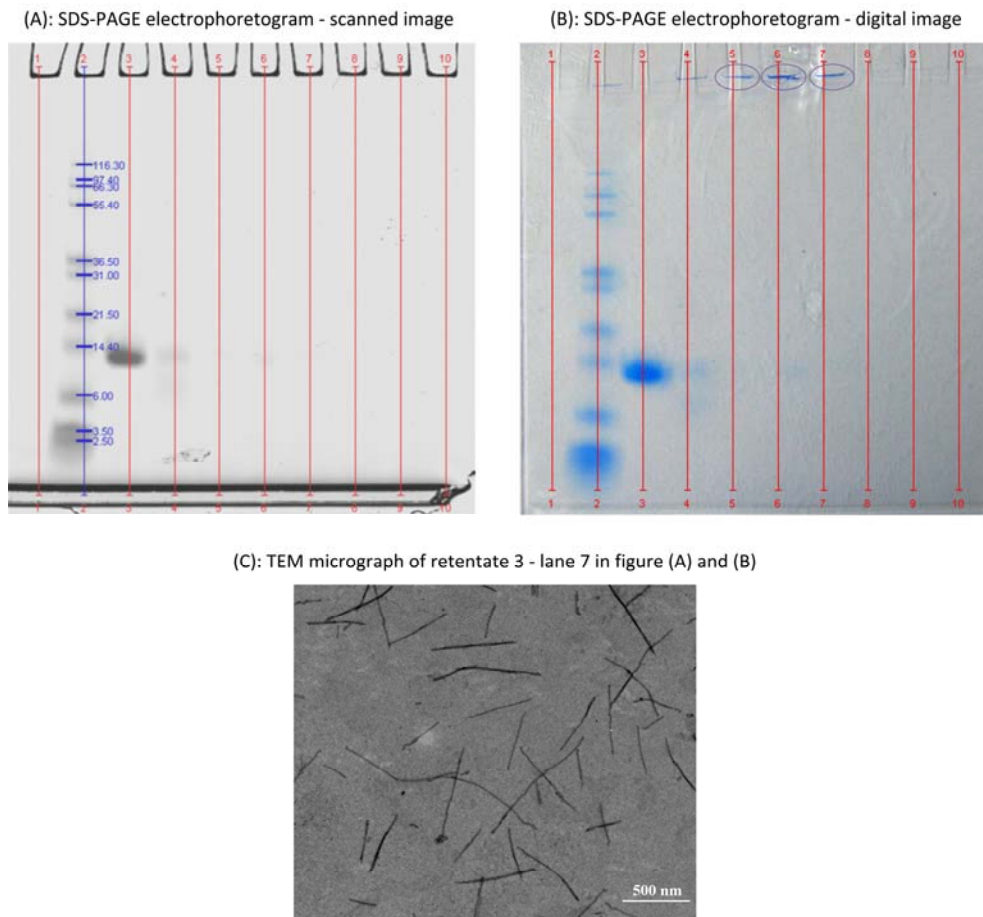

Figure 2.2. Figure (A): Conversion as a function of shear rate for 2% wt Lys heated at 57 °C for 24h. The error bars indicated the deviations from the mean values of duplicate samples; figure (B): Conversion as a function of heating time for 2% wt Lys heated at 57 °C at two stirring rates: ■ 550 rpm; ● 290 rpm.

For most shear rates, the conversions of duplicate samples were comparable, except for samples prepared at shear rates of 220 and 332 s^{-1}. These show a slightly higher variation most likely due to minor deviations from the applied shear rate that occurred in the early stages of these experiments.

A clear trend can be seen in all these samples: an increase of shear rate leads to an increase in conversion. Even at the lowest shear rate, more than 20% of the protein was already aggregated into fibrils after 1 day of shearing, compared to a lag time of 2 days in which no conversion can be detected when Lys solutions were heated at rest as reported by Arnaudov *et al.*[4] This shows the significant effect of shearing on the Lys fibril aggregation.

A similar observation on β-lactoglobulin was reported in a study of Akkermans *et al.*[5] where pulsed and continuous shear applied during heating enhanced fibril growth. However, in the case of β-lactoglobulin, the effect of shear flow on fibril concentration at low protein concentrations (0.5 – 2% wt) was not as pronounced as it was in our Lys samples (for β-lactoglobulin samples the enhancing effect of shear flow on the amount of fibrils starts around a protein concentration of 3% wt).[16] This comparison confirms that although amyloid formation appears to be a generic property of many globular proteins (or their peptide fragments), the mechanism of self-assembly varies and seems to be specific for each one.[7]

(A): SDS-PAGE electrophoretogram - scanned image

(B): SDS-PAGE electrophoretogram - digital image

(C): TEM micrograph of retentate 3 - lane 7 in figure (A) and (B)

Figure 2.3. SDS-PAGE electrophoretograms of filtrates and retentates of samples heated at 290 rpm for 96h – figure (A): scanned image using the software Quality One (Bio-Rad Laboratories GmbH, Munich, Germany); figure (B): digital image – lane 1: blank; lane 2: marker Mark12™ (Invitrogen Corporation, California, USA); lane 3: purified Lys (after dialysis) as starting material; lane 4: LysFib obtained after heating at 57 °C for 96h with a stirring rate of 290 rpm; lane 5 to lane 10: respectively retentate 1, 2 and 3 and filtrate 1, 2 and 3 (obtained after the first, second and last centrifugation step). The presence of a high molecular mass band in the wells of retentate lanes was marked with an ellipse; figure (C): TEM micrograph of retentate 3 (obtained after the last centrifugation step) (scale bar represents 500 nm)

For the stirred samples (turbulent flow), the conversion as a function of time for two different stirring settings is plotted in **Figure 2.2.B**. At a speed of 550 rpm, Lys fibril solutions reached a conversion of around 90% after two days. A conversion of about 60% was found over the same period of time for samples stirred at 290 rpm. These conversions are significantly higher, compared to those for samples at the same conditions (concentration, pH and heating temperature), and heated at rest, reported

by Arnaudov *et al.*[4] In our own samples some fibrils were seen on TEM micrographs of samples heated at rest after 24h of heating (micrographs not shown), but the conversions could not be determined due to the low fibril concentrations. The conversions after 24h of heating in turbulent flow were in the same range as those of sheared samples (between 30 and 60%). So both types of flow enhanced the formation of Lys fibrils significantly.

After centrifugal filtration, the filtrates and retentates were examined using TEM and SDS-PAGE methods. When the filtrates were studied with TEM, no aggregates were observed (micrographs not shown) showing that the loss of fibrils was negligible. In addition, the SDS-PAGE tests (see **Figure 2.3A**) of retentates and filtrates showed that the bands of Lys monomers became less visible after each of the washing steps and entirely disappeared from both retentates and filtrates after the last centrifugation step (for more electrophoretograms, see Appendix). That means that the washing steps were adequately separating aggregates from non-aggregated material. The presence of high molecular mass bands in the wells of retentate lines (see **Figure 2.3B**) indicated the presence of aggregates of molecular mass larger than 200 kDa (marker Mark12™ – Invitrogen Corporation, Carlsbad, California, USA – has a molecular mass range from 2.5 to 200 kDa in the conditions applied). However, no other intermediate aggregates were obvious on the gels. The same observation was reported by Mishra *et al.* of samples at pH 1.6 incubated for more than 40h at 65°C.[12] The high molecular weight material in the final retentate was investigated using TEM (see **Figure 2.3C**). This image clearly shows that this material consists of long fibrils.

Length distributions

In the analyses of TEM micrographs, images of fibrils of sheared samples were captured randomly on the grids and their contour lengths were measured to construct a length distribution. Sample sizes varied from 240 to 380 fibrils. Only fibrils that could be clearly distinguished and had both ends on the image were analyzed. The number of fibrils of length L, N, was weighed by $1/(1 – L/D)$, the probability of finding a fibril of length L in a frame with width D.[21] The results are presented in **Figure 2.4A**.

The maximum in the curves shifted from right to left (from long to shorter fibrils) as a result of increasing shear rates (**Figure 2.4A**). The predominant lengths of Lys fibril solutions sheared at 71, 220 and 436 s^{-1} are approximately 1500, 1300, and 800 nm, respectively. Thus, the increasing shear rate not only induces an increase in the fibril formation rate but also shortens the fibrils formed. A possible explanation for these observations could be that shearing ruptures the fibrils during formation, producing two or more active fragments, which each may grow by addition of Lys monomers (or peptide fragments). Consequently, more and shorter fibrils are formed.

For stirred samples, the TEM analyses were carried out similarly to the sheared samples, but the sample sizes were somewhat smaller (around 100 fibrils per sample were measured). Samples of the same stirring rates but at different heating times were investigated, but no obvious difference in size distribution was observed. So heating time did not have an effect on the size of fibrils formed.
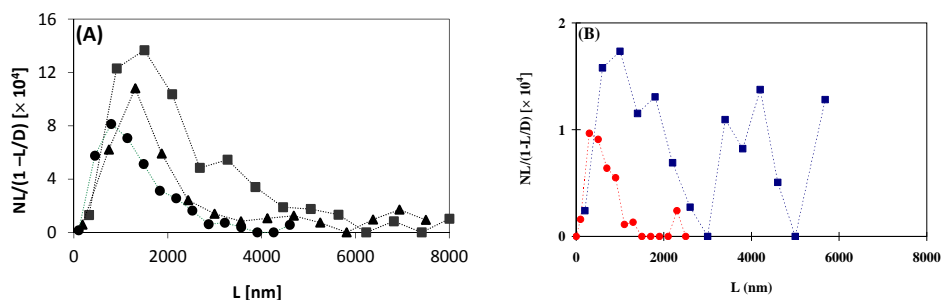
Figure 2.4. Figure (A): Weighted length distribution curves of samples prepared at different shear rates (■: 71.19 s⁻¹; ▲: 220.04 s⁻¹, ●: 435.76 s⁻¹); figure (B): Weighted length distribution curves of samples heated for 48h at different stirring rates (■: 290 rpm; ●: 550 rpm)

The length distributions obtained from TEM of samples in turbulent flow were much wider than those of samples produced in steady shear flows (**Figure 2.4**). At lower stirring rates, polydispersity is more pronounced than at higher stirring rates. This is most likely a result of the inhomogeneity of the flow patterns. At low stirring rates only the portion of the fluid close to the magnetic stirrer bar is exposed to significant shear and extensional rates, whereas the fluid close to the top of the container is hardly sheared at all. Consequently, the sizes of fibrils varied significantly, as can be seen from the presence of a second peak in samples at 290 rpm (**Figure 2.4B**). Inhomogeneous flow apparently leads to the formation of a mixture of very long and short fibrils. Note that at 290 rpm the second peak in **Figure 2.4B** is rather pronounced. In this distribution each fraction is weighted by a factor $1/(1 - L/D)$, where D is the width of the frame of the TEM micrograph. This implies that longer fibrils contribute more to the total length distribution. **Figure 2.4B** shows that fibrils formed at higher stirring rates were shorter than those at lower stirring rate. The peaks in the distribution are at approximately 300 and 650 nm for samples stirred at 550 and 290 rpm respectively, whereas for samples produced in steady shear the peaks where at lengths above 1 μm.

Birefringence of fibril solutions

Birefringence and fibril concentration

Lys fibril solutions with known conversions (determined with the centrifugal filtration method) were subjected to steady shear flow at a shear rate of 200 s⁻¹, for 30 s, in both clockwise and counter-clockwise directions. This shear rate was sufficient to induce maximum alignment of the fibrils. Samples were diluted 10 times prior to measurement of the flow birefringence *Δn'*. This value is related to the length and concentration of fibrils by the equation[21]

$$\nu.\Delta n' = M \int c(L) L dL \qquad (1)$$

where ν is the dilution factor, *M* is a constant,[21] and *c(L)* is the concentration of fibrils with a length between *L* and *(L + dL)*.

Plotting the birefringence versus the fibril concentration (**Figure 2.5**) we obtain a linear relationship, which is basically the inverse of equation **(1)**. The equation of the trend line is given by $C_{fibril} = K_1.\nu\Delta n'$, with a slope $K_1 = 1.22 \cdot 10^5$. From this value for K_1 a value for the constant *M* can be calculated, using[21]

$$M = \frac{\alpha M_{mono}}{10 K_1 N_{av}} \qquad (2)$$

where M_{mono} is the molecular mass of the protein monomers (14.4 kDa), α is the fibril line density (monomers per unit length), and N_{AV} is Avogadro's number (6.022×10^{23} mol⁻¹). The line density, determined by neutron scattering measurements, was approximately equal to the inverse of the monomer diameter.[24,25] On the basis of a mean radius of roughly 1.7 nm for the Lys monomer,[26,27] the fibril line density α was chosen to be 0.294 nm⁻¹. Substituting these values in equation **(2)** resulted in a value for *M* equal to 5.74×10^{-21} m².

In **Figure 2.5B** we have plotted the concentration of fibrils (determined with the centrifugal filtration methods) versus the birefringence νΔn', for the samples produced in turbulent flow at 290 rpm.

The slope of the trend line, K_1, was equal to 3.47×10^5, which gives a value for *M* for these samples equal to 2.03×10^{-21} m². This is almost three times smaller than the value of *M* for fibrils produced in steady shear flow. A possible explanation for this result could be that turbulent flow has an effect on the fibril shaving process as described by Mishra *et al.*,[12] leading to differences in the structure of the fibrils and therefore, to a different value for the anisotropy in polarization per unit length of the

fibrils. However, further research into the actual structure of the fibrils is needed to confirm this hypothesis.

In these birefringence experiments the maximum fibril concentration that could be used was less than 1% wt. When the fibril concentration is higher, domains are formed in the sample with permanent birefringence, and the linear relationship in **Figure 2.5B**, valid only for samples that are isotropic at rest, no longer applies.
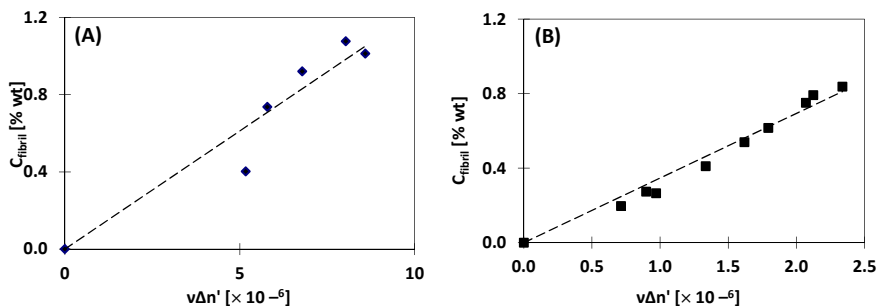

Figure 2.5. Correlation between the measured steady shear birefringence corrected with the dilution factor, $\nu\Delta n'$, and the average fibril concentration based on the conversion of Lys as determined using the centrifugal filtration method, C_{fibril}. Figure (A): Samples produced in steady sheared flow; figure (B): Samples produced in turbulent flow at 290 rpm.

Decay curves and length distributions

Rogers *et al.*[21] developed a method to determine the length distribution of rod-like fibril systems from the decay of flow-induced birefringence after cessation of flow. TEM observations showed that the majority of fibrils formed in the conditions investigated are long, thin, and mostly un-branched. That makes Lys fibril systems suitable for this method, which is based on the Doi-Edwards-Marrucci-Grizutti (DEMG) theory for free, un-branched, non-sticky rods, in the semi-dilute regime. A shear rate of 5 s⁻¹ was applied to all samples. This shear rate ensures that fibrils are sufficiently aligned to accurately study their rotational dynamics, but avoids complete alignment and stretching of the fibrils. At complete alignment the system would be in the dilute regime, where the DEMG theory is no longer applicable.
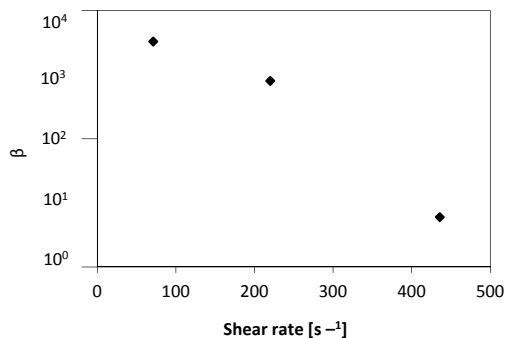
Figure 2.6. The parameter β as a function of applied shear rate.
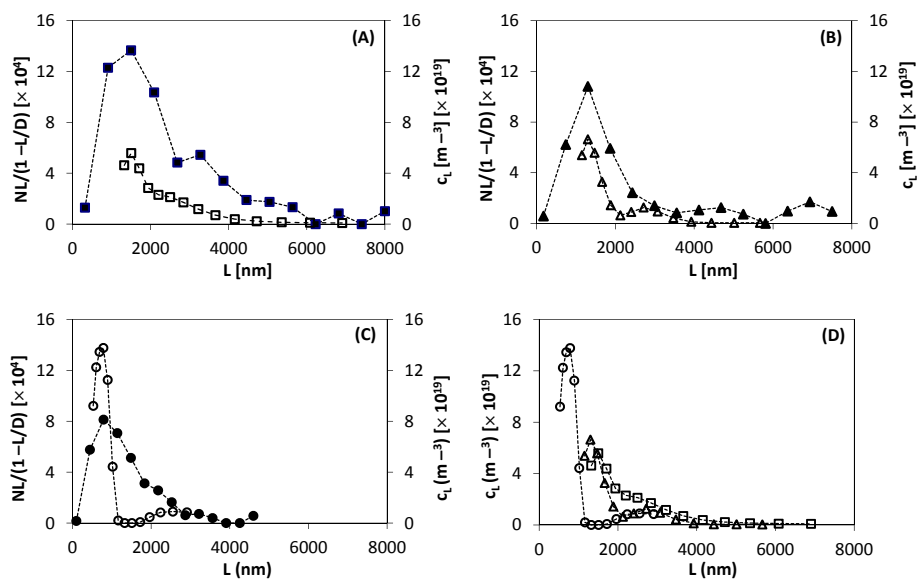
Figure 2.7. Comparison of the length distributions of samples at various shear rates from fitted birefringence decays (open signs) and TEM (closed signs): Figure (A) □, ■: 71.19 s^{-1} (β = 3.3 × 10^3); figure (B) Δ, ▲: 220.04 s^{-1} (β = 800); figure (C) ○, ●: 435.76 s^{-1} (β = 6). figure (D): Length distributions of samples at various shear rate from fitted birefringence decays (□: 71.19 s^{-1} – β = 3.3 × 10^3; Δ: 220.04 s^{-1} – β = 800; ○: 435.76 s^{-1} – β = 6)

The length distribution obtained from the decays was calibrated by comparison with the length distribution from TEM measurements.[21] The calibration was done by adjusting the value for *β* – the pre-factor in the Doi-Edwards expression for the rotational diffusion coefficient of the fibrils. This pre-factor is a measure of the stiffness of the fibrils: it is of order 1 for rod-like fibrils and much higher for semi-flexible fibrils. [19] The adjustment was performed using Matlab software (The

MathWorks, Inc., Natick, Massachusetts, USA) with an iteration of 100 steps. In **Figure 2.6** we have plotted the value for β as a function of the applied shear rate. In **Figure 2.7** we show the size distributions for the same three shear rates.

We clearly see in **Figure 2.6** and **Figure 2.7** that an increase in shear rate resulted in a shift in the size distribution to smaller fibril lengths and a decrease in β, indicating that fibrils are more rod-like. At low shear rates the fibrils appear to be long and semi-flexible, whereas at high shear rates the fibrils appear to be short and more rod-like. The effect of shear treatment on the length distribution of Lys fibrils is much more pronounced than the effect observed for β-lactoglobulin fibrils in about the same shear rate range.[16] In comparison with Lys fibrils formed at rest, fibrils obtained in shear flow experiments tend to be much shorter and more rod-like.[4]

In the case of samples stirred at 550 rpm, the decay of birefringence was too fast (even with non-diluted samples) to get a reliable length distribution. The fibrils were too short and the rotational diffusion was too fast to determine a size distribution from decay of birefringence measurements. Therefore, the determination of the length distribution was performed only for samples stirred at 290 rpm.

Fitting the decay of birefringence measurements for the sample produced with turbulent flow at 290 rpm, with the length distributions determined from TEM, gave a value for β of order 10, comparable to that of samples produced in steady shear, at the highest shear rates. This shows that the fibrils have more rod-like behavior. This can be explained by the fact that the samples consist predominantly of fibrils in the submicron range (**Figure 2.4B**).

CONCLUSIONS

From the results of our study, both steady shear and turbulent flows significantly increase the conversion of Lys proteins into fibrils. The conversion increased with increasing shear or stirring rate. In addition, higher shearing or stirring rates resulted in shorter fibrils that are more rod-like, whereas at rest or at the lowest rates longer semi-flexible fibrils were obtained. In simple shear flows length distributions of fibrils were not as wide as those formed in turbulent flows. This is most likely a result of the inhomogeneity of the flow patterns in turbulent flow. The effect of flow on fibril formation from Lys is much more significant than the effect observed for β-lactoglobulin,[5,16,23] in terms of both conversion and size distributions. The significant effect of flow on the size distribution can be used to control the functionality of the fibrils. A wide range of sizes (from 300 nm to several microns), and flexibilities (from semi-flexible to more rod-like) can be obtained, by adjusting the flow rate during production of the fibrils.

The results from the birefringence measurements show that this technique is an excellent tool to characterize the kinetics of the fibril formation process, and the characteristics (length distribution and flexibility) of the fibrils. The values for K_1, M, and β can be used in fast assays for future Lys fibril formation studies.

ACKNOWLEDGEMENTS

REFERENCES

1   Krebs, M. R. H. *et al.* Formation and Seeding of Amyloid Fibrils From Wild-Type Hen Lysozyme and A Peptide Fragment From The A–Domain. *J Mol Biol* **300**, 541 – 549 (2000).

2   Goda, S. *et al.* Amyloid Protofilament Formation of Hen Egg Lysozyme In Highly Concentrated Ethanol Solution. *Protein Sci* **9**, 369 – 375 (2000).

3   Cao, A., Hu, D. & Lai, L. Formation of Amyloid Fibrils From Fully Reduced Hen Egg White Lysozyme. *Protein Sci* **13**, 319 – 324 (2004).

4   Arnaudov, L. N. & De Vries, R. Thermally Induced Fibrillar Aggregation of Hen Egg White Lysozyme. *Biophys. J.* **88**, 515 – 526 (2005).

5   Akkermans, C. *et al.* Shear Pulses Nucleate Fibril Aggregation. *Food Biophys* **1**, 144 – 150 (2006).

6   Sagis, L. M. C. *et al.* Polymer Microcapsules With A Fiber–Reinforced Nanocomposite Shell. *Langmuir* (2008).

7   Sagis, L. M. C., Veerman, C. & van der Linden, E. Mesoscopic Properties of Semiflexible Amyloid Fibrils. *Langmuir* **20**, 924 – 927 (2004).

8   Veerman, C., Ruis, H. G. M., Sagis, L. M. C. & van der Linden, E. Effect of Electrostatic Interactions On The Percolation Concentration of Fibrillar Beta-Lactoglobulin Gels. *Biomacromolecules* **3**, 869 – 873 (2002).

9   Veerman, C., Sagis, L. M. C., Heck, J. & van der Linden, E. Mesostructure of Fibrillar Bovine Serum Albumin Gels. *Int J Biol Macromol* **31**, 139 – 146 (2003).

10   Schmittschmitt, J. P. & and Scholtz, J. M. The Role of Protein Stability, Solubility, and Net Charge In Amyloid Fibril Formation. *Protein Sci* **12**, 2374 – 2378 (2003).

11   Rochet, J.-C & Lansbury, P. T. Amyloid Fibrillogenesis: Themes and Variations. *Curr Opin Struc Biol* **10**, 60 – 68 (2000).

12   Mishra, R. *et al.* Lysozyme Amyloidogenesis Is Accelerated By Specific Nicking and Fragmentation But Decelerated By Intact Protein Binding and Conversion. *J Mol Biol* **366**, 1029 – 1044 (2007).

13   Vernaglia, B. A., Huang, J. & Clark, E. D. Guanidine Hydrochloride Can Induce Amyloid Fibril Formation From Hen Egg – White Lysozyme. *Biomacromolecules* **5**, 1362 – 1370 (2004).

14   Stathopulos, P. B. *et al.* Sonication of Proteins Causes Formation of Aggregates That Resemble Amyloid. *Protein Sci* **13**, 3017 – 3027 (2004).

15   Krebs, M. R. H., Morozova-Roche, L., Daniel, K., Robinson, C. & Dobson, C. M. Observation of Sequence Specificity In The Seeding of Protein Amyloid Fibrils. *Protein Sci* **13**, 1933 – 1938 (2004).

16   Akkermans, C., A. J. van der Goot, P. Venema, E. van der Linden and R. M. Boom. Formation of Fibrillar Whey Protein Aggregates: Influence of Heat and Shear Treatment, and Resulting Rheology. *Food Hydrocolloid* **22**(7): 1315 – 1325 (2008).

17   Hill, E. K., Krebs, B., Goodall, D. G., Howlett, G. J. & Dunstan, D. E. Shear Flow Induces Amyloid Fibril Formation. *Biomacromolecules* **7**, 10 – 13 (2006).

18   Bolder, S. G., Vasbinder, A. J., Sagis, L. M. C. & van der Linden, E. Heat-Induced Whey Protein Isolate Fibrils: Conversion, Hydrolysis, and Disulphide Bond Formation. *Int Dairy J* **17**, 846 – 853 (2007).

19   Bolder, S. G., Sagis, L. M. C., Venema, P. & van der Linden, E. Thioflavin T and Birefringence Assays To Determine The Conversion of Proteins Into Fibrils. *Langmuir* **23**, 4144 – 4147 (2007).

20   Klein, C. O. *et al.* Optimized Rheo-Optical Measurements Using Fast Fourier Transform and Oversampling. *Appl Rheol* **17**, 45210 – 45211 – 45210 – 45217 (2007).

21   Rogers, S. S., Venema, P., Sagis, L. M. C., van der Linden, E. & Donald, A. M. Measuring The Length Distribution of A Fibril System: A Flow Birefringence Technique Applied To Amyloid Fibrils. *Macromolecules* **38**, 2948 – 2958 (2005).

22   Doi, E. & and Edwards, P. J. B. Dynamics of Rod-Like Macromolecules In Concentrated Solution. Part 2. *J Chem Soc Faraday Trans.* **2**, 918 – 932 (1978).

23   Bolder, S. G., Sagis, L. M. C., Venema, P. & van der Linden, E. Effect of Stirring and Seeding On Whey Protein Fibril Formation. *J. Agric. Food Chem.* **55**, 5661 – 5669 (2007).

24   Rogers, S. S. *Some Physical Properties of Amyloid Fibrils* Doctor of Philosophy Thesis, Wolfson College, Cambrigde University, (2005).

25   Aymard, P., Nicolai, T., Durand, D. & and Clark, A. Static and Dynamic Scattering of β-Lactoglobulin Aggregates Formed After Heat-Induced Denaturation At pH 2. *Marcromolecules* **32**, 2542 – 2552 (1999).

26   Cardinaux, F., Stradner, A., Schurtenberger, P., Sciortino, F. & and Zaccarelli, E. Modeling Equilibrium Clusters In Lysozyme Solution. *EPL* **77** (2007).

27   Broide, M. L., Tominc, T. M. & Saxowsky, M. D. Using Phase Transitions To Investigate The Effect of Salts On Protein Interactions. *Phys Rev E* **53**, 6325 – 6335 (1996).

APPENDIX

SDS-PAGE electrophoretograms of filtrates and retentates obtained after centrifugation steps
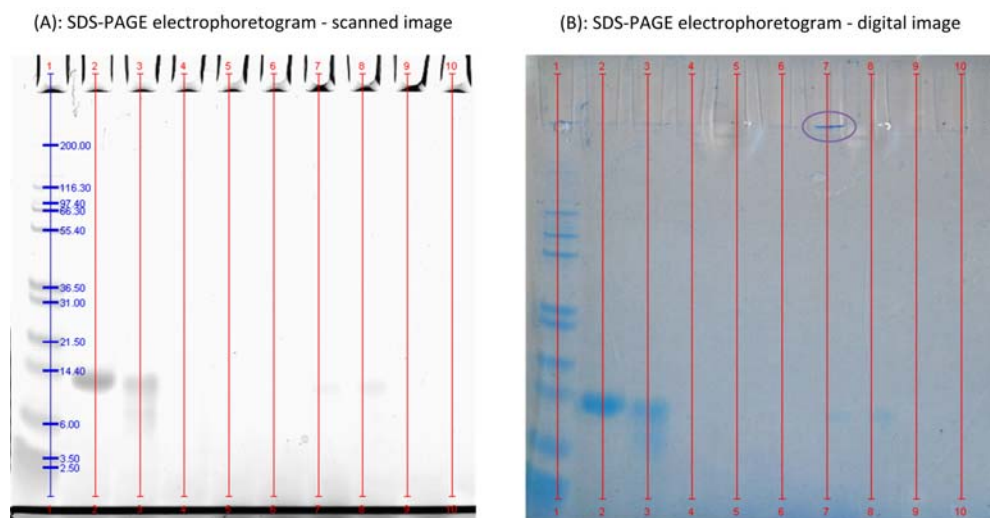
Figure 2.8. SDS-PAGE electrophoretograms of filtrates and retentates of samples heated at 550 rpm for 16h – figure (A): scanned image using the software *Quality One (Bio-Rad* Laboratories GmbH, Munich, Germany); figure (B): digital image – lane 1: marker Mark12™ (Invitrogen Corporation, California, USA); lane 2: purified Lys (after dialysis) as starting material; lane 3: LysFib obtained after heating at 57 °C for 16h with a stirring rate of 550 rpm; lane 4: blank; lane 5 to lane 10: respectively retentate 1, 2, 3 and filtrate 1,2, 3 (obtained after the first, second and last centrifugation step). The presence of a high molecular mass band in the wells of retentate lanes was marked with an ellipse.
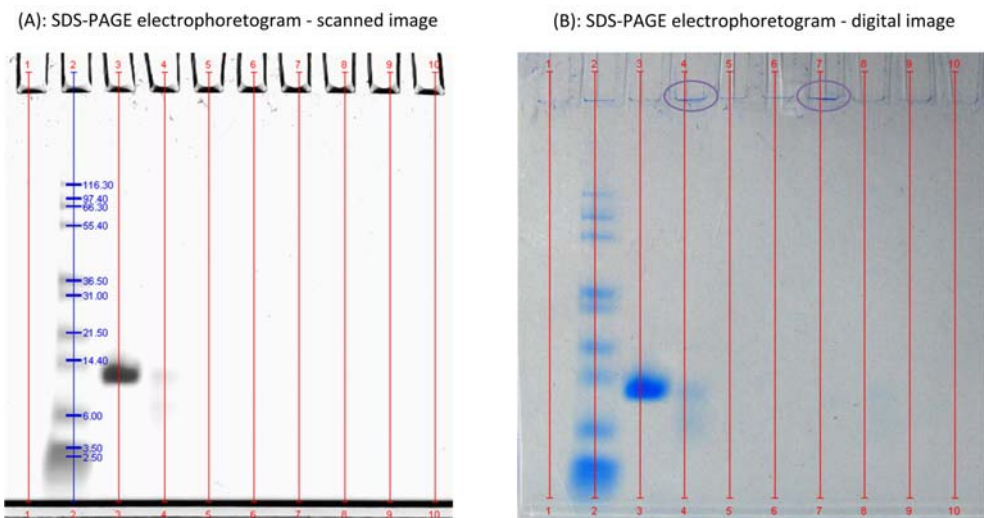
Figure 2.9. SDS-PAGE electrophoretograms of filtrates and retentates of samples heated at 550 rpm for 96h – figure (A): scanned photo using the software *Quality One (Bio-Rad* Laboratories GmbH, Munich, Germany); figure (B): digital photo – lane 1: blank; lane 2: marker Mark12™ (Invitrogen Corporation, California, USA); lane 3: purified Lys (after dialysis) as starting material; lane 4: LysFib obtained after heating at 57 °C for 96h with a stirring rate of 550 rpm; lane 5 to lane 10: respectively retentate 1, 2 and 3 and filtrate 1, 2 and 3 (obtained after the first, second and last centrifugation step). The presence of a high molecular mass band in the wells of retentate lanes was marked with an ellipse.

CHAPTER 3

SURFACE RHEOLOGICAL PROPERTIES OF LIQUID – LIQUID INTERFACES STABILIZED BY PROTEIN FIBRILLAR AGGREGATES AND PROTEIN – POLYSACCHARIDE COMPLEXES

ABSTRACT

In this chapter we have investigated the surface rheological properties of oil – water interfaces stabilized by fibrils from lysozyme (long and semi-flexible, and short and rigid ones), fibrils from ovalbumin (short and semi-flexible), lysozyme – pectin complexes, or ovalbumin – pectin complexes. We have compared these properties with those of interfaces stabilized by the native proteins. The surface dilatational and surface shear moduli were determined using an automated drop tensiometer, and a stress controlled rheometer with biconical disk geometry. Results show that interfaces stabilized by complexes of these proteins with high methoxyl pectin have higher surface shear and dilatational moduli than interfaces stabilized by the native proteins only. The interfaces stabilized by ovalbumin and lysozyme complexes have comparable shear and dilatational moduli though ovalbumin – pectin complexes are twice as large in radius as lysozyme – pectin complexes. At most of the experimental conditions, interfaces stabilized by fibrils have the highest surface rheological moduli. The difference between long semi-flexible lysozyme fibrils or short rigid lysozyme fibrils is not pronounced in interfacial dilation rheology but significant in interfacial shear rheology. The complex surface shear moduli of interfaces stabilized by long semi-flexible fibrils are about 10 times higher than those of interfaces stabilized by short rigid fibrils, over a range of bulk concentrations. Interfaces stabilized by short and more flexible ovalbumin fibrils have a significantly higher surface shear modulus than those stabilized by longer and more rigid lysozyme fibrils. This study has shown that the use of such supra-molecular structural building blocks creates a wider range of microstructural features of the interface, with higher surface shear and dilatational moduli and a more complex dependence on strain rate.

INTRODUCTION

Surface rheological properties have a significant impact on the dynamics and stability of a wide range of multiphase systems.[1] In food products, they may affect the stability and dynamic behavior of foam, emulsions, phase-separated biopolymer systems, or encapsulation systems such as vesicles.[1,2] For these systems the surface dilatational modulus and surface shear modulus are in general considered to be the most relevant surface rheological properties,[1] although in systems such as vesicles or phase-separated biopolymer mixtures the bending rigidity of the interfaces may also affect the dynamics of the system significantly.[2–6]

In food products, proteins are one of the most widely used surface-active ingredients, and they are known to show excellent stabilizing properties in foams, and food emulsions.[7,8] Food emulsions include a wide variety of food products (e.g. dairy products such as milk, yoghurt, ice cream, and infant formula or soft drink, sauces, dressings, etc.),[9] and protein stabilized emulsions form the most important class of food colloids.[10,11]

When proteins adsorb at oil – water interfaces they can form a viscoelastic (multi)layer with a complicated microstructure.[12–17] This viscoelastic layer tends to have dilatational and surface shear moduli much higher than that of interfaces stabilized by low molecular weight surfactants. These moduli depend on composition, thickness and microstructure of the (multi)layer, and influence the emulsion structure, its stability, its rheology, as well as the kinetics of mass transport between droplets.[7,16,18] The primary driving force for the spontaneous adsorption of proteins onto an oil – water interface is the exposure of their non-polar side chains to an unfavorable aqueous environment.[11] Once a protein is adsorbed, it tends to unfold and therefore often cannot be removed from the interface easily by washing.[12,13,19]

Different to proteins, polysaccharides can stabilize oil-in-water emulsions using their thickening and gelling properties to form a macromolecular barrier in the aqueous medium between the dispersed droplets. Protein – polysaccharide complexes have been used more and more as emulsifiers and stabilizers since they have the combined advantages of both components. In theory, soluble protein – polysaccharide complexes can be ideal steric stabilizers because they can attach firmly to an interface like a protein and be able to solvate in the aqueous medium like a polysaccharide to form a gel-like charged film of significant thickness, with polymer chains extending extensively from the interface.[15,20] The mechanical strength of the adsorbed layer, together with the electrostatic repulsion (of like charged emulsion droplets) and steric effects (due to the thick layer as a barrier) are the most important factors affecting the kinetic stability of oil in water emulsions.[21]

The mesoscopic structure of the interfacial layer containing both protein and polysaccharide depends not only on factors like pH and ionic strength but also on the procedure used to make the emulsion.[22,23] There are two main methods to prepare emulsion stabilized with a combination of protein and polysaccharide. In the first method, protein – polysaccharide complexes are first prepared and then used as emulsifiers during droplet formation. Previous studies have confirmed that using soluble protein – polysaccharide complexes results in a substantial improvement in emulsion stability compared to the native protein, without changing the emulsifying capacity significantly.[15,16,24–27] In the second method, the emulsion is first prepared with protein as emulsifier and then the washed emulsion is mixed with a polysaccharide solution. The polysaccharide will adsorb onto the protein layer as a complexing sencondary layer, forming bilayer emulsions.[11,19,22,23,28,29] The two different methods will result in different interfacial compositions and structures, and different emulsion stabilities against creaming or flocculation.[28] Jourdain *et al.* compared the stability of mixed-layer and bilayer emulsion stabilized by sodium caseinate-dextran sulphate, and found that the bilayer emulsion was more inclined to flocculate upon pH decrease.[29]

The surface rheological properties of the interface either formed by proteins or protein – polysaccharide complexes can be determined by interfacial rheology, where mechanical stresses are applied to the interface. Two common surface rheology measurements are dilatation and surface shear rheology.[14,30] In dilatation measurements, the interfacial area is changed resulting in changing of the interface concentration. These measurements provide important information related to stabilizing interfaces during making emulsions or foams.[30] Interfacial dilatational rheology is sensitive to the structural relaxation of molecules under compression and/or expansion and kinetics of exchange of material between interface and bulk phase.[18,19] In surface shear experiments, an in-plane velocity gradient is applied, while the interface area remains constant, and consequently, the interface concentration is constant.[14,30] Interfacial shear rheology can provide information about the interfacial composition, the structural state and the interactions between adsorbed species.[7,19,31,32] Since the deformations in droplet collision are a combination of shear and dilation, emulsion stability is most likely influenced by both dilatational and shear properties[18]

Egg albumen proteins are widely used as functional ingredients in foods because of their excellent interfacial properties.[33,34] Ovalbumin (Ova) and lysozyme (Lys) are two globular proteins in egg white that have been extensively investigated and used as model proteins in studies of protein adsorption at interfaces.[33–35] They are known to be effective emulsifiers, to be able to form complexes with polysaccharides.[36,37] An additional feature of these proteins it their ability to yield fibrillar aggregates.[38–40]

Such fibrils are, like their original proteins, also acting as interface stabilizers.[41–43] For example, in a study of Jung *et al.*, β-lactoglobulin fibrils have been shown to be efficient stabilizers of air – water and oil – water interfaces.[41,42] Other studies of Jung *et al*. and Isa *et al*. found that β-lactoglobulin fibrils induce the development of liquid-crystalline phases during adsorption, thereby, enhancing interfacial stability.[41,43,44]

In general, the use of such supra-molecular structural building blocks creates a wider range of microstructural features of the interface, and accordingly richer interfacial rheological behavior. In this study, we have chosen to investigate how properties of three different individual structural elements (with different properties) affect oil – water interface shear and dilatational rheology. One element is proteins in their (initially) native form, another is complexes of protein with high methoxyl pectin (HMP), and the third consists of fibrils. In this way we cover small and compact spherical structures (protein), larger spherical and softer structures (complexes), and short or long thin structures (fibrils), that can be either flexible or stiff.

The polysaccharide chosen is pectin, a commonly used polysaccharide as a gelling agent in food products. Its elementary chain segment is negatively charged and the charge is varied through the change in its degree of methylation and pH: below pH 3.5, high methoxyl pectin carboxylic functions are not sufficiently dissociated[45] and at pH 7.4, pectin is fully dissociated.[36]

MATERIALS AND METHODS

Materials

Ova was purchased from Sigma-Aldrich Co., Missouri, USA (product no. A5503) (at least 98% purity). It has a molecular weight of 42 kDa with approximate molecular dimensions of 7 × 4.5 × 5 nm.[46] Its isoelectric point is 4.6

Lys from hen egg white was obtained from Sigma-Aldrich Co., Missouri, USA (3 × crystallized, lyophilized powder, product no. L6876). Lys has a molecular weight of 14.3 kDa with approximate molecular dimensions of 3 × 3 × 4.5 nm.[47] Its isoelectric point is above 10.

HMP was supplied by CP Kelco ApS, Lille Skensved, Denmark (JMH-6, batch no. 16849, degree of methoxylation 69.8%). It was characterized in a study of Sagis *et al.*[48] and has a molecular weight of 2.7×10^3 kDa and a radius of gyration of 46 nm.

The oil n-hexadecane was from Merck Schuchardt OHG, Hohenbrunn, Germany (CAS-no. 544-76-3). MCT (medium chain triglyceride oil) was from Sasol Germany GmbH, Witten, Germany (article no. 6330, batch no. 080526).

All other chemicals used were of analytical grade, unless stated otherwise. All solutions were prepared with Millipore water (Millipore Corporation, Billerica, Massachusetts, USA). Samples were diluted to the desired concentration (if applicable) with the same buffer or solution used for the primary solutions

Proteins solutions

Proteins were dissolved in 10 mM phosphate buffer at desired pH and stirred overnight at 4 °C. After that, Ova solutions were centrifuged at 20,000 ×g for 30 min to remove un-dissolved materials. Lys solutions were extensively dialyzed against the same buffer at 4 °C to remove dissolved salts present (around 5 wt %). The dialyzed Lys solution was filtered using filters with a 0.2 μm pore size (FP 30/0.2 CA-S, Schleicher & Schuell, Germany). The concentration of the protein stock solutions was determined with a UV spectrophotometer (Cary 50 Bio, Varian, Inc., Palo Alto, California, USA) at a wavelength of 280 nm and an extinction coefficient of $E^{1\% \, (wt)}$ equal to 6.68145 for Ova and 25.769 for Lys.

Preparing fibrils

Ova fibrils were prepared as described in a previous study of Veerman *et al.*[39] According to this study, Ova fibrils formed by heating Ova solutions of 7% wt at pH 2, 80 °C were short, with a contour length L_c of about 200 nm, a persistence length of the same order of magnitude (L_p of about 300 nm)[49], and can therefore be considered to be semi-flexible.

Lys fibrils were prepared by heating Lys solutions at pH 2 at 57°C on a heating plate (RT15, IKA Werke, Germany) using magnetic stirring bars (20 mm × 6 mm, VWR International, West Chester, PA) as described in *chapter 2.*[38] Stirring rates of approximately 290 and 550 rpm were applied. At 290 rpm, fibrils were obtained with L_c of about 1.2 – 1.5 μm and a pre-factor β in the Doi-Edwards expression for the rotational diffusion coefficient of the fibrils,[50] of order 10 . Because β can be used as a measure for the stiffness of the fibrils – of order 1 for rod-like fibrils and of higher order for semi-flexible ones[51] – these fibrils are considered as semi-flexible. At 550 rpm, fibrils formed were short with L_c of about 500 nm and more rod-like (L_c <L_p).[38]

Preparing protein – HMP complexes

HMP was dissolved in 10mM phosphate buffers at pH 3.5 and pH 7 and was stirred overnight at 4 °C. The solutions were centrifuged at 20,000 ×g for 30 min to remove un-dissolved materials. The supernatants were filtered through Millipore Millex-HP filters (Hydrophilic PES 0.45 μm) (Millipore Corporation, Billerica, Massachusetts, USA). These solutions were further diluted to desired concentrations using the same buffer.

Ova and Lys were dissolved in 10mM phosphate buffers at pH 3.5 and pH 7 respectively. These solutions were stirred overnight at 4 °C, and then were centrifuged at 20,000 ×g for 30 min to remove un-dissolved materials. The concentrations of these solutions were determined with a UV spectrophotometer. These solutions were further diluted to 0.1% wt using the same buffer.

0.1% wt protein and HMP solutions were mixed at various ratios ranging from proteins:HMP (wt:wt) 1:4 to 12:1. Electron micrographs of the complex coacervates were taken using a Philips CM 12 electron microscope (TEM).

Methods

Turbidity measurement

To determine the stability of the complexes, turbidity measurements were performed using a TurbiScan MA 2000 (Formulaction SA, L'Union, France). The stability of protein – HMP complex solution was evaluated by measuring the transmission and backscattering intensity percentages of incident light (wavelength of 860 nm). The obtained profile gives a qualitative indication of the distribution of the aggregates along the height of the tube.

Light scattering measurements

The size distributions and ξ-potentials of the protein:HMP complexes were determined using a Zetasizer Nano (Malvern Instruments, Ltd. Worcestershire, UK). On each sample, three size distribution and five ξ-potential measurements were performed.

Automated drop tensiometer

The interfacial tension (γ) and dilatational elastic modulus (E_d) of the oil – water interface were measured using an automated drop tensiometer (Tracker™, Teclis-IT Concept, Longessaigne, France). Two different types of oils were used for the oil – water interface: n-hexadecane and MCT. Details of the experiments are summerized in **Table 3.1**.

Surface shear rheometer

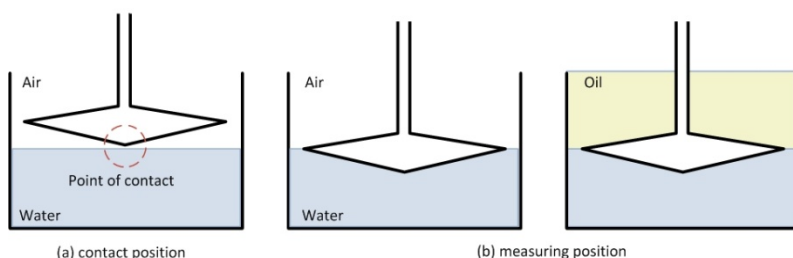Interfacial shear rheology measurements were performed using a Physica MCR 501 rheometer (Anton Paar) and a bicone geometry (Bi-C 68 2 × 50, part no. 14340, serial no. 3903, diameter 68.29 mm, angle 9.981°). The oil phase was MCT oil. The bicone was first positioned at the water – air interface. When the bicone was at the right position, MCT was carefully poured in along the shaft (**Figure 3.1**).

Table 3.1. Experiment setup for the dilatational rheology measurements with an ADT

Interface	*n-hexadecane – water*	*MCT – water*	
Drop status	Rising	Rising	
Volume of drop (µL)	8	20	
Type of test	Time sweep	Amplitude	Frequency
• Aging time (h)	**7 and 15**	15	15
• Amplitude (% v/v)	6	**2.5 to 17.5**	5 and 10
• Frequency (Hz)	0.1	0.05	**0.01 to 0.1**
Bulk concentration (% wt)	0.05	0.01	

Recording of data started about 1 min after the MCT – water interface was formed. A time sweep was performed with an oscillation amplitude of 0.5% at a frequency of 1 Hz. From strain sweep tests it was known that this amplitude is within the linear viscoelastic regime where the storage and loss modulus (G' and G") are independent of the strain amplitude. After 24h of aging, the interface was subjected to a strain sweep with strains ranging from 0.1% to 100%, at the same frequency.

Figure 3.1. Positioning of the geometry in the interfacial shear rheology measurements

RESULTS AND DISCUSSIONS

Complex formation

It is well known that the mixing ratios between protein and polysaccharide have a major effect on the characteristics of the complexes formed, including their size.[52,53] When the mixture composition contains a high proportion of proteins, very large

complexes containing an excess amount of protein will form.[53] For Ova and Lys at the specific conditions used, ratios of protein:HMP of 12:1 and 8:1 (wt:wt) resulted in co-precipitate complexes leading to phase separation: a dense phase rich in protein and HMP and a dilute phase rich in solvent (results not shown).

Size and ζ-potential distribution

The size and ζ-potential distribution of protein – HMP complexes are summarized in **Table 3.2**. Protein:HMP ratios of 4:1 and 2:1 appear to be most suitable for formation of stable complexes, for both OvaHMP at pH 3.5 and LysHMP at pH 7 mixtures. On the basis of these results, we chose to use a ratio of Ova:HMP equal to 2:1 for the complexes for further investigation, because of the smaller size these have compared to the 4:1 complexes. For LysHMP, at both ratios 4:1 and 2:1, complexes were formed with suitable sizes and net charges. The ratio Lys:HMP equal to 4:1 had, however, a narrower size distribution curve (data not shown). It was therefore chosen for further investigation. Factors determining the characteristics of the complexes include extrinsic factors such as mixing ratio, pH, and ionic strength, and intrinsic factors related to the molecules, such as the molecular weight, net charge and flexibility of the chains.[53] Therefore, even though both Ova and Lys are small ellipsoidal molecules with similar dimensions, of approximately 5 × 5 × 7 nm (Ova)[46,49] and 3 × 3 × 4.5 nm (Lys),[54,55] at the same mixing ratios, OvaHMP complexes are larger than LysHMP complexes (see **Table 3.2**).

Table 3.2. Average size (nm) and ζ-potential (mV) of protein – HMP complexes at various wt/wt ratios

| Ratio	OvaHMP at pH 3.5			LysHMP at pH 7		
	Z – average (nm)	ξ-potential (mV)	Distribution	Z – average (nm)	ξ-potential (mV)	Distribution
4:1	622	– 9.1	One narrow peak	184	– 18.7	One narrow peak
2:1	352	– 10.5	One narrow peak	180	– 19.3	One narrow peak
1:1	269	– 11.6	Polydispersed	175	– 21.9	Polydispersed
1:2	279	– 13.2	Polydispersed	208	– 23.5	Polydispersed
1:4	388	– 14.4	Polydispersed	301	– 23.2	Polydispersed

TEM micrographs (**Figure 3.2**) showed that the protein – HMP complexes were roughly spherical, and diameters obtained from the TEM images are in agreement with values measured by light scattering techniques.

OvaHMP 2:1 pH 3.5   LysHMP 4:1 pH 7
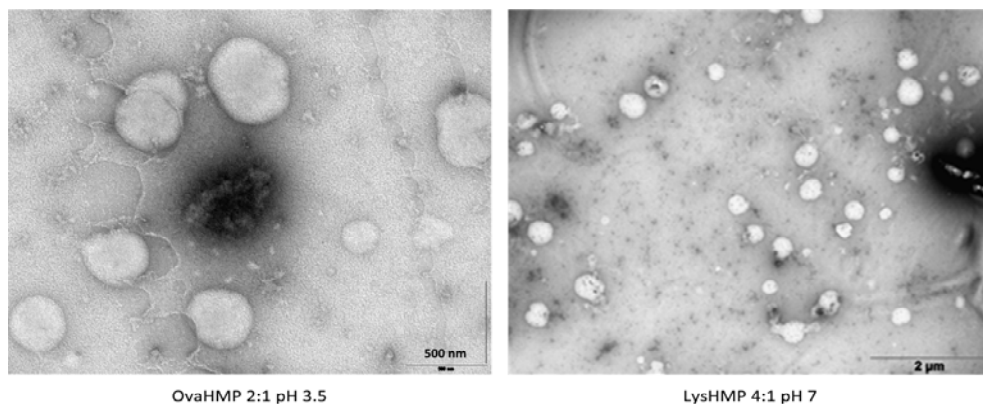
Figure 3.2. TEM micrographs of OvaHMP 2:1 complexes (left figure) and Lys:HMP 4:1 complexes (right figure). Scale bar represents 500 nm (left) or 2 µm (right).

*Growth and Stability*

The growth of the size of the OvaHMP 2:1 and LysHMP 4:1 complexes in time was measured using a Zetasizer Nano, and the results for these measurements are shown in **Figure 3.3.** We see that after a few hours the size of the complexes no longer increases, and the complexes appear to be stable in time.
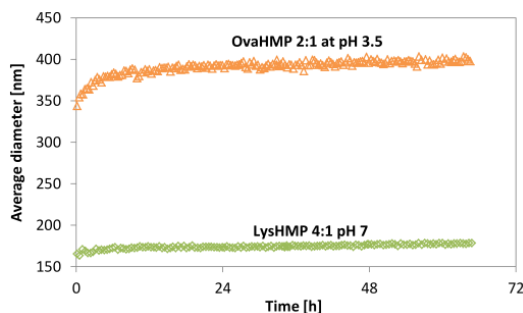
Figure 3.3. Growth of protein:HMP complex coacervates (diameter vs. time)

Stability of the complexes was also investigated using turbidity measurements (**Figure 3.4**). During the 20h of measuring, the transmission profiles of LysHMP 4:1 complexes at pH 7 do not change, indicating that these complexes are stable. For OvaHMP 2:1 complexes at pH 3.5, there is a significant change between the scan at t=0 and the scan at t=1h, showing that the complexes were still changing in size and composition during that time. After 1h, the differences in data were small, indicating that no significant changes in the particle sizes; and no particle migration has taken place. These results correspond to those of the light scattering experiments (**Figure 3.3**): stable LysHMP 4:1 complexes were formed instantly after mixing while OvaHMP 2:1 complexes required some time to reach their equilibrium size. Light scattering measurements also showed that these complexes were stable for at least 4 weeks (data not shown).
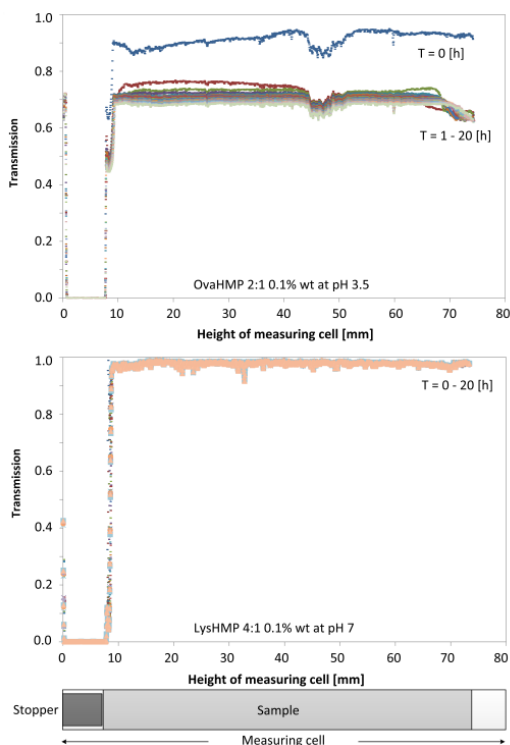
Figure 3.4. Transmission *vs.* sample height as a function of time of OvaHMP 2:1 complexes, at a concentration of 0.1% wt, and a pH of 3.5 (above figure), and LysHMP 4:1 complexes, 0.1% wt, at pH 7 (below figure).

Dilatational rheology of n-hexadecane – water interfaces

In the dilatational rheology experiments, the interfacial tensions of the interfaces stabilized by proteins, their complexes with HMP and their fibrillar aggregates as a function of time were measured. When these values reached equilibrium, dilatational oscillation was performed and the dilatational elastic moduli were determined. The interfacial dilatational rheology results of the n-hexadecane – water interface are plotted in **Figure 3.5** and **Figure 3.6** while those of the MCT – water interface are plotted in **Figure 3.7** to **Figure 3.11**.

The surface dilatational modulus $E_d = d\gamma/d\ln A$ (where γ is the surface tension and A is the surface area) is dependent on the amount of protein adsorbed on the oil – water interface, and this in turn depends on (besides other factors, such as pH, ionic strength, temperature) the bulk concentration.[14,29,47,56–58] The typical reported bulk concentration for monolayer adsorption of proteins at an oil – water interface is about 10^{-4}% wt, which results in monolayers with a film thickness of about 5nm and surface excess concentration of about 2 – 3 mg/m^2.[59] At the concentrations of materials used in our experiments (0.05 and 0.01% wt for n-hexadecane – water and MCT – water interface, respectively), we are far above the monolayer concentrations and multilayer films may have formed at the interface.

Interfacial tension (γ) and dilatational elastic modulus (E_d)

In the measurements on n-hexadecane – water interfaces, two aging times were applied: 7h and 15h. The results did not show a significant difference between these two, meaning that after 7h, equilibrium is more or less reached.

For Ova the surface tension of the n-hexadecane – water interface stabilized by OvaHMP complexes was comparable to that of interfaces stabilized by pure Ova, but the complexes formed viscoelastic interfacial films with a significantly higher dilatational modulus (**Figure 3.5**). The same observation was reported by Schmitt *et al.* when the authors compared pure β-lactoglobulin and its complexes with acacia gum at the air – water interface.[25,60]

For Lys the difference in surface tension and dilatational modulus of n-hexadecan – water interfaces stabilized by Lys or LysHMP complexes at pH 7 is not significant (**Figure 3.6**). That could be due to the more compact structure of LysHMP complexes in comparison with OvaHMP complexes: at the same bulk concentration (0.01% wt), OvaHMP complexes have a radius twice as large as LysHMP complexes. The latter also has higher protein content in the complexes, and relatively less HMP, and this may result in comparable interfacial activity between Lys and LysHMP 4:1.
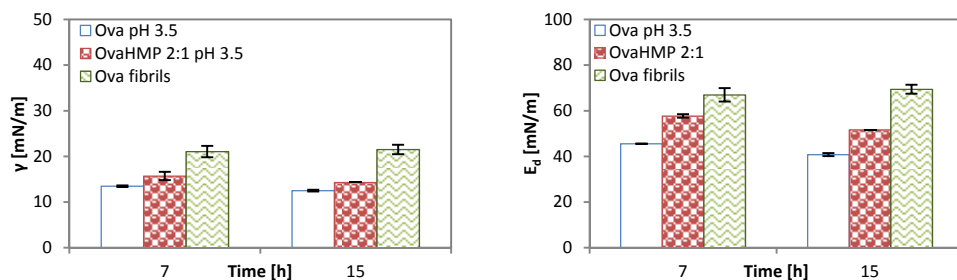
Figure 3.5. Values of the interfacial tension (γ) (left figure) and elastic modulus (E_d) (right figure) of the n-hexadecane – water interface stabilized by Ova, OvaHMP complexes and Ova fibrils at two different aging times: 7h and 15h. Oscillations were performed at conditions: bulk concentration 0.01% wt, drop volume 8 µL, strain 6% v/v and frequency 0.1 Hz
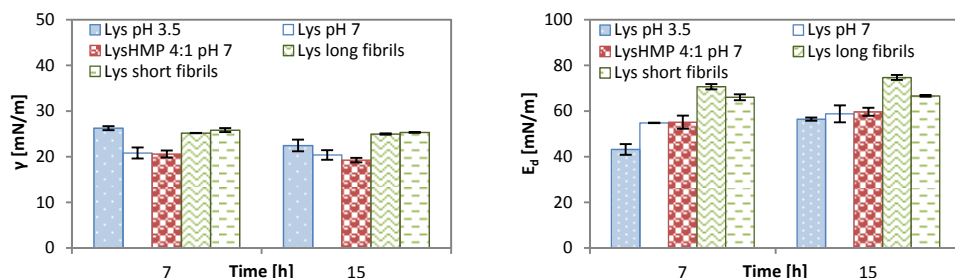
Figure 3.6. Values of the interfacial tension (γ) (left figure) and elastic modulus (E_d) (right figure) of the n-hexadecane – water interface stabilized by Lys, LysHMP, and Lys fibrils at two different aging times: 7h and 15h. Oscillations were performed at conditions: bulk concentration 0.01% wt, drop volume 8 µL, strain 6% v/v and frequency 0.1 Hz

At an aging time of 7h, a significant difference in surface properties of n-hexadecane – water interfaces stabilized by native Lys monomer is observed between interfaces formed at pH 3.5 or 7. At the same bulk concentration, interfaces stabilized by native Lys at pH 7 show a lower surface tension and higher dilatational modulus than interfaces stabilized by native Lys at pH 3.5 (**Figure 3.6**), most likely due to the difference in the molecular net charge. The isoelectric point of Lys is above 10, therefore, at both pH 3.5 and 7, Lys is positively charged, and Lys at pH 3.5 is more positively charged than Lys at pH 7. The higher the molecular net charge, the higher the electrostatic repulsion between the protein molecules is. Near the pI, proteins are therefore thought to be more surface active and form denser films at the interface.[30,47,61] At an aging time of 15 hours, the difference in surface tension and surface dilatational modulus between oil – water interfaces stabilized by native Lys at pH 3.5 or 7 is no longer significant (**Figure 3.6**). So it appears that the increased

surface charge of the proteins at pH 3.5 merely decreases the rate of the adsorption process, but has only a minor effect on the equilibrium surface properties.

From the interfacial tension results for Lys fibrils, there is no significant difference between short and long fibrils. In a study of Jung *et al.*, the authors have observed the same behavior for β-lactoglobulin fibrils where the adsorption kinetics of these fibrils at an oil – water interface seemed to be independent from length and flexibility.[42]

For both Ova and Lys, the surface tension of n-hexadecane – water interfaces stabilized by fibrils was higher than that of interfaces stabilized by native proteins or their complexes with HMP, but the fibrils formed interfaces with significantly higher dilatational moduli (**Figure 3.5** and **Figure 3.6**). To understand these differences, detailed knowledge on the interfacial structure of the fibril stabilized interfaces is needed. Currently this information is not yet available, so it is unknown whether the fibrils form entangled networks at the interface, or, perhaps, liquid crystalline phases.

Concerning the pure protein solutions, results show that Ova monomer can lower the interfacial tension of the n-hexadecane – water interface more than Lys monomer (**Figure 3.5** and **Figure 3.6**). Le Floch-Fouere *et al.* observed the same behavior in the adsorption of these two proteins at the air – water interface.[33]

In summary, at n-hexadecane – water interfaces, Ova and Lys complexes with HMP give comparable surface tensions as protein monomer. Fibrils of these proteins do not increase the surface pressure as much as the native protein and complexes but they do form viscoelastic films at the interface with significantly higher dilatational moduli.

Dilatational rheology of MCT – water interfaces

Interfacial tension (γ)

For the MCT – water interface, native Ova and Lys lower the surface tension more than complexes and fibrils do (**Figure 3.7**) (just like we observed for the n-hexadecane – water interfaces). The initial bulk concentration was 0.01% wt. After 15h of aging, an oscillatory deformation was applied to determine the dilatational modulus (strain amplitude 5 and 10% v/v). In this experiment, bilayer adsorption of Lys and HMP was also performed and compared to mixed layers formed by LysHMP complexes. Bilayers were formed by first replacing 50% of the volume of the continuous phase in the cuvette of the ADT (Lys solution 0.01% wt at pH 7) with buffer and repeating this step 10 times, until the Lys bulk phase concentration is diluted by a factor of about 1,000. After that, 50% volume of the final solution was replaced by HMP solution at pH 7, and the HMP was subsequently allowed to adsorbed onto the already present Lys layer for 2h before applying oscillation. **Figure 3.7** shows that after the washing steps, the interfacial tension of the pendant drops

slightly increased due to desorption of Lys from the interface. This observation was earlier reported in a study of Erni *et al.*[17] In their pendant drop measurements with various proteins (including Lys), minor desorption and small changes in interfacial tension of the protein-stabilized interface are seen when washing steps with buffer solution were applied.[17] The adsorption of HMP after the washing step did not affect the interfacial tension (**Figure 3.7**).
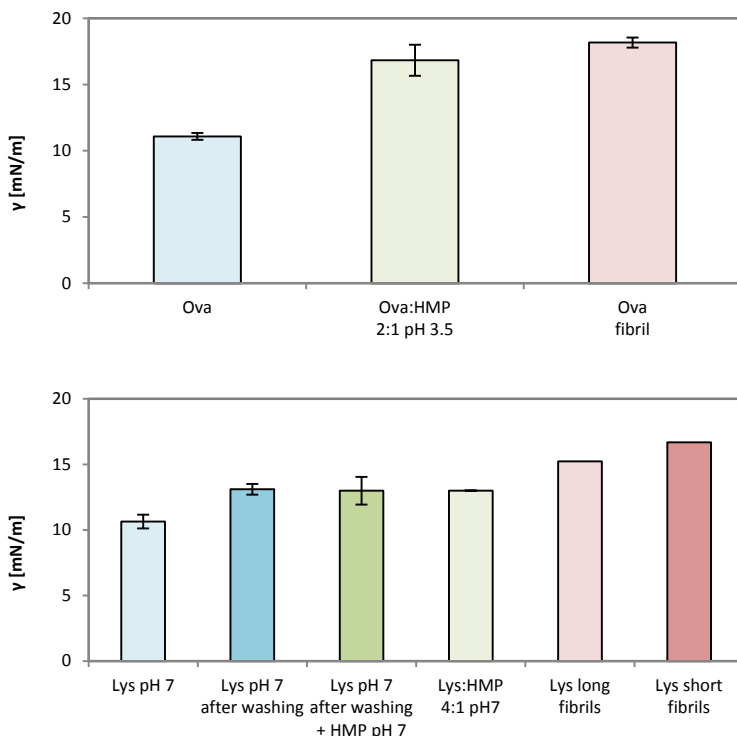
Figure 3.7. Values of the interfacial tension (γ) of the MCT – water interface stabilized by Ova (above figure) and Lys (below figure). Conditions of measurements: bulk concentration 0.01% wt, drop volume 20 µL and aging time 15h.

Dilatational elastic modulus (E_d)

Frequency sweeps

In order to study the specific relaxation mechanisms including exchange with the surface or surface structural changes, the rheological response at various frequencies must be measured.[18] In the range of frequencies applied from 0.01 to 0.1 Hz, there is no significant change in the dilatational modulus of the MCT – water interface when

frequency increases, for interfaces stabilized by either native proteins, or protein HMP complexes, or protein fibrils (**Figure 3.8** and **Figure 3.9**). Freer *et al.*[18] observed the same behavior at the same range of frequency for Lys monomer at pH 7 at n-hexadecane – water interfaces.
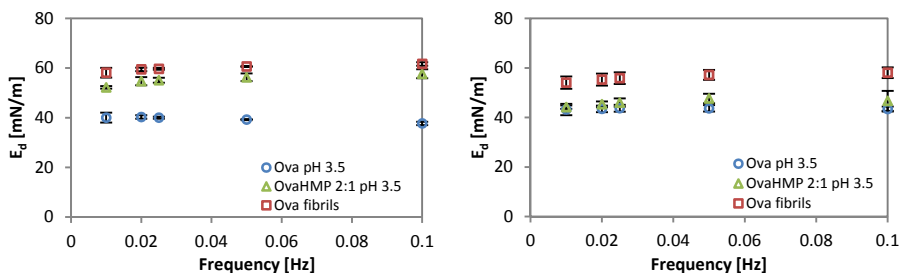
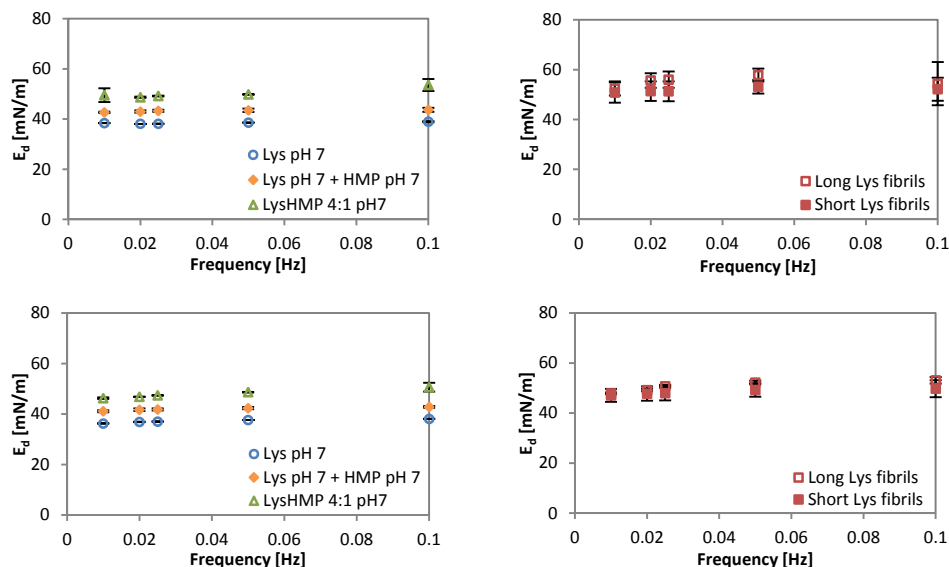**Figure 3.8.** Dilatation rheology: dilatational modulus (E_d) of the MCT – water interface stabilized by Ova vs. frequency at two amplitudes: 5% v/v (left figure) and 10% v/v (right figure). The interface was aged for 15h in a 10 mM phosphate buffer with a bulk concentration of 0.01% wt and initial drop volume of 20 μL. Open circle (○): Ova; open triangle (△): Ova:HMP 2:1 pH 3.5; open square (□): Ova fibrils

Figure 3.8 shows that Ova fibrils formed interfaces with the highest dilatational modulus and Ova monomer formed the interfaces with the lowest modulus at the MCT – water interface, similar to what was observed in the experiments with the n-hexadecane – water interface described above.

Figure 3.9 shows that the dilatational modulus of MCT – water interfaces stabilized by a mixed layer film of LysHMP 4:1 pH 7 complexes is higher than that of an interface stabilized by a bilayer film of native Lys (first layer) and HMP (second layer). In the case of the mixed layer adsorbed film, the presence of polysaccharide during interface formation results in a thicker and more highly charged layer.[19,22]

Also from **Figure 3.9**, the difference in dilatational modulus between MCT – water interfaces stabilized by long and short Lys fibrils is not significant, just as for the n-hexadecane – water interfaces (**Figure 3.6**). The difference in surface properties between n-hexadecane – water interfaces stabilized by native Ova or native Lys is not observed for MCT – water interfaces. Nevertheless, at both interfaces, complexes of protein and HMP formed interfaces with higher dilatational moduli than the native proteins, confirming the advantageous combination of these two common biopolymers. The difference between the interfacial tensions and elastic moduli of the MCT – water interface stabilized by OvaHMP 2:1 pH 3.5 and that stabilized by LysHMP 4:1 pH 7 was also small, even though OvaHMP complexes are twice as large in radius as LysHMP complexes.

Figure 3.9. Dilatation rheology: dilatational modulus (E_d) of the MCT – water interface stabilized by Lys vs. frequency at two amplitudes: 5% v/v (above figure) and 10% v/v (below figure). The interface was aged for 15h in a 10 mM phosphate buffer with a bulk concentration of 0.01% wt and initial drop volume of 20 μL. Open circle (○): Lys pH 7; filled triangle (▲): Lys pH 7 + HMP pH 7; open triangle (△): LysHMP 4:1 pH 7; open square (□): long Lys fibrils; filled square (■): short Lys fibrils

For both Ova and Lys, the elastic moduli decreased when the amplitude of oscillation increased from 5% v/v to 10% v/v (**Figure 3.8** and **Figure 3.9**). This is an important observation, since it may indicate that the results of the dilatational rheology were obtained in the nonlinear response regime. To check this, amplitude sweeps were performed, at a fixed frequency of 0.05 Hz.

Amplitude sweeps

To check if the results of the frequency sweep experiments were in the linear response regime, we applied amplitude sweeps to our interfaces. Contrary to bulk shear rheology, where amplitude sweeps are seen as a standard and necessary test to check the validity of obtained results, in dilatational rheology these sweeps are rarely applied.[1]. The amplitude sweep started from the lower limit of the apparatus (which is 0.5 μL for a syringe volume of 500 μL) up to 20% v/v deformation. The results (**Figure 3.10** and **Figure 3.11**) show that in the range of the amplitude sweep, the elastic moduli E_d of protein:HMP complexes and fibrils are not in the linear regime, even at the lowest strains which can be applied with the ADT. Besides, the decrease in modulus with increasing strain is most significant for MCT – water interfaces stabilized by fibrils, and almost negligible for interfaces stabilized by native proteins.

This could be due to slower diffusion of fibrils from the bulk to the interface and/or the slower rearrangement of the fibrils at the interface when the area is increased or decreased. It can be seen that at MCT – water interfaces, the difference between two different types of Lys fibrils (long and semi-flexible, and short and rod-like) is again not significant (**Figure 3.11**). We also observe that mixed adsorbed layers formed by LysHMP complexes have a higher dilatational modulus than bilayers formed by Lys and HMP over the entire range of strains tested (**Figure 3.11**).
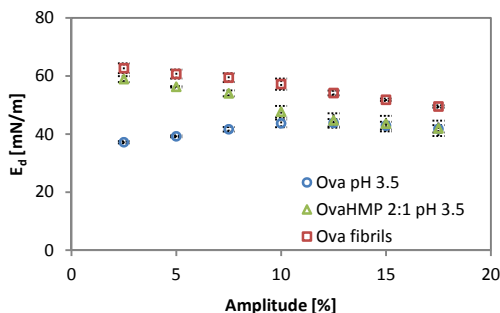
Figure 3.10. Dilatational modulus (E_d) of the MCT – water interface stabilized by Ova vs. amplitude at 0.05 Hz. The interface was aged for 15h in a 10 mM phosphate buffer with a bulk concentration of 0.01% wt and an initial drop volume of 20 µL.
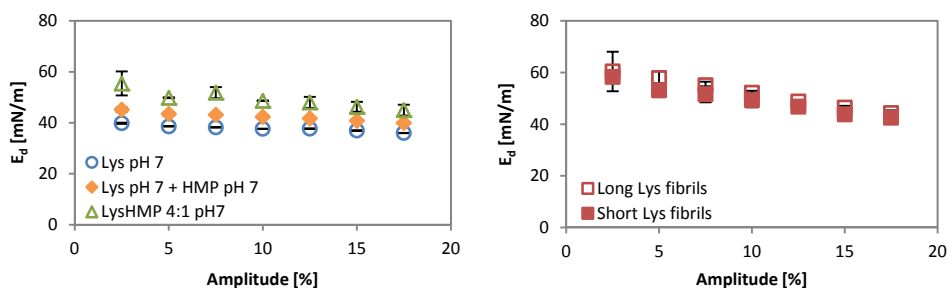
Figure 3.11. Dilatation modulus (E_d) of the MCT – water interface stabilized by Lys vs. amplitude at 0.05 Hz. Left figure: Lys, bilayer Lys and HMP, and mixed-layer LysHMP 4:1.0. Right figure: long Lys fibrils and short Lys fibrils. The interface was aged for 15h in a 10mM phosphate buffer with a bulk concentration of 0.01% wt and an initial drop volume of 20 µL.

The results from the dilatational rheology experiments have shown that fibrils from Ova and Lys do not produce oil – water interfaces with interfacial pressures as high as those produced by the native proteins or complexes of these proteins with HMP. But they form viscoelastic films at the interface with significantly higher dilatational moduli (**Figure 3.10** and **Figure 3.11**). Between the two methods of stabilizing the oil

– water interface with a combination of these proteins and a polysaccharide, the method of forming a mixed layer using protein HMP complexes resulted in interfaces with a higher dilatational modulus than the method of forming bilayers (**Figure 3.11**).

Interfacial shear rheology

As mentioned in the introduction, interfacial shear is sensitive to the composition and interactions between the adsorbed surface-active species. In general, the factors that tend to strengthen the interactions between adjacent molecules or larger structural elements in the adsorbed film will also tend to lead to an increase in the interfacial shear elasticity and interfacial shear viscosity.[7]

In this series of measurements, bulk concentration from 0.001 to 0.1% wt were used. Note that at concentrations lower than 0.01% wt, the size and net charge of protein:HMP complexes slightly decreases. In all measurements, the surface storage moduli G' were much higher than the surface loss moduli G", showing that all components formed highly elastic layers at the MCT – water interface. For this reason we report the magnitude of the complex surface shear modulus G*, rather than reporting both parameters. The low value of the surface loss tangent makes accurate determination of the surface loss modulus very difficult.

Interfacial complex shear modulus
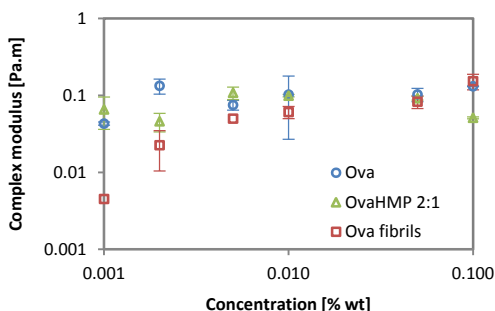
Figure 3.12. Complex surface shear modulus of MCT – water interfaces stabilized by Ova, OvaHMP 2:1 complexes and Ova fibrils vs. concentration, determined at a strain of 0.5% and a frequency of 1 Hz

The complex moduli of protein-stabilized MCT – water interfaces after 24h of aging were plotted as a function of bulk concentration in **Figure 3.12** and **Figure 3.13**. **Figure 3.12** shows that the complex moduli of the adsorbed layer of native Ova and OvaHMP complexes are more or less independent of the bulk concentration in the range tested here, while the moduli of layers formed by Ova fibrils are still increasing

when the bulk concentration increases. These results indicate that in this range of bulk concentrations, for interfaces stabilized by native Ova and OvaHMP complexes, the interface is already saturated and densely packed while, in the case of Ova fibrils, more material still adsorbs to the interface upon increasing the bulk concentration.

For bulk concentrations upwards of 0.005% wt MCT – water interfaces stabilized by native Ova, OvaHMP complexes and semi-flexible Ova fibrils have complex surface shear moduli which are roughly equal, and are of order of 10^{-1} Pa m.

This is, however, not seen in interfaces stabilized by various forms of Lys (**Figure 3.13**). At lower bulk concentrations, LysHMP complexes form films with a significantly higher complex surface shear modulus than native Lys at the same concentration. The clear difference in surface shear rheology between native Lys and its complexes with HMP at low concentrations may be the result of how these materials adsorb at the interface. Lys was found to adsorb strongly at oil – water interfaces but maintains its compact structure,[46,47] because although it unfolds, disulfide bonds limit its conformational flexibility. This may lead to surface layers with limited connectivity between the proteins. Complexes, on the other hand, at the same concentration, may form thicker layers with more connectivity or entanglement, leading to a higher value of the complex shear modulus. For both native Lys and complex, complex moduli become independent of bulk concentration at a concentration of about 0.01% wt and these moduli also reach values of the order of 10^{-1} Pa m (**Figure 3.13**).
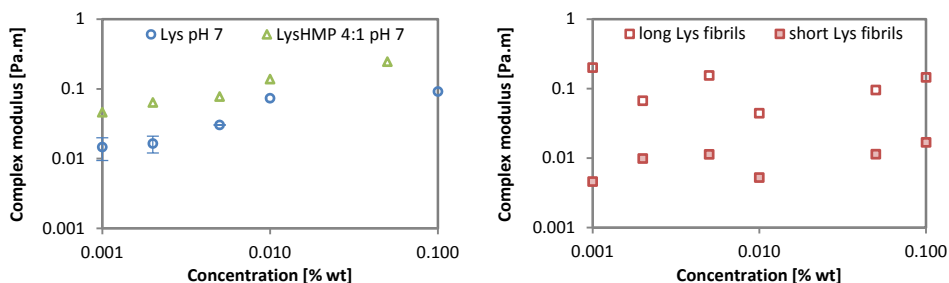
Figure 3.13. Complex surface shear modulus of the MCT – water interface stabilized by Ova, OvaHMP 2:1 complexes (left figure) and Lys fibrils (right figure) vs. concentration, determined at a strain of 0.5% and a frequency of 1 Hz

Results from dilatation and surface shear rheology show that at bulk concentration above 0.01% wt, native Ova and Lys formed adsorbed layers at the MCT – water interface with similar dilatational and shear properties (**Figure 3.7** to **Figure 3.9**,

Figure 3.12 and **Figure 3.13**). Apparently the structure of the adsorbed films of the native proteins is very similar at these bulk concentrations.

The addition of HMP to the protein solutions results in complexes with different sizes and charges. However, when these complexes are adsorbed onto the MCT – water interface, they form layers with similar surface shear and dilatational properties, again indicating a similar structural rearrangement of these complexes at the interface (**Figure 3.7** to **Figure 3.9**, **Figure 3.12** and **Figure 3.13**).

At low bulk concentration, the complex surface shear modulus of interfaces stabilized by native Lys is comparable to that of interfaces stabilized by short rigid fibrils. At higher bulk concentrations, the complex surface shear modulus of native Lys stabilized interfaces is comparable to that of interfaces stabilized by long semi-flexible fibrils.

Concerning the Lys fibrils, the complex moduli obtained from Lys fibril-stabilized interfaces are of the order of 10^{-1} Pa m for long fibrils and 10^{-2} Pa m for short fibrils. So, films formed by long Lys fibrils have a complex modulus 10 times higher than films formed by short Lys fibrils. For β-lactoglobulin fibrils, the same phenomenon was reported: long fibrils formed interfaces with a higher interfacial shear modulus than short ones.[42] Moreover, in a study of Isa *et al.* on the alignment of β-lactoglobulin fibrils as a function of fibril length and bulk concentration, the authors have found that by increasing the bulk concentration of long and semi-flexible fibrils (1 – 10 µm) from 0.001 to 0.1 % wt they could observe an alignment transition within their observation time (less than 1h).[43] For these long fibrils, at a bulk concentration of 0.01 % wt, nematic islands were formed upon interface creation, and anisotropy grew with time. At 0.1% wt, interfacial diffusion became sub-diffusive as a result of the long-range nematic order. For shorter β-lactoglobulin fibrils (50 – 300 nm), Isa *et al.* observed that increasing bulk concentration and adsorption time resulted only in a transition from a dilute isotropic interfacial layer to a strongly viscoelastic layer.[43] These observations on long and short β-lactoglobulin fibrils, which are of similar length as the Lys fibrils in this study, may also explain the difference in complex shear moduli obtained for long and short Lys fibrils. For short and rigid fibrils, the system may already be fixed in a disordered, isotropic network of fibrils,[43] before the interfacial concentration necessary for an isotropic – nematic transition to happen is reached. For long and semi-flexible fibrils, this transition happens at lower concentrations, and their larger aspect ratio and flexibility allow them to rearrange into nematic domains at the interface upon adsorption, before a rigid viscoelastic interface builds up.[43,61]

At a bulk concentration below 0.01% wt the complex moduli obtained from Ova fibril-stabilized interfaces are of the same order of magnitude as those of short Lys fibrils (**Figure 3.12** and **Figure 3.13**). At bulk concentration above 0.01% wt the complex

moduli obtained from Ova fibril-stabilized interfaces are of the same order of magnitude as those of long Lys fibrils (**Figure 3.12** and **Figure 3.13**). Apparently, at lower bulk concentration, the short Ova fibrils form an open isotropic structure at the interface similar to that of short Lys fibrils. The fact that increasing the Ova fibril bulk concentration leads to an increase of the complex surface shear moduli to values similar to those of interfaces stabilized by long Lys fibrils, suggests that also for the Ova fibrils an alignment transition occurs. **Figure 3.14** summarizes our hypotheses, for the structure of fibrils at the liquid – liquid interface as a function of the fibril morphology and the bulk concentration.
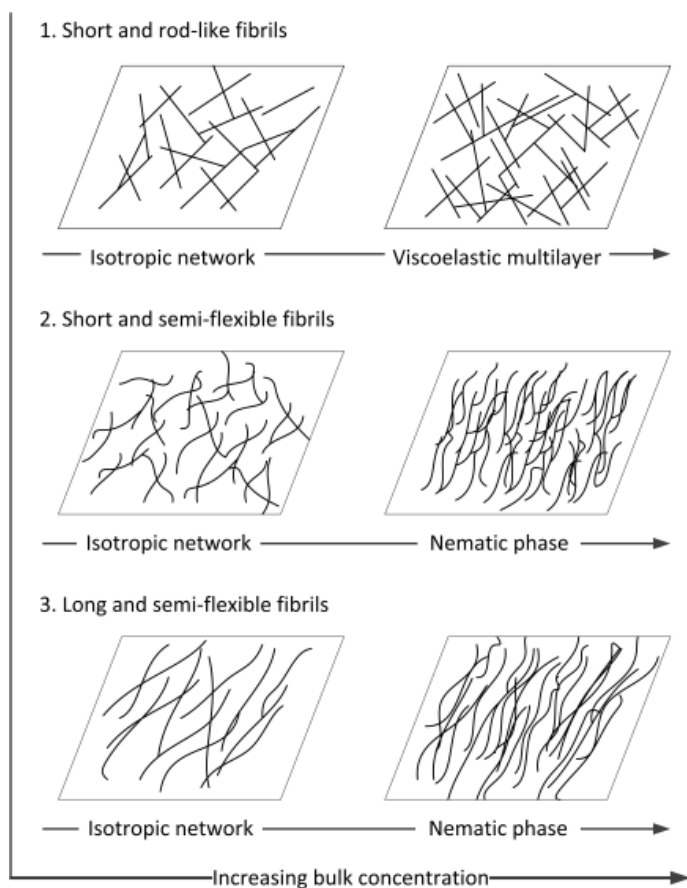

Figure 3.14. Model for fibril alignment at a liquid – liquid interface vs. bulk concentration

Our results show that for a detailed analysis of the surface rheology of interfaces stabilized by complex mesostructures, information on the microstructure of the

interface and its evolution upon deformation is very important. This information is however difficult to obtain. The field of surface rheology could benifit substantially from the development of surface rheo-optical methods which allow for simultaneous probing of the stress deformation behavior and interfacial structure.[62]

Strain sweep

Strain sweep experiments were performed on 24h aged interfaces. The calculated complex moduli are plotted against the strain in **Figure 3.15** and **Figure 3.16**. For all samples, decay in moduli occurs only after 1% of strain. The difference of moduli at various bulk concentrations is only obvious at low strains. At 100% strain, the complex moduli of all samples were of the same order and independent of the bulk concentration. The results also show that the interfaces stabilized by the more flexible Ova fibrils and long Lys fibrils yield at lower strains than those stabilized by the native proteins, complexes and short rod-like Lys fibrils. It means that at the interface, the interaction between the more flexible fibrils is weaker than the interactions between the monomers, the complexes or even the rod-like fibrils.
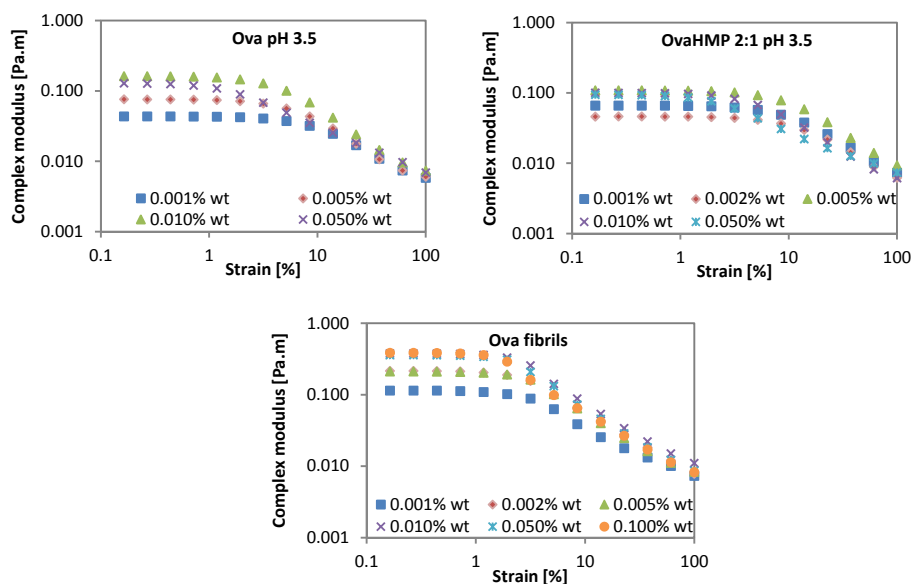
Figure 3.15. Complex surface shear modulus of the MCT – water interface stabilized by Ova vs. strain at 1 Hz. Left above figure: Ova; right above figure: OvaHMP 2:1; below figure: Ova fibrils
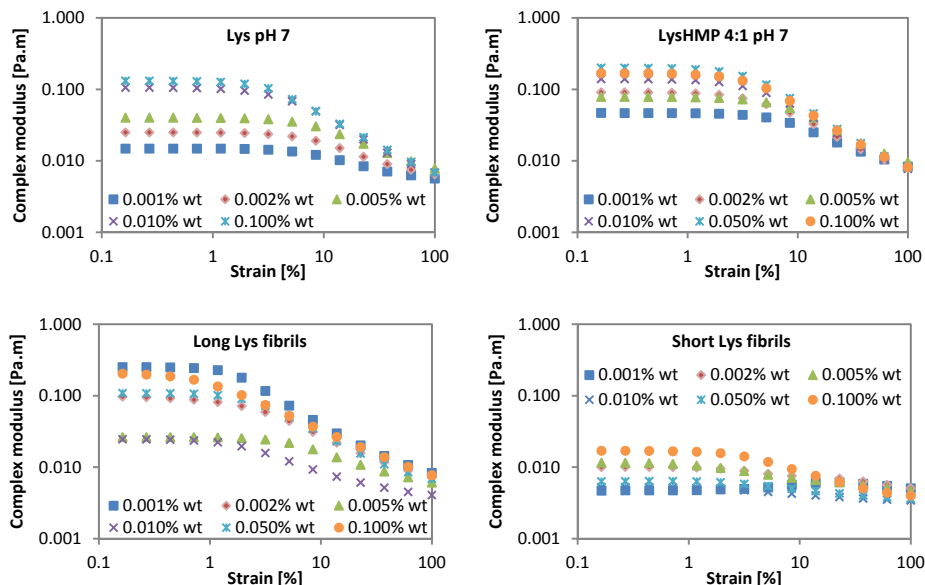
Figure 3.16. Complex surface shear modulus of the MCT – water interface stabilized by Lys vs. strain at 1 Hz. Left above figure: Lys; right above figure: LysHMP 4:1; left below figure: long Lys fibrils; right below figure: short Lys fibrils

CONCLUSIONS

We have studied the rheological properties oil – water interfaces stabilized by different structural elements: small and compact spherical structures (Lys or Ova protein), larger spherical and softer structures (their complexes with HMP), and short or long thin structures (fibrils) that can be either flexible or stiff. At both interfaces (n-hexadecane – water and MCT – water) and for both proteins, fibrils formed the films with the highest dilatational elastic modulus while native proteins had the lowest elastic modulus. Native proteins are the components most efficient in lowering the surface tension.

At the n-hexadecane – water interface, the effect of pH (3.5 and 7) on the surface charge of Lys merely decreases the rate of the adsorption process, but has only a minor effect on the equilibrium surface properties.

At the MCT – water interfaces, the difference between the mixed LysHMP adsorbed layer and the Lys – HMP bilayer can be distinguished: mixed layers are more resistant against compression and expansion than bilayers.

The dilation strain sweep test has shown that increasing the amplitude has only small effects on the interfaces stabilized by smaller structures (in our case, native proteins)

but has significant influence on the interfaces stabilized by meso structures (such as complexes and fibrils). Most measurements performed with the ADT appeared to be in the non-linear response regime, even at the smallest amplitude which could be applied.

The difference between interfaces stabilized by short and long Lys fibrils was only observed in shear rheology and not in dilatational measurements. Films formed by long fibrils have a complex modulus 10 times higher than films formed by short fibrils. At higher bulk concentration, the complex shear modulus of interface stabilized by short and semi-flexible Ova fibrils is of the same order of magnitude as that of interface stabilized by long and semi-flexible Lys fibrils.

When comparing the two proteins, results showed that the native proteins Ova and Lys formed adsorbed layers at the MCT – water interface with similar dilatational and shear properties. The addition of HMP to the protein solutions results in complexes with different sizes and charges. However, when these complexes are adsorbed onto the MCT – water interface, they form layers with similar dilatational and complex shear moduli. In both cases, the addition of HMP to the oil – water interfaces increases the dilatational and complex shear moduli of the interface.

In conclusion, this study has shown that the use of supra-molecular structural building blocks creates a wider range of microstructural features of the interface, having increased surface shear and dilatational moduli and a more complex dependence on strain (rate).

ACKNOWLEDGEMENT

REFERENCES

1   Sagis, L. M. C. Dynamic Properties of Interfaces In Soft Matter: Experiments and Theory. *Rev Mod Phys* **83**, 1367 – 1403 (2011).

2   Sagis, L. M. C. Dynamics of Controlled Release Systems Based On Water – In – Water Emulsions: A General Theory. J *Control Release* **131**, 5 – 13 (2008).

3   Scholten, E., Sagis, L. M. C. & van der Linden, E. Bending Rigidity of Interfaces In Aqueous Phase – Separated Biopolymer Mixtures. *J Phys Chem B* **108**, 12164 – 12169 (2004).

4   Scholten, E., Sagis, L. M. C. & van der Linden, E. Coarsening Rates of Bicontinuous Structures In Polymer Mixtures. *Macromolecules* **38**, 3515 – 3518 (2005).

5   Scholten, E., Sprakel, J., Sagis, L. M. C. & van der Linden, E. Effect of Interfacial Permeability On Droplet Relaxation In Biopolymer – Based Water – In – Water Emulsions. *Biomacromolecules* **7**, 339 – 346 (2006).

6   Scholten, E., Sagis, L. M. C. & van der Linden, E. Effect of Bending Rigidity and Interfacial Permeability On The Dynamical Behavior of Water – In – Water Emulsions. *J Phys Chem B* **110**, 3250 – 3256 (2006).

7   Murray, B. S. Interfacial Rheology of Food Emulsifiers and Proteins. *Curr Opin Colloid In* **7**, 426 – 431 (2002).

8   Van Aken, G. A. & Merks, M. T. E. Adsorption of Soluble Proteins To Dilating Surfaces. *Colloid Surface A* **114**, 221 – 226 (1996).

9   McClements, D. J., Stefan, K., Norton, I., T. & Ubbink, J., B. . In Modern Biopolymer Science 129 – 166 (Academic Press, 2009).

10   Dickinson, E. Faraday Research Article. Structure and Composition of Adsorbed Protein Layers and The Relationship To Emulsion Stability. *J Chem Soc Faraday T* **88** (1992).

11   Dickinson, E. In *Food Macromolecules and Colloids* 1 – 19 (The Royal Society of Chemistry, 1995).

12   Cases, E., Rampini, C. & Cayot, P. Interfacial Properties of Acidified Skim Milk. *J Colloid Interf Sci* **282**, 133 – 141 (2005).

13   Alahverdjieva, V. S. *et al.* Adsorption Behaviour of Hen Egg – White Lysozyme At The Air/Water Interface. *Colloid Surface A* **323**, 167 – 174 (2008).

14   Baldursdottir, S. G., Fullerton, M. S., Nielsen, S. H. & Jorgensen, L. Adsorption of Proteins At The Oil/Water Interface—Observation of Protein Adsorption By Interfacial Shear Stress Measurements. *Colloid Surface B* **79**, 41 – 46 (2010).

15   Dickinson, E. & Galazka, V. B. Emulsion Stabilization By Ionic and Covalent Complexes of β-Lactoglobulin With Polysaccharides. *Food Hydrocolloid* **5**, 281 – 296 (1991).

16   Dickinson, E. Interfacial Interactions and The Stability of Oil-In-Water Emulsions. *Pure Appl Chem* **64**, 1721 – 1724 (1992).

17   Erni, P., Windhab, E. J. & Fischer, P. Emulsion Drops With Complex Interfaces: Globular Versus Flexible Proteins. *Macromol Mater Eng* **296**, 249 – 262 (2011).

18   Freer, E. M., Yim, K. S., Fuller, G. G. & Radke, C. J. Shear and Dilatational Relaxation Mechanisms of Globular and Flexible Proteins At The Hexadecane/Water Interface. *Langmuir* **20**, 10159 – 10167 (2004).

19   Dickinson, E. Mixed Biopolymers At Interfaces: Competitive Adsorption and Multilayer Structures. *Food Hydrocolloid* **25**, 1966 – 1983 (2011).

20   Ye, A. Complexation Between Milk Proteins and Polysaccharides Via Electrostatic Interaction: Principles and Applications – A Review. *Int J Food Sci Tech* **43**, 406 – 415 (2008).

21   McClements, D. J. Theoretical Analysis of Factors Affecting The Formation and Stability of Multilayered Colloidal Dispersions. *Langmuir* **21**, 9777 – 9785 (2005).

22   Dickinson, E. Interfacial Structure and Stability of Food Emulsions As Affected By Protein – Polysaccharide Interactions. *Soft Matter* **4** (2008).

23   Dickinson, E. Hydrocolloids As Emulsifiers and Emulsion Stabilizers. *Food Hydrocolloid* **23**, 1473 – 1482 (2009).

24   Dickinson, E. Stability and Rheological Implications of Electrostatic Milk Protein – Polysaccharide Interactions. *Trends Food Sci Tech* **9**, 347 – 354 (1998).

25   Schmitt, C., Kolodziejczyk, E. & Leser, M. E. In *Food Colloids* (Ed Eric Dickinson) 284 – 300 (The Royal Society of Chemistry, 2005).

26   Santipanichwong, R., Suphantharika, M., Weiss, J. & McClements, D. J. Core – Shell Biopolymer Nanoparticles Produced By Electrostatic Deposition of Beet Pectin Onto Heat-Denatured β-Lactoglobulin Aggregates. *J Food Sci* **73**, N23 – N30 (2008).

27   Santipanichwong, R. & Suphantharika, M. Influence of Different β-Glucans On The Physical and Rheological Properties of Egg Yolk Stabilized Oil-In-Water Emulsions. *Food Hydrocolloid* **23**, 1279 – 1287 (2009).

28   Turgeon, S. L., Schmitt, C. & Sanchez, C. Protein – Polysaccharide Complexes and Coacervates. *Curr Opin Colloid In* **12**, 166 – 178 (2007).

29   Jourdain, L., Leser, M. E., Schmitt, C., Michel, M. & Dickinson, E. Stability of Emulsions Containing Sodium Caseinate and Dextran Sulfate: Relationship To Complexation In Solution. *Food Hydrocolloid* **22**, 647 – 659 (2008).

30   Dickinson, E. Milk Protein Interfacial Layers and The Relationship To Emulsion Stability and Rheology. *Colloid Surface B* **20**, 197 – 210 (2001).

31   Martin, A. H., Bos, M. A. & Van Vliet, T. Interfacial Rheological Properties and Conformational Aspects of Soy Glycinin At The Air/Water Interface. *Food Hydrocolloid* **16**, 63 – 71 (2002).

32   Hotrum, N. E., Cohen Stuart, M. A., Van Vliet, T. & Van Aken, G. A. Flow and Fracture Phenomena In Adsorbed Protein Layers At The Air/Water Interface In Connectin To Spreading Oil Droplets. *Langmuir* **19**, 10210 – 10216 (2003).

33   Le Floch-Fouéré, C. *et al.* Synergy Between Ovalbumin and Lysozyme Leads To Non-Additive Interfacial and Foaming Properties of Mixtures. *Food Hydrocolloid* **23**, 352 – 365 (2009).

34   Le Floch-Fouéré, C. *et al.* Sequential Adsorption of Egg-White Proteins At The Air – Water Interface Suggests A Stratified Organization of The Interfacial Film. *Food Hydrocolloid* **24**, 275 – 284 (2010).

35   Malcolm, A. S., Dexter, A. F. & Middelberg, A. P. J. Mechanical Properties of Interfacial Films Formed By Lysozyme Self-Assembly At The Air –Water Interface. *Langmuir* **22**, 8897 – 8905 (2006).

36   Schmidt, I., Cousin, F., Huchon, C., Boué, F. & Axelos, M. A. V. Spatial Structure and Composition of Polysaccharide – Protein Complexes From Small Angle Neutron Scattering. *Biomacromolecules* **10**, 1346 – 1357 (2009).

37   Kudryashova, E. V., Visser, A. J. W. G., Van Hoek, A. & De Jongh, H. H. J. Molecular Details of Ovalbumin – Pectin Complexes At The Air/Water Interface: A Spectroscopic Study. *Langmuir* **23**, 7942 – 7950 (2007).

38   Humblet-Hua, N.-P., Sagis, L. M. C. & van der Linden, E. Effects of Flow On Hen Egg White Lysozyme (HEWL) Fibril Formation: Length Distribution, Flexibility, and Kinetics. *J Agr Food Chem* **56**, 11875 – 11882 (2008).

39   Veerman, C., De Schiffart, G., Sagis, L. M. C. & van der Linden, E. Irreversible Self-Assembly of Ovalbumin Into Fibrils and The Resulting Network Rheology. *Int J Biol Macromol* **33**, 121 – 127 (2003).

40   Arnaudov, L. N. & De Vries, R. Thermally Induced Fibrillar Aggregation of Hen Egg White Lysozyme. *Biophys. J.* **88**, 515 – 526 (2005).

41   Jones, O. G. & Mezzenga, R. Inhibiting, Promoting, and Preserving Stability of Functional Protein Fibrils. *Soft Matter* **8**, 876 – 895 (2012).

42   Jung, J.-M., Gunes, D. Z. & Mezzenga, R. Interfacial Activity and Interfacial Shear Rheology of Native β-Lactoglobulin Monomers and Their Heat-Induced Fibers. *Langmuir* **26**, 15366 – 15375 (2010).

43   Isa, L., Jung, J.-M. & Mezzenga, R. Unravelling Adsorption and Alignment of Amyloid Fibrils At Interfaces By Probe Particle Tracking. *Soft Matter* **7**, 8127 – 8134 (2011).

44   Jung, J.-M. & Mezzenga, R. Liquid Crystalline Phase Behavior of Protein Fibers In Water: Experiments Versus Theory. *Langmuir* **26**, 504 – 514 (2009).

45   Thibault, J. F. & Ralet, M. C. In *Advances In Pectin and Pectinase Research* (Eds Voragen, F., Schols, H., & Visser R.) 91 – 106 (Kluwer Academic Publishers, 2003).

46   Beverung, C. J., Radke, C. J. & Blanch, H. W. Protein Adsorption At The Oil/Water Interface: Characterization of Adsorption Kinetics By Dynamic Interfacial Tension Measurements. *Biophysical Chemistry* **81**, 59 – 80 (1999).

47   Lu, J. R., Su, T. J. & Howlin, B. J. The Effect of Solution pH On The Structural Conformation of Lysozyme Layers Adsorbed On The Surface of Water. *J Phys Chem B* **103**, 5903 – 5909 (1999).

48   Sagis, L. M. C. *et al.* Polymer Microcapsules With A Fiber–Reinforced Nanocomposite Shell. *Langmuir* **24**, 1608 – 1612 (2008).

49   Sagis, L. M. C., Veerman, C. & van der Linden, E. Mesoscopic Properties of Semiflexible Amyloid Fibrils. *Langmuir* **20**, 924 – 927 (2004).

50   Rogers, S. S., Venema, P., Sagis, L. M. C., van der Linden, E. & Donald, A. M. Measuring The Length Distribution of A Fibril System: A Flow Birefringence Technique Applied To Amyloid Fibrils. *Macromolecules* **38**, 2948 – 2958 (2005).

51   Bolder, S. G., Sagis, L. M. C., Venema, P. & van der Linden, E. Thioflavin T and Birefringence Assays To Determine The Conversion of Proteins Into Fibrils. *Langmuir* **23**, 4144 – 4147 (2007).

52   Weinbreck, F., Nieuwenhuijse, H., Robijn, G. W. & De Kruif, C. G. Complexation of Whey Proteins With Carrageenan. *J Agr Food Chem* **52**, 3550 – 3555 (2004).

53   Turgeon, S. L., Laneuville, S. I. Chapter 11 - Protein + Polysaccharide Coacervates and Complexes: From Scientific Background to their Application as Functional Ingredients in Food Products. In *Modern Biopolymer Science* (Eds Kasapis, S., Norton, I. T., & Ubbink, J. B.) 327-363 (Academic Press: San Diego, 2009).

54   Broide, M. L., Tominc, T. M. & Saxowsky, M. D. Using Phase Transitions To Investigate The Effect of Salts On Protein Interactions. *Phys Rev E* **53**, 6325 – 6335 (1996).

55   Cardinaux, F., Stradner, A., Schurtenberger, P., Sciortino, F. & and Zaccarelli, E. Modeling Equilibrium Clusters In Lysozyme Solution. *EPL* **77**, 48004 (2007).

56   Lucassen-Reynders, E. H., Fainerman, V. B. & Miller, R. Surface Dilational Modulus Or Gibbs' Elasticity of Protein Adsorption Layers. *J Phys Chem B* **108**, 9173 – 9176 (2004).

57   Benjamins, J., Lucassen-Reynders, E. H. & Dietmar Möbius and Reinhard, M. In *Studies In Interface Science* Vol. Volume 7 341 – 384 (Elsevier, 1998).

58   Mellema, M., Clark, D. C., Husband, F. A. & Mackie, A. R. Properties of B-Casein At The Air/Water Interface As Supported By Surface Rheological Measurements. *Langmuir* **14**, 1753 – 1758 (1998).

59   Dickinson, E., Murray, B. S. & Stainsby, G. Coalescence Stability of Emulsion-Sized Droplets At A Planar Oil – Water Interface and The Relationship To Protein Film Surface Rheology. *J Chem Soc Faraday T 1* **84**, 871 – 883 (1988).

60   Schmitt, C. & Turgeon, S. L. Protein/Polysaccharide Complexes and Coacervates In Food Systems. *Adv Colloid Interfac* **167**, 63 – 70 (2011).

61   Magdassi, S. & Kamyshnu, A. In *Surface Activity of Proteins : Chemical and Physicochemical Modifications* (Ed Shlomo Magdassi) Ch. 1, 1 – 38 (Dekker, 1996).

62   van der Linden, E., Sagis, L. M. C. & Venema, P. Rheo-Optics and Food Systems. *Curr Opin Colloid In* **8**, 349 – 358 (2003).

CHAPTER 4

ENCAPSULATION SYSTEM BASED ON OVALBUMIN FIBRILS AND HIGH METHOXYL PECTIN

ABSTRACT

In this study we produced microcapsules using layer-by- layer adsorption of food-grade polyelectrolytes. The shell was built with alternating layers of ovalbumin fibrils and high methoxyl pectin. By varying the number of layers, the release of active ingredients can be controlled – increasing the number of layers of the shell from 4 to 8, decreases the release rate by a factor 6. The formation of the capsules involves merely standard operations that can easily be scaled up to industrial production.

INTRODUCTION

Since the first introduction of microencapsulation in the 1950s,[1] encapsulation technology has developed significantly and is applied in various fields such as pharmaceuticals, cosmetics, and food.[2] In food, encapsulation of functional ingredients using microcapsules is found in various applications, either to improve or enhance nutritional value, or to use for preservation purposes. These functional ingredients can be fats and oils, aromas, oleoresins, vitamins, minerals, colorants, antioxidants, probiotics and enzymes. They have been encapsulated,[2–6] either using coacervation, molecular inclusion, interfacial polymerization, or mechanical techniques like spray-drying, spray chilling/cooling, extrusion, or fluidized bed coating.[2,7–9]

Creating multilayer films based on electrostatic interactions between oppositely charged components was introduced in 1991 by Decher *et al.*[10–12] layer-by-layer (LbL) polyelectrolyte deposition has become a popular technique for preparing polyelectrolyte capsules because of its ability to create highly tailored capsule shells through a simple, inexpensive and easily controllable adsorption process.[13] It has been applied to produce capsules of various sizes, ranging from the nanometer to micrometer scale,[14,15] with well-defined barrier properties.[15] In this technique, self-assembly is driven by the electrostatic attraction of oppositely charged materials (polycations and polyanions) to form polyelectrolyte shells.[16–18] Excess of materials in the solution is removed by centrifuging and/or washing. At last, the inner phase (the core) can be removed to obtain hollow capsules.[13,14,19] The materials for assembly can be small organic molecules, inorganic compounds, macromolecules, bio-macromolecules or colloids.[18,20–28] Polyelectrolyte microcapsules made by this technique have many potential applications including controlled release of materials.[28,29]

The structure of the polyion layered capsule shell is determined mainly by the electrostatic interactions between the polyions used.[13] The mechanical strength and permeability of the capsules can be controlled by varying the number of layers or by changing the characteristics of the encapsulating materials.[15] The average charge of the shell can easily be tuned by the acidity of the continuous phase, thus offering the possibility to control the interactions between the charged materials. The foundation of multilayers with pH-sensitive characteristics has got considerable attention.[20,21,26,27,29]

Food proteins have excellent emulsification and film-forming abilities. Their charge can be adjusted by changing the pH of the solvent which makes them excellent candidates for encapsulation based on electrostatic LbL self-assembly.

In this study, we used the LbL self-assembly technique to produce microcapsules using oil in water emulsion droplets as a template, and food-grade protein fibrils and polysaccharides as wall materials. By using emulsion droplets as a liquid – core template, we were able to control the size distribution by adjusting the energy input and the concentration of the stabilizer.[15] Ovalbumin (Ova) – a major globular protein in egg white – has valuable functional properties such as surface activity.[30,31] When heated at 80 °C (above the denaturation temperature of 63.9 °C) at pH 2 (far below the isoelectric point) and low ionic strength (0.01 – 0.035 M), Ova monomers assemble irreversibly into semi-flexible fibrils with a contour length of a few hundred nanometer and effective diameters of a few nanometer.[32–34] The surface activity of Ova fibril solution allows it to be used as the primary stabilizer of the emulsion – in other words, forming the first layer of the LbL process. Our choice of the second polyelectrolyte is high methoxyl pectin (HMP). Pectin is a soluble diet polysaccharide widely used in food production and is claimed to have health benefits.[35] HMP has a negative charge in mildly acidic solutions due to the presence of ionized carboxylic groups along its backbone that have pK_a values of about 3.6.[36]

In order to ensure that the LbL sefl – assembly process will occur and to prevent undesirable effects (such as flocculation), the pH of the polyelectrolyte solutions should be chosen to obtain a suitable degree of polyion ionization. [13,16] The Ova fibril and HMP solutions used were at pH 3.5. At this pH, the protein fibrils adsorbed to the oil – water interface provide the emulsion droplets with a positive charge while HMP, as the alternating material, is negatively charged.

We used simple and standard operations in order to increase the potential for scaling up to industrial production volumes.

MATERIALS AND METHODS

Materials

Ova was obtained from Sigma-Aldrich Co., Missouri, USA (product no. A5503) with a purity of at least 98%. HMP was supplied by CP Kelco ApS, Lille Skensved, Denmark (JMH-6, batch no. 16849, degree of methoxylation 69.8%). HMP was characterized in a study of Sagis *et al.*[15] and has a molecular weight of 2.7×10^3 kDa and a radius of gyration of 46 nm.

The oil n-hexadecane was obtained from Merck Schuchardt OHG, Hohenbrunn, Germany (CAS-no. 544-76-3). (R)-(+)-Limonene 97% was supplied by Sigma-Aldrich Co., Missouri, USA (CAS-no. 5989-27-5)

Thioflavin T (ThT) was obtained from Merck Schuchardt OHG, Hohenbrunn, Germany, (CAS-no. 2390-54-7, C.I. No. 49005).

All other chemicals used were of analytical grade, unless stated otherwise. All solutions were prepared with Millipore water (Millipore Corporation, Billerica, Massachusetts, USA). Samples were diluted to the desired concentration (if applicable) with the same buffer or solution used for the primary solutions

Preparing Ova fibrils

Ova was dissolved in water and the pH was adjusted to pH 2 using a 1M HCl solution. The Ova solution was stirred overnight at 4 °C. After that, the solution was centrifuged at 20,000 ×g for 30 min to remove un-dissolved materials. The concentration of the stock solution was determined with a UV spectrophotometer at a wavelength of 280 nm and an extinction coefficient of $E^{1\% \, (wt)} = 6.68145$. Based on results from a study of Veerman *et al*.,[32] Ova solutions of 5% wt were heated at 80 °C for at least 3h. After heating, the sample was quenched by cooling the samples immediately on ice, and subsequently stored at 4 °C for further investigations.

Electron micrographs of the Ova fibrils were taken using a Philips CM 12 electron microscope (Transmission electron microscopy – TEM) as described in previous studies.[37 – 39] TEM micrographs showed that Ova fibrils obtained had a contour length of a few hundreds nanometer (see **Figure 4.1**), in agreement with values reported in literature.[32] Sagis *et al.* found that Ova fibrils prepared in these conditions were semi-flexible with a contour length/persistence length ratio equal to 0.6.[40]
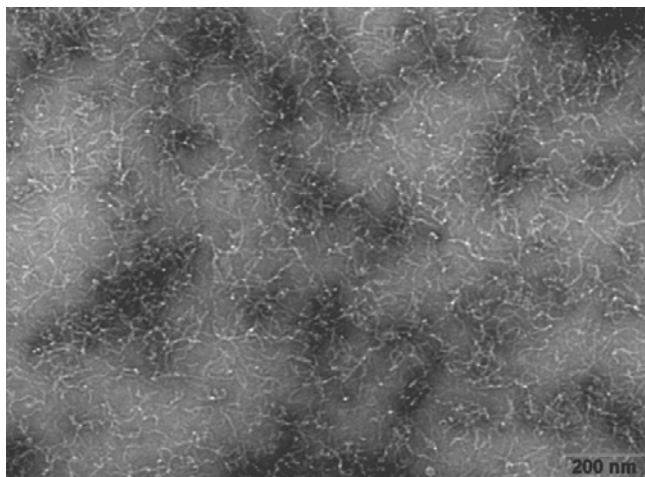
Figure 4.1. TEM micrograph of Ova fibrils at pH 3.5.

Preparing HMP solution

HMP was dissolved in a pH 3.5 buffer of 10 mM citric acid and 20 mM Na_2HPO_4, and was stirred overnight at 4 °C. The solution was centrifuged at 20,000 ×g for 30 min to remove un-dissolved materials. The supernatant was filtered through Millipore Millex-HP filters (Hydrophilic PES 0.45 µm) (Millipore Corporation, Billerica, Massachusetts, USA). This solution was further diluted to desired concentrations using the same buffer.

Methods

Production of microcapsules
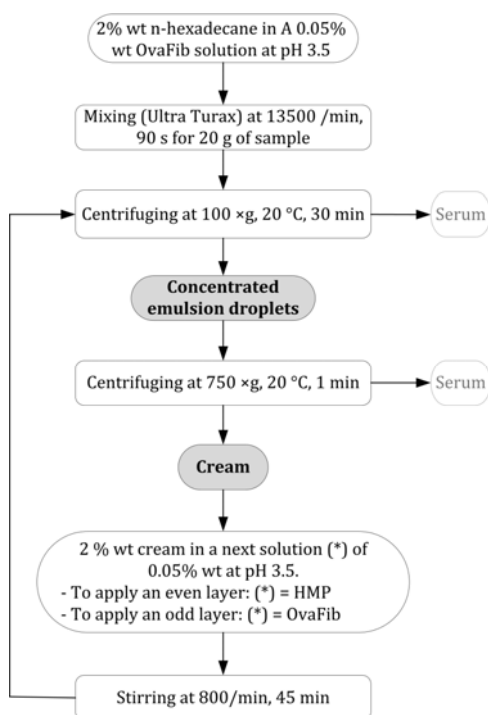
Figure 4.2. Scheme showing the process of making capsules

A 2% wt emulsion of n-hexadecane in a 0.05% wt Ova fibril solution at pH 3.5 was made by mixing with a rotor – stator mixer (Ultra Turrax) using a setting of 13,500 rpm for 90 s for a sample of 25 g of emulsion. To remove the non-adsorbed Ova fibrils, the emulsion droplets were separated from the serums by centrifuging at 50 ×g for 45 min at 20 °C. The concentrated emulsion droplets ("cream") were centrifuged again at

750 ×g for 1 min to remove excess solution. After that, the positively charged droplets were dispersed in a HMP solution of 0.05% wt at pH 3.5. At this pH, HMP is negatively charged which allowed self-assembly driven by electrostatic interaction to form bilayered droplets. These bilayered droplets were isolated and dispersed in the same solution used for the first layer. By repeating this process, additional layers of encapsulating materials can be added (see **Figure 4.2**).

Light scattering measurements

To determine the size distribution and ξ-potential of the isolated emulsion droplets, a MasterSizer 2000 and a Zetasizer Nano (Malvern Instruments, Ltd. Worcestershire, UK) were used. Creams were re-dispersed in buffer at pH 3.5 prior to measurements to ensure that presence of excess polyelectrolytes (not adsorbed on the templates) was minimized. On each sample, three size distribution and five ξ-potential measurements were performed.

Confocal Laser Scanning Microscopy (CLSM)

To study the distribution of Ova fibrils on the emulsion droplets, ThT was used to label the Ova fibrils. ThT adsorbs to the β-sheets formed during the amyloid fibril formation.[41–43] The fluorescence of ThT was also found to increase by this specific binding to β-sheets. The emulsion droplets were then observed under a Zeiss LSM5 Pascal confocal system mounted on an inverted microscope (Zeiss Axiovert 200). The 458 nm line of an argon laser was used to excite the samples, and the emission fluorescence was observed after passing a 475 nm LP filter.

Scanning Electron Microscopy (SEM)

To examine the structure of the shell of the microcapsules with SEM, samples were dried and the oil phase was evaporated using critical point drying. Dried microcapsules were fixed onto double-stick carbon tape, placed in a dedicated preparation chamber (Oxford Instruments CT 1500 HF, Eynsham, England), and sputter coated with 5 nm of platinum. Samples were analyzed with a field emission scanning electron microscope (JEOL 6300 F, Tokyo, Japan) at room temperature at a working distance of 8 mm with SE detection at 3.5 – 5 kV. All images were recorded digitally (Orion, 6 E.L.I. sprl., Belgium) at a scan rate of 100 s (full frame).

Proton Transfer Reaction – Mass Spectrometry (PTR – MS) measurements

The PTR-MS measurements were carried out as described in a study of Zuidam *et al.*[44] The controlled release of limonene from the microcapsules into the headspace was measured real-time by a High-Sensitivity PTR-MS from Ionicon Analytik,

Innsbruck, Austria. The limonene release profiles of different microcapsules were measured at 80 °C.

The first minute of PTR-MS measurement recorded the base line without sample, and after 1 minute the sample was introduced. The PTR-MS measurements lasted for 30 minutes and recorded ion trace 137 and 81, respectively the MW of limonene + 1 (from the proton) and its major fragment ion. The data of the different samples were combined and plotted against time.[44]

RESULTS AND DISCUSSIONS

Size distributions and ξ-potential

One of the most common problems reported in previous studies using the LbL technique to produce multilayer particles, is the tendency for flocculation.[13,17,45–47] In this system, that problem was not observed. The size distribution of isolated emulsion droplets (templates) did not change significantly from 1-layer droplets to 7-layer droplets (**Figure 4.3** and **Figure 4.4**), even after storage for 24h (all samples) and for a week (only samples of 3-layer to 7-layer droplets were measured). In other words, the emulsion droplets were stable against flocculation after applying more layers of polyelectrolytes. The Sauter mean diameters D(3,2) of these droplets fluctuated between 5 and 6 μm and slightly increased as the number of layers increased (**Figure 4.5**). Note that the emulsion droplets were poly-disperse. Another possible problem that may occur using the LbL technique is complex formation between non-adsorbed protein and pectin molecules. These complexes with a typical diameter smaller than 1 μm were not detected here.
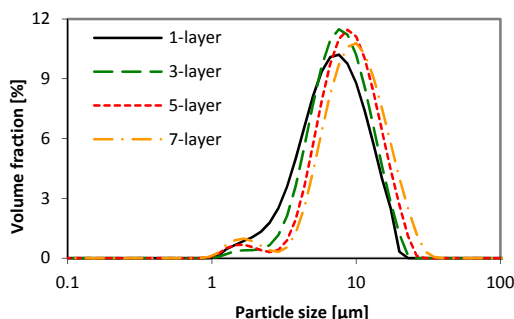
Figure 4.3. Size distribution of emulsion droplets with Ova fibrils as outer layer: solid line (–) – 1-layer, dashed line (– –) – 3-layer, dotted line (..) – 5-layer; dot – dashed line (. - . -) – 7-layer
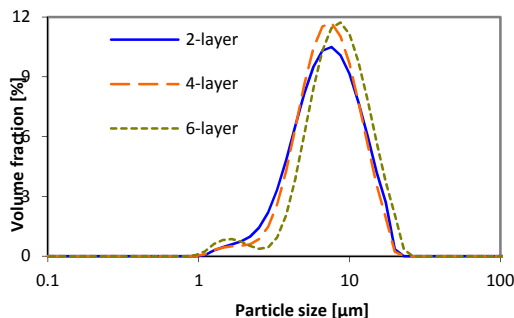
Figure 4.4. Size distribution of emulsion droplets with HMP as outer layer: solid line (–) – 2-layer; dashed line (- - -) – 4-layer droplets; and dotted line (...) – 6-layer.
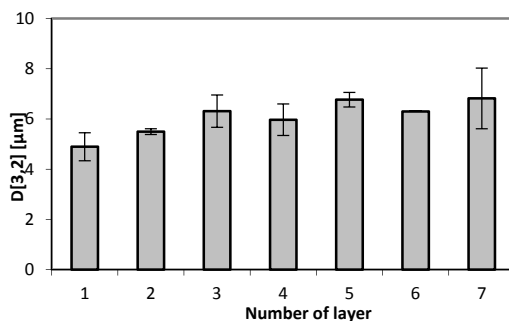
Figure 4.5. Surface mean diameter – Sauter mean diameter D (3,2) – of emulsion droplets with various number of encapsulating layers. Odd layer number represents the deposition of Ova fibrils. Even layer numbers represents the deposition of HMP. The error bars indicate deviation from the mean values of various samples.

During the self-assembly process adsorption of oppositely charged polyions results in a surface charge reversal,[13,16,48] i.e. the final outer layer normally determines the interfacial net charge.[17,18] **Figure 4.6** shows that the ξ-potential distribution of emulsion droplets reverses from about plus (+) 30 mV (odd number of layers with Ova fibrils as outer layers) to about negative (–) 20 mV (even number of layers with HMP as outer layers) confirming the layer-by- layer adsorption based on electrostatic attraction.
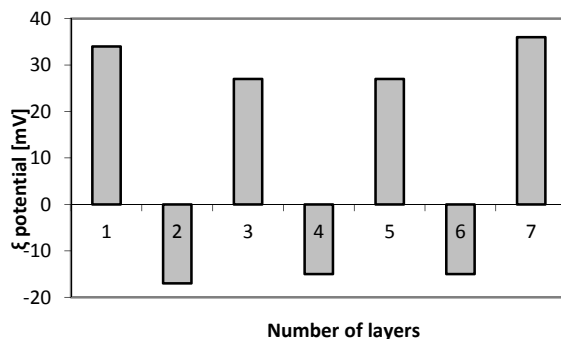
Figure 4.6. ζ-potential distribution of emulsion droplets with various layers of encapsulating materials Odd layer number represents the deposition of Ova fibrils. Even layer numbers represents the deposition of HMP.

CLSM

The dye ThT is known for its specific binding to amyloid fibrils.[33,34,41–43] In order to observe the adsorption of fibrils on the emulsion droplets, ThT was used as dye agent for confocal microscopy. The fluorescence signals (**Figure 4.7**) confirm the adsorption of Ova fibrils on the emulsion droplet templates, in line with the results of ξ-potential measurements. In comparison with a 3-layer shell made of whey protein isolate (WPI) fibrils and HMP (at the same pH 3.5) by Sagis *et al.*,[15] the distribution of Ova fibrils on the shell is more homogenous. The morphology of the two fibrils were different: WPI fibrils were stiff and about 1,5 μm long (microcapsule with a D(3,2) of about 25 μm) and Ova fibrils were semi-flexible and about 200 nm long (microcapsules with a average D(3,2) of about 6 μm). Short and flexible fibrils can easily be adsorbed and arrange themselves along the interface while longer and more rigid ones have difficulties organizing themselves on spheres resulting in a hairy structure with extreme thickness. From the fluorescence intensity distribution (see **Figure 4.7 (c)**), the thickness of a microcapsule shell constructed with 5 layers can be estimated to be about a few hundred nanometers. From literature,[29,48] it is known that multilayer shells exhibit a swelling behavior. The interactions between polyelectrolyte segments versus those between polyelectrolytes and water molecules determine the water uptake. This water content is important for the internal dynamics and stability of the deposited layers since it affects the charge coupling between oppositely charged polyelectrolytes.[48] In a dry state, as used for example in the SEM analysis, the shell thickness may appear to be much smaller.
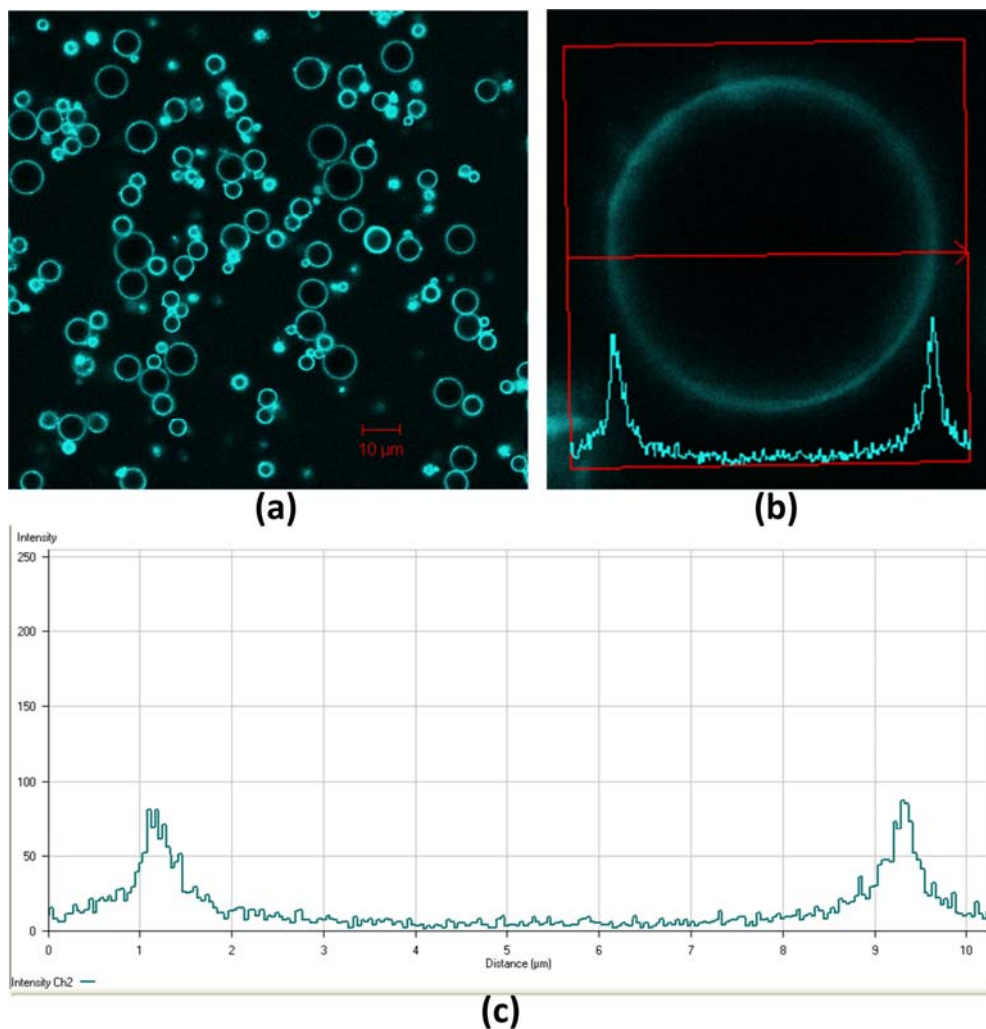
Figure 4.7. CSLM picture showing the ovalbumin fibril adsorption of 5-layer microcapsules (a): overview; (b): distribution of Ova fibrils (dyed with ThT) on an emulsion droplet template; (c): fluorescence intensity scan through a microcapsule along an arrow shown on (b)

SEM

The inner-phase of the emulsion droplets was removed by critical point drying to obtain hollow microcapsules. After that, they were studied using a scanning electron microscope (see **Figure 4.8**). Comparing microcapsules with different materials at the outer layers, it can be seen that when the outer layers of the microcapsules consist of Ova fibrils, the shell looks smoother than when the outer layers consist of HMP.

(a) and (b): 4-layer microcapsules (outer layer: HMP pH 3.5)

(c) and (d): 5-layer microcapsules (outer layer: OvaFib pH 3.5)

(e) and (f): 6-layer microcapsules (outer layer: HMP pH 3.5)

(g) and (h): 7-layer microcapsules (outer layer: OvaFib pH 3.5)
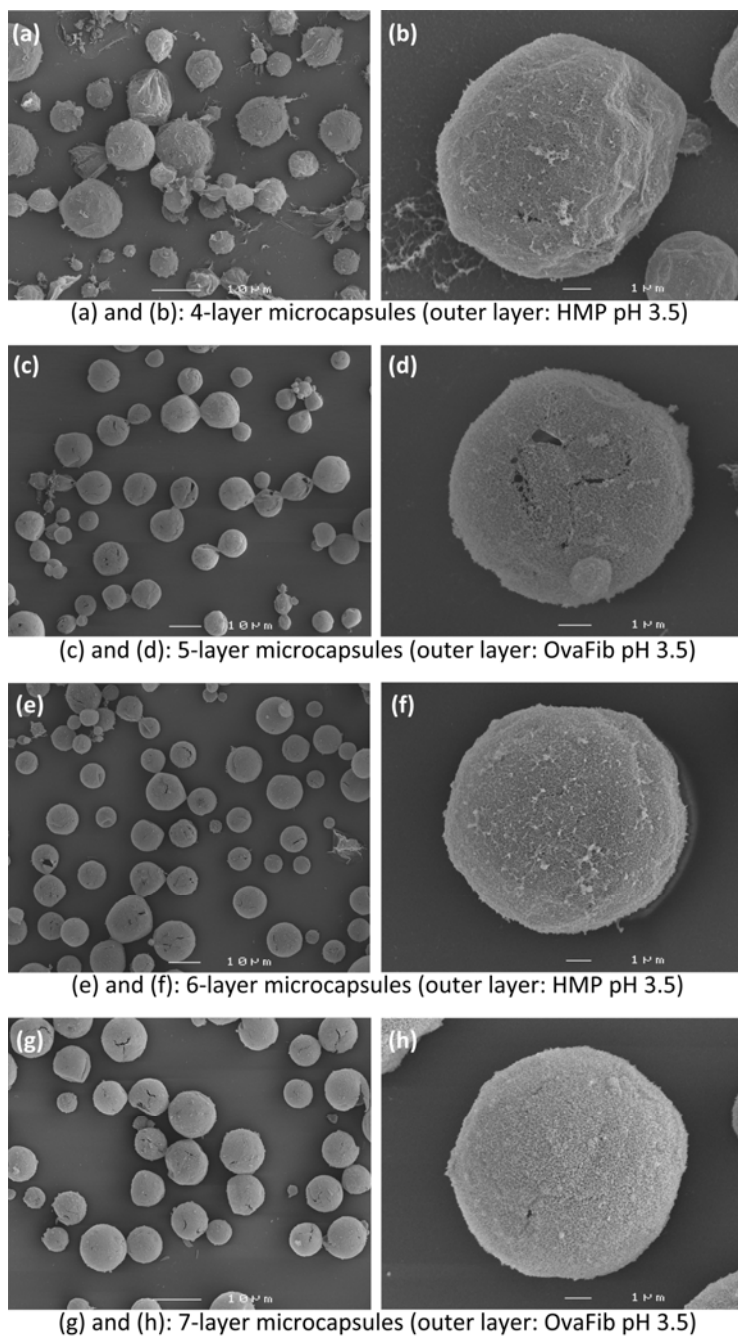
Figure 4.8. SEM pictures showing the structure of the outer layer of (a) and (b): 4-layer; (c) and (d): 5-layer; (e) and (f): 6-layer; (g) and (h): 7-layer microcapsules. Microcapsules with odd layers have Ova fibrils as outer layers and those with even layers have HMP as outer layers. The microcapsules were obtained by critical point drying to remove the inner-phase (oil).

Comparing microcapsules with various numbers of layers, an improvement in shell strength can be seen. Indentation is observed on 4-layer microcapsules showing that the shell was not strong enough to resist the drying process. Some of 5-layer microcapsules have maintained their spherical shapes but there are defects on the shell. They could be formed during the drying process or they are shell defects due to incomplete coverage of materials, meaning more layers are needed to fully cover the microcapsule shell. These defects are seen less on 6-layer and 7-layer microcapsules. More intact microcapsules can be found in samples of 7-layers than those of 6-layers. These observations indicate that the more layers the shell consist of, the more resistant it is against the physical drying process.

Release of limonene

The diffusion-controlled release of limonene from the microcapsules was analyzed by PTR-MS measurements. Limonene was released by diffusion through the polyelectrolyte shells and/or through the pores in the shell.[49]

Results show that the time of the maximum in release shifts to higher values as the number of layers of the capsules increased. From **Figure 4.9** and **Figure 4.10** we clearly see that increasing the number of layers in the shell of the capsules leads to a delay of the release of limonene. Going from four layers to eight the maximum release time (the time were the release curves in **Figure 4.9** have their maximum value) increases by about a factor 6.
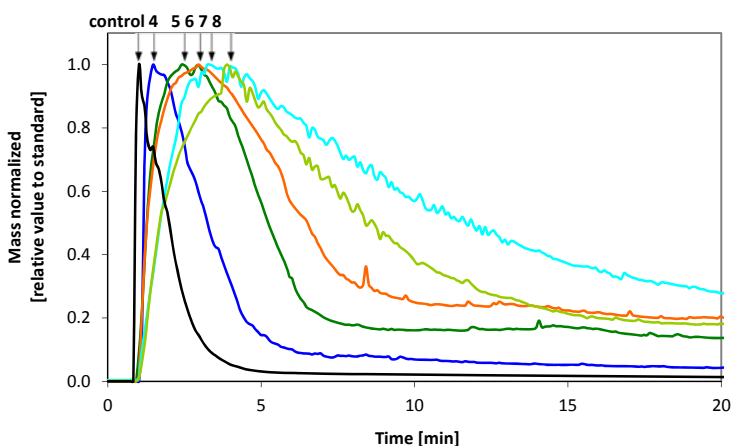
Figure 4.9. Normalized limonene release profile of microcapsules with various numbers of encapsulating layers (10% wt of limonene loading). The numbers indicate the number of layers of the microcapsules. Control is sample without encapsulating materials.
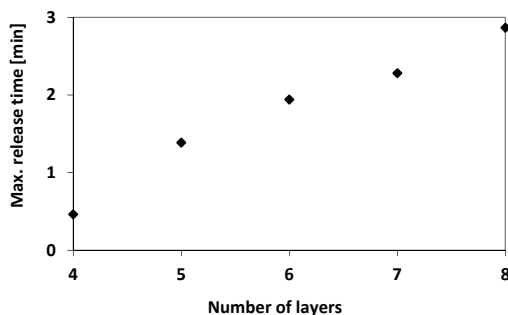
Figure 4.10. Time at maximal release (time at which highest limonene concentration is released) vs. number of encapsulating layers (samples with 10% wt of limonene load).

Figure 4.10 shows the maximal release time (time at which highest limonene concentration is released) as a function of the number of layers is increasing steadily which show the release can be delayed even more by adding additional layers. These results prove that the release properties of the multi-layer capsules can be tuned by controlling the number of layers in the shell of the capsules.

CONCLUSIONS

Microcapsules with different layers of food-grade protein fibrils and polysaccharides can be prepared using merely standard operations (mixing, centrifuging, and stirring). In this study we have produced microcapsules using the LbL technique and food-grade Ova fibrils and HMP. The microcapsules have a poly-disperse size distribution. No flocculation of microcapsules during applying of additional layers is observed. We have found that by increasing the number of layers from 4 to 8, the release rate of active ingredients (in our case: limonene) decreases by a factor 6. Since the materials are food-grade, the applications of these microcapsules can include food products or pharmaceutical purposes.

ACKNOWLEDGEMENTS

REFERENCE

1   Green, B. K. Pressure Sensitive Record Material. U.S. Patent 2712507 (1955).

2   Madene, A., Jacquot, M., Scher, J. & Desobry, S. Flavour Encapsulation and Controlled Release: A Review. *Int J Food Sci Tech* **41**, 1 – 21 (2006).

3   Dziezak, J. D. Microencapsulation and Encapsulated Ingredients. *Food Technol.* **42**, 136 – 151 (1988).

4   Schrooyen, P. M. M., Meer, R. V. D. & Kruif, C. G. D. Microencapsulation: Its Application In Nutrition. *P Nutr Soc* **60**, 475 – 479 (2001).

5   Jackson, L. S. & Lee, K. Microencapsulation and The Food Industry. *Lebensm Wiss Technol* **24**, 289 – 297 (1991).

6   Shahidi, F. & Han, X.-Q. Encapsulation of Food Ingredients. *Crit Rev Food Sci* **33**, 501 – 547 (1993).

7   Gibbs, B. F., Kermasha, S., Alli, I. & Mulligan, C. N. Encapsulation In The Food Industry: A Review. *Int J Food Sci Nutr* **50**, 213 – 224 (1999).

8   Dewettinck, K. & Huyghebaert, A. Fluidized Bed Coating In Food Technology. *Trends Food Sci Tech* **10**, 163 – 168 (1999).

9   Rosenberg, M. & Sheu, T. Y. Microencapsulation of Volatiles By Spray-Drying In Whey Protein-Based Wall Systems. *Int Dairy J* **6**, 273 – 284 (1996).

10   Decher, G. & Hong, J. D. Buildup of Ultrathin Multilayer Films By A Self-Assembly Process: I. Consecutive Adsorption of Anionic and Cationic Bipolar Amphiphiles. *Makromol. Chem., Macromol. Symp.* **46**, 321 – 327 (1991).

11   Decher, G. & Hong, J. D. Buildup of Ultrathin Multilayer Films By A Self-Assembly Process: II. Consecutive Adsorption of Anionic and Cationic Bipolar Amphiphiles and Polyelectrolytes On Charged Surfaces. *Ber. Bunsenges. Phys. Chem.* **95**, 1430 – 1434 (1991).

12   Decher, G., Hong, J. D. & Schmitt, J. Buildup of Ultrathin Multilayer Films By A Self-Assembly Process: III. Consecutively Alternating Adsorption of Anionic and Cationic Polyelectrolytes On Charged Surfaces. *Thin Solid Films* **210 – 211**, 831 – 835 (1992).

13   Peyratout, C. S. & Dähne, L. Tailor-Made Polyelectrolyte Microcapsules: From Multilayers To Smart Containers. *Angew Chem Int Edit* **43**, 3762 – 3783 (2004).

14   Yow, H. N. & Routh, A. F. Formation of Liquid Core– Polymer Shell Microcapsules *Soft Matter* **2**, 940 – 949 (2006).

15   Sagis, L. M. C. *et al.* Polymer Microcapsules With A Fiber-Reinforced Nanocomposite Shell. *Langmuir* **24**, 1608 – 1612 (2008).

16   Ai, H., Jones, S. A. & Lvov, Y. M. Biomedical Applications of Electrostatic Layer-By-Layer Nano-Assembly of Polymers, Enzymes, and Nanoparticles *Cell Biochem Biophys* **39**, 23 – 43 (2003).

17   McClements, D. J. Theoretical Analysis of Factors Affecting The Formation and Stability of Multilayered Colloidal Dispersions. *Langmuir* **21**, 9777 – 9785 (2005).

18   Decher, G. (Eds Gero Decher & Joseph B. Schlenoff) 1 – 46 (Wiley – VCH, 2003).

19   Schönhoff, M. Self-Assembled Polyelectrolyte Multilayers. *Curr Opin Colloid In* **8**, 86 – 95 (2003).

20   Déjugnat, C. & Sukhorukov, G. B. pH-Responsive Properties of Hollow Polyelectrolyte Microcapsules Templated On Various Cores. *Langmuir* **20**, 7265 – 7269 (2004).

21   Kietzmann, D., Béduneau, A., Pellequer, Y. & Lamprecht, A. pH-Sensitive Microparticles Prepared By An Oil/Water Emulsification Method Using N-Butanol. *Int J Pharm* **375**, 61 – 66 (2009).

22   Kim, J.-H., Hwang, J.-H. & Lim, T.-Y. A Layer-By-Layer Self-Assembly Method For Organic – Inorganic Hybrid Multilayer Thin Films. *J Ceram Process Res* **10**, 770 – 773 (2009).

23   Richert, L. *et al.* Layer By Layer Buildup of Polysaccharide Films: Physical Chemistry and Cellular Adhesion Aspects. *Langmuir* **20**, 448 – 458 (2003).

24   Rmaile, H. H. & Schlenoff, J. B. "Internal Pka's" In Polyelectrolyte Multilayers: Coupling Protons and Salt. *Langmuir* **18**, 8263 – 8265 (2002).

25   Schneider, G. & Decher, G. Functional Core/Shell Nanoparticles Via Layer-By-Layer Assembly. Investigation of The Experimental Parameters For Controlling Particle Aggregation and For Enhancing Dispersion Stability. *Langmuir* **24**, 1778 – 1789 (2008).

26   Sukhorukov, G. B., Antipov, A. A., Voigt, A., Donath, E. & Möhwald, H. pH-Controlled Macromolecule Encapsulation In and Release From Polyelectrolyte Multilayer Nanocapsules. *Macromol Rapid Comm* **22**, 44 – 46 (2001).

27   Tong, W., Gao, C. & Möhwald, H. Stable Weak Polyelectrolyte Microcapsules With pH-Responsive Permeability. *Macromolecules* **39**, 335 – 340 (2005).

28   Wang, C. *et al.* Microcapsules For Controlled Release Fabricated Via Layer-By-Layer Self-Assembly of Polyelectrolytes. *J Exp Nanosci* **3**, 133 – 145 (2008).

29   Mauser, T., Déjugnat, C. & Sukhorukov, G. B. Balance of Hydrophobic and Electrostatic Forces In The pH Response of Weak Polyelectrolyte Capsules. *J Phys Chem B* **110**, 20246 – 20253 (2006).

30   Delben, F. & Stefancich, S. Interaction of Food Polysaccharides With Ovalbumin. *Food Hydrocolloid* **12**, 291 – 299 (1998).

31   Kudryashova, E. V., Visser, A. J. W. G., Van Hoek, A. & De Jongh, H. H. J. Molecular Details of Ovalbumin – Pectin Complexes At The Air/Water Interface: A Spectroscopic Study. *Langmuir* **23**, 7942 – 7950 (2007).

32   Veerman, C., De Schiffart, G., Sagis, L. M. C. & van der Linden, E. Irreversible Self-Assembly of Ovalbumin Into Fibrils and The Resulting Network Rheology. *Int J Biol Macromol* **33**, 121 – 127 (2003).

33   Azakami, H., Mukai, A. & Kato, A. Role of Amyloid Type Cross B-Structure In The Formation of Soluble Aggregate and Gel In Heat-Induced Ovalbumin. *J Agr Food Chem* **53**, 1254 – 1257 (2005).

34   Khodarahmi, R., Soori, H. & Karimi, S. A. Chaperone-Like Activity of Heme Group Against Amyloid-Like Fibril Formation By Hen Egg Ovalbumin: Possible Mechanism of Action. *Int J Biol Macromol* **44**, 98 – 106 (2009).

35   Sriamornsak, P. Chemistry of Pectin and Its Pharmaceutical Uses : A Review. *Silpakorn University International Journal* **3**, 206 – 228 (2003).

36   Morris, E. R., Gidley, M. J., Murray, E. J., Powell, D. A. & Rees, D. A. Characterization of Pectin Gelation Under Conditions of Low Water Activity, By Circular Dichroism, Competitive Inhibition and Mechanical Properties *Int J Biol Macromol* **2**, 327 – 330 (1980).

37   Humblet-Hua, N.-P., Sagis, L. M. C. & van der Linden, E. Effects of Flow On Hen Egg White Lysozyme (HEWL) Fibril Formation: Length Distribution, Flexibility, and Kinetics. *J Agr Food Chem* **56**, 11875 – 11882 (2008).

38   Bolder, S. G., Vasbinder, A., Sagis, L. M. C. & van der Linden, E. Heat-Induced Whey Protein Isolate Fibrils: Conversion, Hydrolysis, and Disulphide Bond Formation. *Int Dairy J* **17**, 846 – 853 (2007).

39   Akkermans, C., van der Goot, A. J., Venema, P., van der Linden, E. & Boom, R. M. Formation of Fibrillar Whey Protein Aggregates: Influence of Heat and Shear Treatment, and Resulting Rheology. *Food Hydrocolloid* **22**, 1315 – 1325 (2008).

40   Sagis, L. M. C., Veerman, C. & van der Linden, E. Mesoscopic Properties of Semiflexible Amyloid Fibrils. *Langmuir* **20**, 924 – 927 (2004).

41   Krebs, M. R. H., Bromley, E. H. C. & Donald, A. M. The Binding of Thioflavin–T To Amyloid Fibrils: Localisation and Implications. *J. Struct. Biol.* **149**, 30 – 37 (2005).

42   Bolder, S. G., Sagis, L. M. C., Venema, P. & van der Linden, E. Thioflavin T and Birefringence Assays To Determine The Conversion of Proteins Into Fibrils. *Langmuir* **23**, 4144 – 4147 (2007).

43   Nilsson, M. R. Techniques To Study Amyloid Fibril Formation In Vitro. *Methods* **34**, 151 – 160 (2004).

44   Zuidam, N. J., Jublot, L., Suijker, M. J., Ziere, A. & Smit, G. In *XVII International Conference On Bioencapsulation.*

45   Cariso, F. Nanoengineering of Particle Surfaces. *Adv Mater* **13**, 11 – 22 (2001).

46   Ogawa, S., Decker, E. A. & McClements, D. J. Production and Characterization of O/W Emulsions Containing Cationic Droplets Stabilized By Lecithin – Chitosan Membranes. *J Agr Food Chem* **51**, 2806 – 2812 (2003).

47   Ogawa, S., Decker, E. A. & McClements, D. J. Production and Characterization of O/W Emulsions Containing Droplets Stabilized By Lecithin – Chitosan – Pectin Mutilayered Membranes. *J Agr Food Chem* **52**, 3595 – 3600 (2004).

48   Schönhoff, M. Layered Polyelectrolyte Complexes: Physics of Formation and Molecular Properties. *Journal of Physics: Condensed Matter*, R1781 (2003).

49   Pothakamury, U. R. & Barbosa – Cánovas, G. V. Fundamental Aspects of Controlled Release In Foods. *Trends Food Sci Tech* **6**, 397 – 406 (1995).

CHAPTER 5

MICROCAPSULES WITH PROTEIN FIBRIL REINFORCED SHELLS: EFFECTS OF FIBRIL PROPERTIES ON MECHANICAL STRENGTH OF THE SHELL

ABSTRACT

In this study, we produced microcapsules using layer-by- layer adsorption of food-grade polyelectrolytes on an emulsion droplet template. We compared the mechanical stability of microcapsules with shells consisting of alternating layers of ovalbumin – high methoxyl pectin complexes (OvaHMP) and semi-flexible ovalbumin fibrils (OvaFib) (average contour length $L_c{\sim}200nm$), with microcapsules built of alternating layers of lysozyme – high methoxyl pectin complexes (LysHMP) and lysozyme fibrils (LysFib). Two types of lysozyme fibrils were used: short and rod-like ($L_c{\sim}500$ nm), and long and semi-flexible ($L_c =1.2 – 1.5$ μm). At a low number of layers (≤ 4), microcapsules from ovalbumin complexes and fibrils were stronger than microcapsules prepared from lysozyme complexes and fibrils. With an increase of the number of layers, the mechanical stability of microcapsules from LysHMP/LysFib increased significantly and capsules were stronger than those prepared from OvaHMP/OvaFib with the same number of layers. The contour length of the Lysozyme fibrils did not have a significant effect on mechanical stability of the LYsHMP/LysFib capsules. The stiffer lysozyme fibrils produce capsules with a hard but more brittle shell, whereas the semi-flexible ovalbumin fibrils produce capsules with a softer but more stretchable shell. These results show that mechanical properties of this type of capsule can be tuned by varying the flexibility of the protein fibrils.

INTRODUCTION

In the 1950s, Green and Schleicher introduced microencapsulation,[1] since then encapsulation technology has been developed and applied in various fields including medicine and pharmacy, and food [2]. In food products, different components, including aromas, vitamins, probiotics, and enzymes, have been encapsulated,[2–6] using either physical chemical techniques (such as interfacial polymerization, solidification, coacervation, molecular inclusion, gelation, or evaporation) or mechanical techniques (such as spray-drying, spray chilling/cooling, extrusion, or fluidized bed coating).[2,7–9]

In 1991, Decher *et al.* developed microencapsulation by layer-by- layer (LbL) assembly.[10–12] This technique is the sequential adsorption of oppositely charged materials on a template, to form polyelectrolyte shells.[13–15] It is a simple and inexpensive technique to control the shell thickness of the microcapsules[16–18] and the release of encapsulated materials.[18–20]

In this study, we prepared microcapsules by LbL assembly, using oil in water emulsion droplets as templates. Surface-active complexes of food-grade proteins and polysaccharides were used as the emulsifier of the template emulsion. After preparation of the template emulsion, alternating layers of fibrillar protein aggregates and protein – polysaccharide complexes were adsorbed to build the shell of the microcapsule.

Protein – polysaccharide complexes have previously been used as emulsion stabilizers and were shown to have high surface activity and the ability to form thick, gel-like, and charged adsorbed layers.[21,22] The mechanical strength of that adsorbed layer, together with the electrostatic and steric repulsion it induces, is the most important factor influencing the kinetic stability of the oil-in-water emulsion droplets,[13] and will also affect the stability of microcapsules produced with these complexes.

For the complexes, we have chosen ovalbumin (Ova) and lysozyme (Lys), two major egg white proteins, and high methoxyl pectin (HMP). Ova (60– 65% of the total proteins in egg white) is available in large quantities and widely used in studies of protein structures and properties.[23] Lys is a well-characterized protein[24] and is a model protein in studying the interaction between proteins and polysaccharides.[25] Pectin is an anionic polysaccharide present in plant cell walls and is commonly used in food products.[25,26] It was found to form complexes with various proteins, such as gelatin,[26] Ova,[27] Lys[25] and milk proteins.[28–31] The main parameters controlling the formation of stable protein – polysaccharide complexes are pH, ionic strength, charge density, concentration, and protein – polysaccharide ratio.[21,25,32] At chosen pH's (3.5 for Ova and 7 for Lys), the proteins are positively charged while HMP is negatively charged, resulting in attractive electrostatic interactions to form complexes. A high

ionic strength (I) will lead to charge screening of the polymers and, hence, affect the formation of complexes.[21,31] Therefore, no extra salts were added to the polymer solutions. We have mixed proteins and HMP at various ratios, and the optimum ratio to obtain stable complexes was determined by visual observation, light scattering and ξ-potential distribution measurements.

The assembly of food-grade proteins, such as milk proteins, Ova, and Lys, into fibrils[33–36] has the potential of broadening the functional properties of these proteins.[37] Fibrils have previously been used to develop microcapsules for encapsulation,[17,18] but a detailed study on how protein fibril properties affect mechanical stability of microcapsule has so thus far not been performed.

When heated at 80 °C, at pH 2, Ova monomers assemble irreversibly into semi-flexible fibrils with a contour length of a few hundred nanometer and effective diameters of a few nanometer.[38] For Lys the optimum conditions to form fibrils were at pH 2 and 57 °C.[36] Applying flow during heating was found to influence the morphology of fibrils: higher shearing or stirring rates resulted in shorter fibrils that are more rod-like, whereas at rest or at lower rates, longer semi-flexible fibrils were obtained.[39] In this study, both short and rod-like and long and semi-flexible fibrils were used as encapsulating materials.

From these two types of protein complexes and fibrillar aggregates, two encapsulation systems were developed. System 1 was composed of OvaHMP complexes and Ova fibrils. The microcapsules of this system were prepared at pH 3.5. At this pH, OvaHMP complexes have a negative net charge while Ova fibrils are positively charged. System 2 was composed of LysHMP complexes and Lys fibrils. LysHMP complexes were adsorbed on the template at pH 7 and negatively charged, and Lys fibrils were adsorbed at pH 5 and, hence, positively charged. Both systems were prepared using simple and standard operations as described in previous studies.[17,18] Using a range of fibrils (short and semi-flexible Ova, short and rod-like Lys, long and semi-flexible Lys) allowed us to investigate the effect of fibril properties on mechanical stability of the multilayer capsules. The contribution to the mechanical strength by the "complex" layers is not much different for both complexes used.

MATERIALS AND METHODS

Materials

Ova was obtained from Sigma-Aldrich Co., Missouri, USA (product no. A5503) with a purity of at least 98%. Lys from hen egg white was obtained from Sigma-Aldrich Co., Missouri, USA (3 × crystallized, lyophilized powder, product no. L6876). HMP was supplied by CP Kelco ApS, Lille Skensved, Denmark (JMH-6, batch no. 16849, degree of

methoxylation 69.8%). It was characterized in a study of Sagis *et al.*[17] and has a molecular weight of 2.7×10^3 kDa and a radius of gyration of 46 nm.

The oil n-hexadecane was from Merck Schuchardt OHG, Hohenbrunn, Germany (CAS-no. 544-76-3). The oil (R)-(+)-Limonene 97% was supplied by Sigma-Aldrich Co., Missouri, USA (CAS-no. 5989-27-5)

Thioflavin T (ThT) was obtained from Merck Schuchardt OHG, Hohenbrunn, Germany, (CAS-no. 2390-54-7, C.I. No. 49005). Fluorescein isothiocyanate isomer (FITC) was from Sigma-Aldrich Co., Missouri, USA (product no. CAS-no. 3326-32-7, F7250-1G)

All other chemicals used were of analytical grade, unless stated otherwise. All solutions were prepared with Millipore water (Millipore Corporation, Billerica, Massachusetts, USA). Samples were diluted to the desired concentration (if applicable) with the same buffer or solution used for the primary solutions

Preparing fibrils

On the basis of results from a study of Veerman *et al.*,[38] Ova solutions of 5% wt at pH 2 were heated at 80 °C for 24h to obtain Ova fibrils.

Lys fibrils with various lengths were prepared as described in a *chapter 2*.[39] Lys solutions of 2% wt at pH 2 were heated at 57 °C in a heating plate (RT15, IKA Werke, Germany) using magnetic stirring bars (20 mm × 6 mm, VWR International, West Chester, PA). Bottles containing about 18 mL of sample have an inner diameter of 24 mm. Stirring rates of approximately 290 and 550 rpm were applied. At these conditions, two types of fibrils were obtained: long and semi-flexible (called long Lys fibrils) (290 rpm); and short and rod-like (called short Lys fibrils) (550 rpm)

After heating, samples were quenched by cooling immediately on ice and subsequently stored at 4 °C for further investigations. Electron micrographs of the Ova and Lys fibrils were taken using a Philips CM12 electron microscope (Philips, Eindhoven, Netherlands) (Transmission electron microscopy – TEM).

Preparing protein – HMP complexes

HMP was dissolved in 10 mM phosphate buffers at pH 3.5 and pH 7 and was stirred overnight at 4 °C. The solutions were centrifuged at 20,000 ×g for 30 min to remove undissolved materials. The supernatants were filtered through Millipore Millex-HP filters (Hydrophilic PES 0.45 μm) (Millipore Corporation, Billerica, Massachusetts, USA). These solutions were further diluted to desired concentrations using the same buffer.

Ova and Lys were dissolved in 10 mM phosphate buffers at pH 3.5 and pH 7 respectively. These solutions were stirred overnight at 4 °C, and then were

centrifuged at 20,000 ×g for 30 min to remove un-dissolved materials. The concentrations of these solutions were determined with a UV spectrophotometer. These solutions were further diluted to 0.1% wt using the same buffer.

Protein and HMP solutions (0.1% wt) were mixed at ratios 2:1 and 4:1 for Ova and Lys respectively. OvaHMP 2:1 pH 3.5 complexes were spherical with a diameter of about 400 nm and negatively charged with a ξ-potential of about minus (–) 10 mV. LysHMP 4:1 pH 7 complexes were spherical with a diameter of about 200 nm and negatively charged with a ξ-potential of about minus (–) 20 mV (see *Chapter 3*). Dilutions of complexes up to 0.01% wt did not show significant changes in size and ξ-potential of the complexes.

Methods

Production of microcapsules
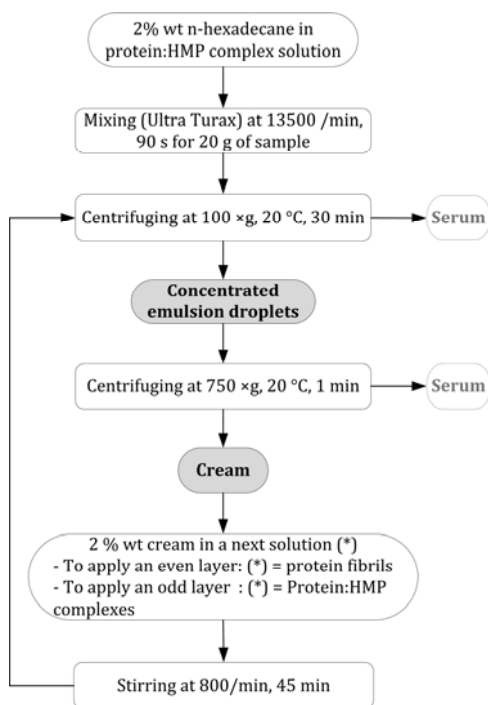
Figure 5.1. Scheme showing the process of making capsules

Microcapsules were prepared as described in *chapter 4*.[18] A 2% wt emulsion of n-hexadecane in 0.1% wt OvaHMP complex solution at pH 3.5 or 0.05% wt LysHMP solution at pH 7, was made by mixing with a rotor – stator mixer (Ultra Turrax) using a setting of 13,500 rpm for 90 s for a sample of 20 g of emulsion. Non-adsorbed

materials were removed from the emulsion droplets by centrifuging at 100 ×g for 30 min at 20 °C. The concentrated emulsion droplets ("cream" or one-layer microcapsules) were centrifuged again at 750 ×g for 1 min to remove excess solution. After that, the negatively charged droplets were dispersed in a fibril solution of 0.06% wt Ova fibrils at pH 3.5, or 0.03% wt Lys fibrils at pH 5. At these pH values, fibrils are positively charged, which allowed assembly driven by electrostatic interaction to form bi-layer microcapsules. These bilayer microcapsules were isolated by the same process and dispersed in the same solution used for the first layer. When this process is repeated, additional layers of encapsulating materials can be added (see **Figure 5.1**).

Microcapsules for mechanical stability experiments were prepared using an oil mixture of 75% wt n-hexadecane and 25% wt limonene. All other material concentrations and process conditions were as described above.

Light scattering measurements

The size distributions and ξ-potentials of the protein – HMP complexes were determined using a Zetasizer Nano (Malvern Instruments, Ltd. Worcestershire, UK). The size distribution and ξ-potential of the emulsion droplets and microcapsules were determined using a MasterSizer 2000 and a Zetasizer Nano (Malvern Instruments, Ltd. Worcestershire, UK). Creams were re-dispersed in buffer with the same pH prior to measurements to ensure that presence of excess polyelectrolytes (not adsorbed on the templates) was minimized. On each sample, three size distribution and five ξ-potential measurements were performed.

Confocal Laser Scanning Microscopy (CLSM)

To study the distribution of encapsulating materials on the emulsion droplets, ThT was used to label the fibrils and FITC was used to label either the HMP or the proteins in the complexes.

The dye ThT can have a specific binding to the β-sheets in amyloid fibrils[40 – 44] and is therefore widely used to determine the presence of fibrils.[42,45 – 50] A 3 mM ThT solution at pH 7 was prepared and filtered with Millex-GP filters of 0.22 μm pore size. This solution was diluted 50 times with the fibril solutions.

Covalently labeled HMP was prepared for labeling OvaHMP complexes. A HMP solution of 2 mg/mL at pH 9 was prepared. To each mL of the HMP solution, 1 μL of FITC solution (1 mg/mL DMSO) was added and stirred overnight at 4 °C. The excess of FITC was removed by centrifuging samples at approximately 90,000 ×g at 15 °C for 2h. The pellet was dissolved in a buffer pH 3.5. This labeled HMP was then used to make complexes with Ova.

A 2 mg/ml Lys solution was brought to pH 9. Then 1 μL of FITC solution (1 mg/ml DMSO) was added to every mililiter of protein solution. This solution was dialyzed against a phosphate buffer pH 9 under continuous stirring overnight in a cool room to remove the excessive FITC. Then, labeled Lys solution was diluted with phosphate buffer pH 7 to mix with the unlabeled HMP solution pH 7, forming labeled LysHMP complexes.

The emulsion droplets were observed under a Zeiss LSM5 Pascal confocal system mounted on an inverted microscope (Zeiss Axiovert 200). Images were taken with a Leica TCS SP under conditions described in **Table 5.1**

Table 5.1. Excitation wavelengths and emission maxima of the different fluorescent dyes

Fluorescent dye	Excitation wavelength (nm)	Emission maximum (nm)
Thioflavin T (ThT)	458	482
Fluorescein isothiocyanate (FITC)	488	518

Scanning Electron Microscopy (SEM)

To examine the structure of the shell of the microcapsules with SEM, samples were dried and the oil phase was evaporated using critical point drying (CPD). Dried microcapsules were fixed onto double-stick carbon tape, placed in a dedicated preparation chamber and sputter coated with 2 nm Tungsten (MED 020, Leica, Vienna, Austria). Samples were analyzed with a field emission scanning electron microscope (Magellan 400, FEI, Eindhoven, Netherlands) at room temperature at a working distance of 4 mm with SE detection at 2 kV. All images were recorded digitally.

Cryo – SEM imaging

Small drops of samples were placed between two aluminium (HPF) platelets (Wohlwend, Sennwald, Switzerland). Then, all samples were plunge-frozen in liquid ethane with a KF 80 (Leica, Vienna, Austria).

The frozen samples were mounted on a clamping sample holder under LN_2. After that, they were transferred to a non-dedicated cryo-preparation system (MED 020/VCT 100, Leica, Vienna, Austria) onto a sample stage at minus (–) 94 °C in high vacuum (1,3 × 10^{-6} mBar). In this cryo-preparation system, the samples were kept for 3 min, subsequently freeze-fractured, and immediately sputter coated with 5 nm Tungsten. The samples were transferred into the field emission scanning microscope (Magellan

400, FEI, Eindhoven, Netherlands) on the sample stage at minus (–) 121 °C (vacuum in the sample chamber of 4×10^{-7} mBar).

The analysis was performed at a working distance between 2 and 4 mm with ETD and TLD SE detection at 2 kV, 13 pA. All images were recorded digitally

Mechanical stability

The mechanical stability of the microcapsules was studied using a standard microscope connected to a temperature controlled stage (Analysa LTS120, Linkam Scientific Instruments Ltd., Surrey, U.K.). All samples (prepared at room temperature) were placed on a pre-heated stage at 90 °C, and the heat resistance time – the period for which the microcapsules maintain their spherical shape – was measured. Because the thermal coefficient of the internal oil phase differs from that of the aqueous continuous phase, the temperature increase results in a mechanical strain on the shell. This resistance time is a qualitative measure for the mechanical strength of the shells of capsules. Images of the process were recorded with a digital camera.

RESULTS AND DISCUSSIONS

Size and ξ-potential distribution

Light scattering measurements show that micocapsules from either system 1 or 2 are polydisperse (**Figure 5.2**). The Sauter mean diameters D (3,2) of the droplets from system 2 with either long or short Lys fibrils fluctuated between 4 and 6 μm which was in the same range as microcapsules from a previously studied system with Ova fibril and pure HMP (*chapter 4*).[18] Droplets from system 1, however, have diameters twice as large as those from the other systems. The size difference is already present in the template emulsion, and this shows that the ability to reduce the amount of free energy required to form droplets is lower for OvaHMP complexes than for LysHMP complexes. [51]

Droplets with even number of layers (outer layers are fibrils) are larger than those with odd number of layers (outer layers are protein – HMP complexes), even when the number of layers is lower. This is particularly true for capsules made with the stiffer Lys fibrils. This fluctuation in diameter could be due to the properties of the encapsulating materials: when stiffer fibrils with a persistence length close to the diameter of the capsules are adsorbed on the surface of the microcapsule, they may not be able to bend sufficiently to adsorb flat on the interface. They will then form a "hairy" layer around the capsule, with parts of the fibrils protruding into the solution. When the "hairy" surface structure of the even-layer droplets was brought into

contact with the complexes, it might be smoothened by interacting with the complexes, resulting in slightly smaller odd-layer droplets.
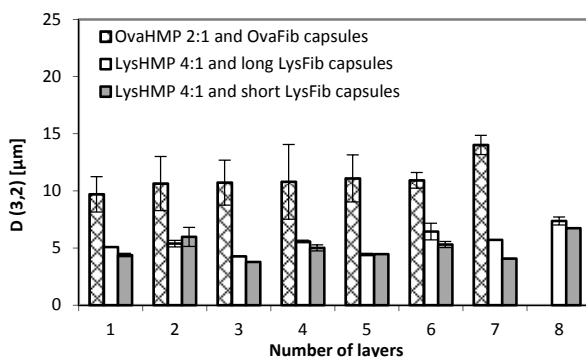
Figure 5.2. Sauter mean diameter D (3,2) of microcapsules with various number of layers. Odd layer number represents capsules with an outer layer of protein – HMP complexes. Even layer numbers represent capsules with an outer layer of protein fibrils. The error bars indicate the width of the distribution around the mean diameter values. First column: Capsules prepared with OvaHMP 2:1 complexes and Ova fibrils. Second column: capsules prepared with LysHMP 4:1 complexes and long Lys fibrils. Third (filled) column: capsules prepared with LysHMP 4:1 complexes and short Lys fibrils.
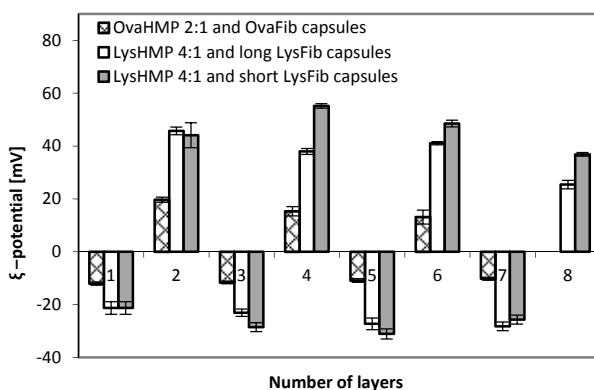
Figure 5.3. ζ-potential distribution of microcapsules with various layers of encapsulating materials. Bar sequence is similar to that in **Figure 5.2**.

The microcapsules from both systems did not show significant change in size distribution from one layer to seven or eight layers, even after weeks of storage. This shows that microcapsules made by LbL deposition of protein – HMP complexes and protein fibrils are highly stable over long periods of time.

One of the parameters to monitor the adsorption of oppositely charged polyelectrolytes on microcapsules in the LbL process is to measure their surface net charge. LbL adsorption based on electrostatic interaction leads to a surface charge reversion;[14,16,52,53] i.e., the final outer layer normally determines the interfacial net charge.[13, 15] The ξ-potential distribution of microcapsules switches from negative (odd number of layers with protein – HMP complexes as outer layers) to positive (even number of layers with protein fibrils as the outer layer), confirming the LbL adsorption of materials (**Figure 5.3**). There is a slight decrease in the positive charges as a function of number of (even) layers while the charges of odd-layer droplets were stable or increased as the layer number increased.

CLSM

Results from the imaging of the microcapsules with CSLM are shown in **Figure 5.4**. ThT adsorbs to the β-sheets formed in amyloid fibril.[42,43] Therefore, it is used to observe the adsorption of fibrils on the microcapsules. FITC was bound covalently to one component of the protein – HMP complexes. The fluorescence signals (**Figure 5.4**) confirm the adsorption of alternating layers of fibrils and complexes on the emulsion droplet templates, in line with the results of ξ-potential measurements. These signals also visualize the inhomogeneity of the shells of the microcapsules. The inhomogeneous distribution of encapsulating materials was observed for both materials: complexes and fibrils. Because the excitation maxima of ThT (482 nm) and FITC (518 nm) are close to each other, it was not possible to observe their signals at the same time to be able to visualize their interaction in the shell.
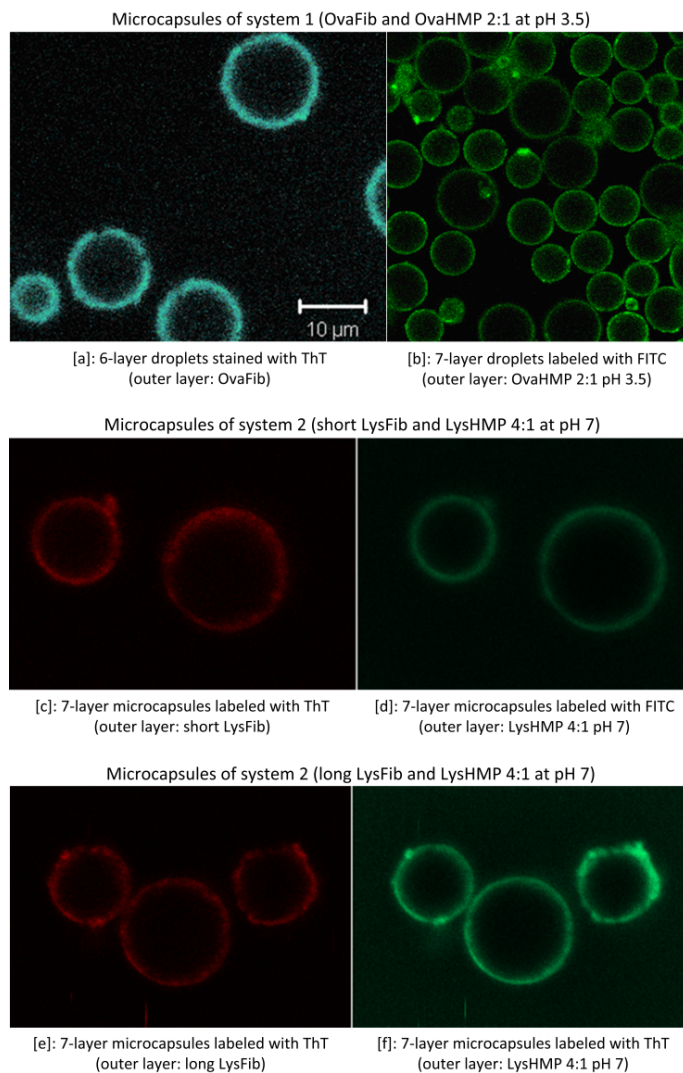
Figure 5.4. CSLM picture showing the material adsorption on microcapsules of system 1 ((a) and (b)) and system 2 ((c) – (f)). (a): 6-layer microcapsules stained with ThT (outer layer: Ova fibrils); (b): 7-layer microcapsules labeled with FICT (outer layer: OvaHMP 2:1); (c) and (d): 7-layer microcapsules labeled with ThT (c) and FITC (d) prepared with short Lys fibrils; (e) and (f): 7-layer microcapsules labeled with ThT (e) and FITC (f) prepared with long Lys fibrils.

SEM and Cryo – SEM

The results from the analysis of the capsules with SEM and Cryo – SEM are shown in **Figure 5.5** to **Figure 5.8.** Microcapsules of both systems were dried by the same critical point drying method. Because SEM pictures of microcapsules with short Lys fibrils were quite similar in surface structure to those with long Lys fibrils, they were not included in **Figure 5.6.** Apparently, the difference in size and flexibility between these two types of Lys fibrils did not have a significant effect on the structure of the shell of the microcapsules.
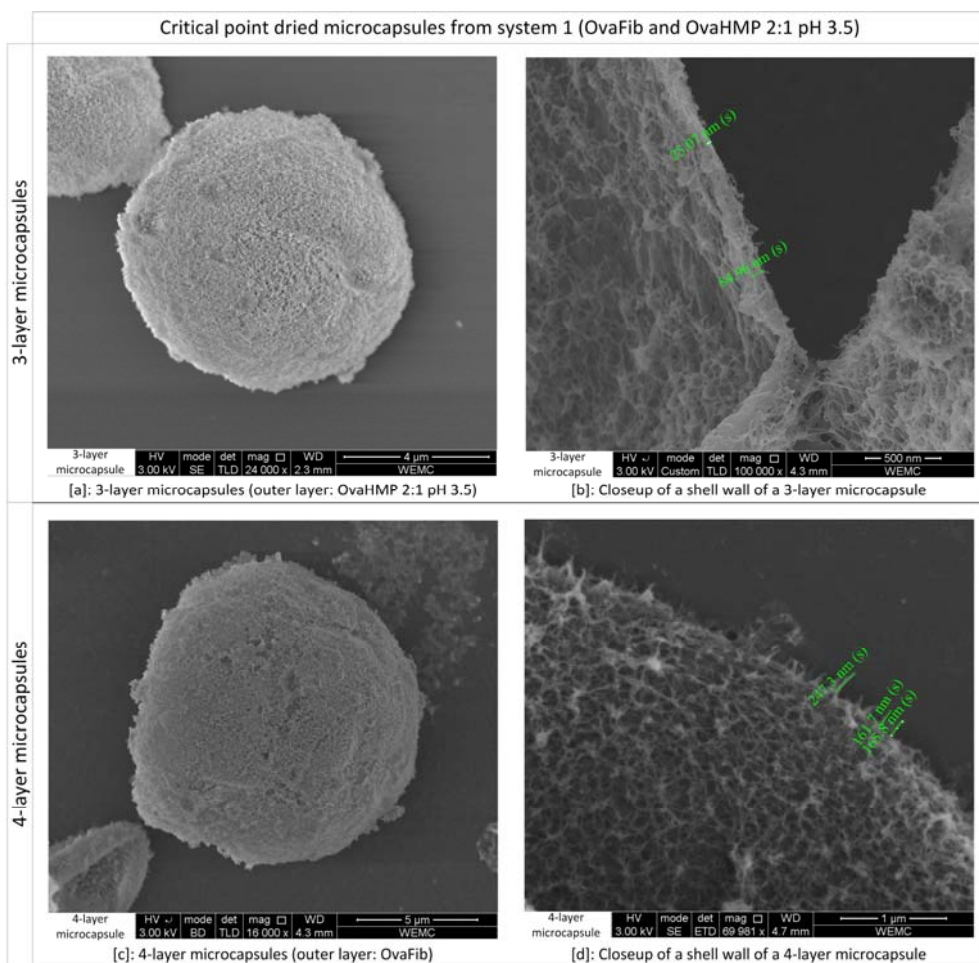
Figure 5.5. [A] SEM pictures showing the structure of the outer layer of microcapsules from system1 (OvaHMP 2:1 and OvaFib). (a) and (b): 3-layer; (c) and (d): 4-layer
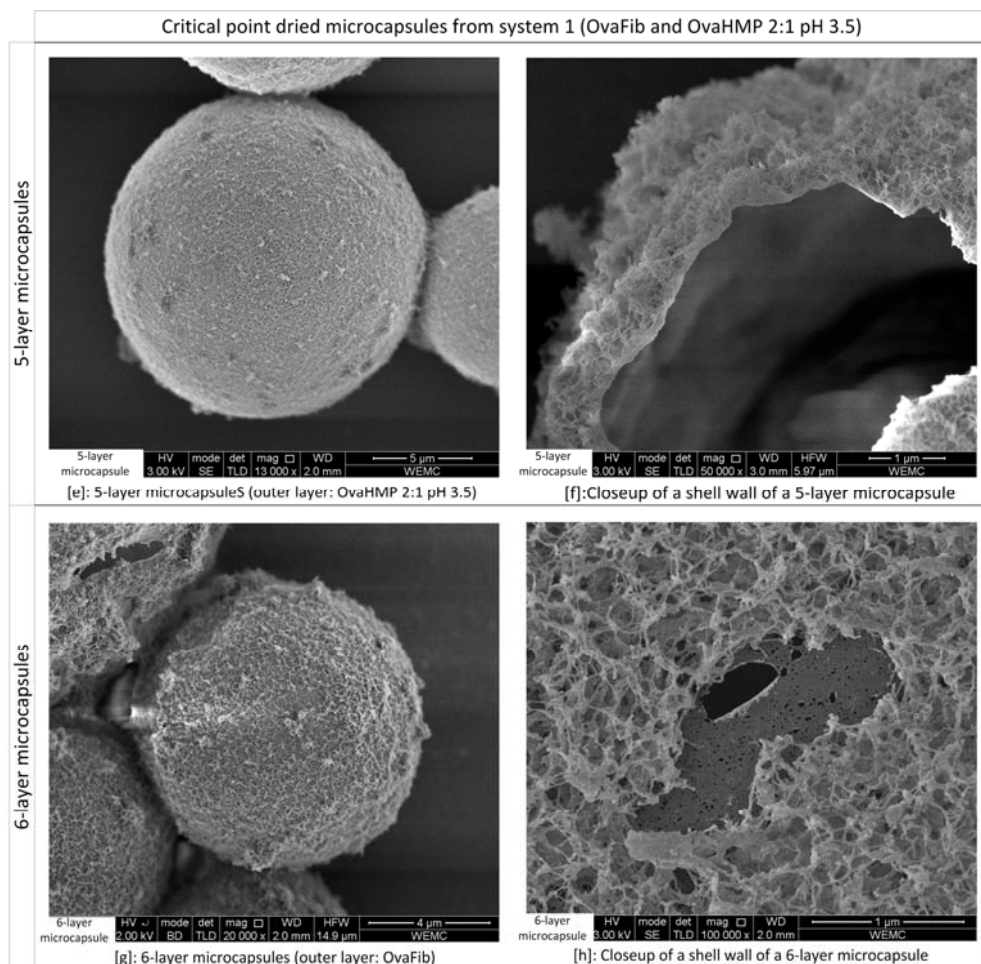
Figure 5.5. [B] SEM pictures showing the structure of the outer layer of microcapsules from system1 (OvaHMP 2:1 and OvaFib). (e) and (f): 5-layer; (g) and (h): 6-layer

Figure 5.5 and **Figure 5.6** show that microcapsules prepared with OvaHMP 2:1 and Ova fibrils (system 1) were more resistant to the drying process than those prepared with LysHMP 4:1 and Lys fibrils (system 2). The shell structure of microcapsules from system 1 was also denser than that of microcapsules from system 2.

In system 1, the "hairy" structure of microcapsules with an even number of layers could clearly be observed. In the SEM picture of a 4-layer microcapsule, it can be seen that adsorbed Ova fibrils were protruding from the surface. When the next layer of material was adsorbed, the shell was smoothened. Unfortunately, that phenomenon could not be observed in system 2, due to collapsing of the microcapsules after drying, for capsules with five or fewer layers. For system 2, the images clearly indicate that

the strength of the microcapsule shell increases when the number of adsorbed layers increases. Whereas shells with five or fewer layers have all collapsed after drying, capsules with six or more layers remain spherical.

Figure 5.6. [A] SEM pictures showing the structure of the outer layer of microcapsules from system 2 (LysHMP 4:1 and long LysFib). (a) and (b): 3-layer; (c) and (d): 4-layer
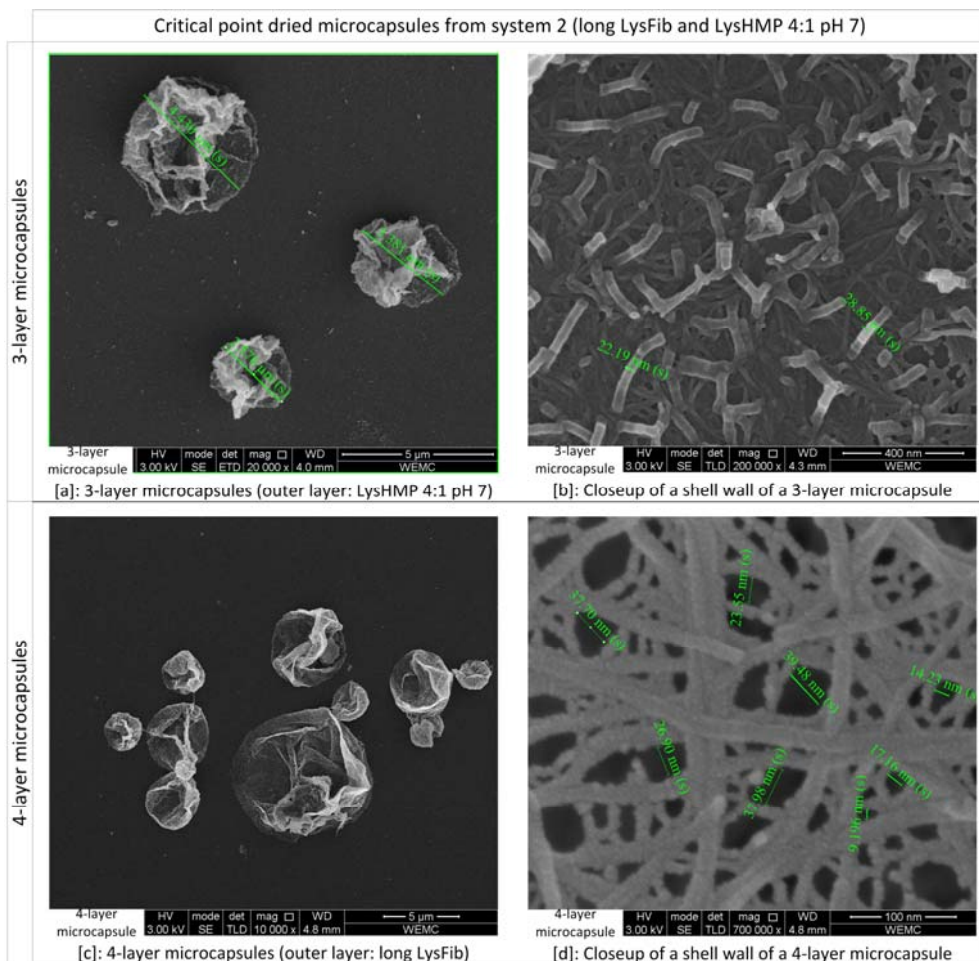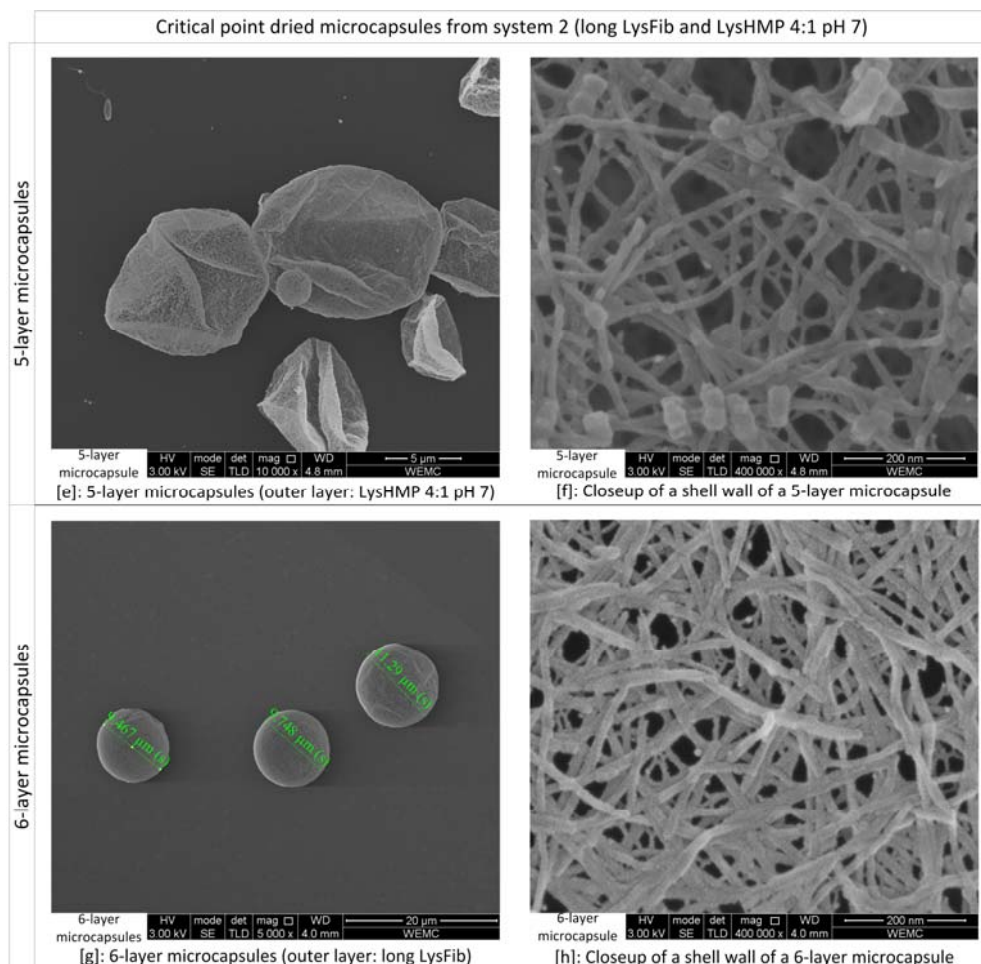
Figure 5.6. [B] SEM pictures showing the structure of the outer layer of microcapsules from system 2 (LysHMP 4:1 and long LysFib). (e) and (f): 5-layer; (g) and (h): 6-layer

Close-up pictures of the microcapsules of system 1 (**Figure 5.7**) and system 2 with long Lys fibrils (**Figure 5.6**) show that their shells are quite inhomogeneous and consist of layers of networks of fibrils with relatively large pores and a considerable number of defects. Increasing the number of layers does seem to decrease the sizes of pores and decrease the number of defects. The thicknesses of the strands in the network are similar to the diameter of a single protein fibril.
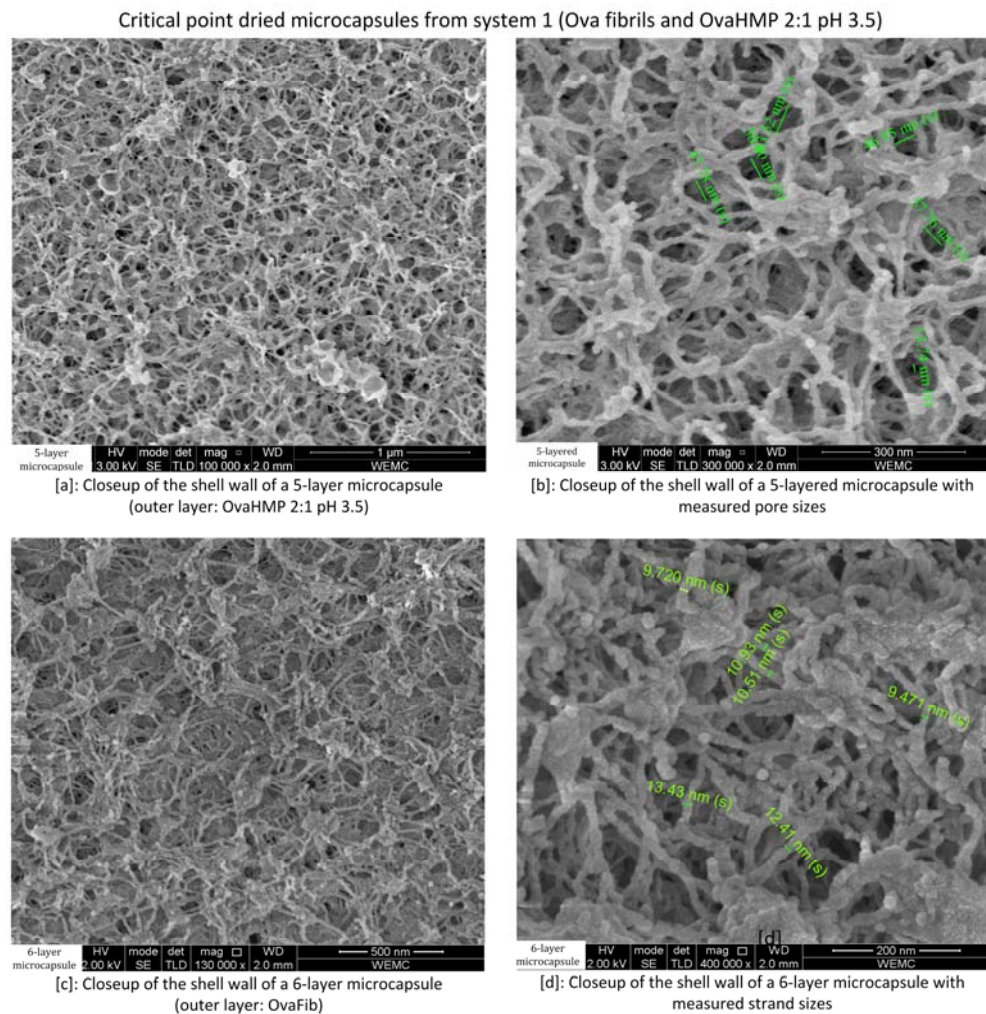
Figure 5.7. SEM pictures showing the structure of the outer layer of (a) and (b): 5-layer with OvaHMP 4:1 as the outer layer; (c) and (d): 6-layer microcapsules from system 2 with Ova fibrils as the outer layer. The microcapsules were obtained by critical point drying to remove the inner phase (oil).

Freeze-fractured 8-layer microcapsules from system 2 (long Lys fibrils and LysHMP 4:1 pH 7)

[a] and [b]: 8-layer microcapsules with measured shell wall thickness. Spherical objects are frozen inner oil phase.

[c] and [d]: Closeup of 8-layer microcapsules with measured shell wall thickness (left) and shell wall structure (right).
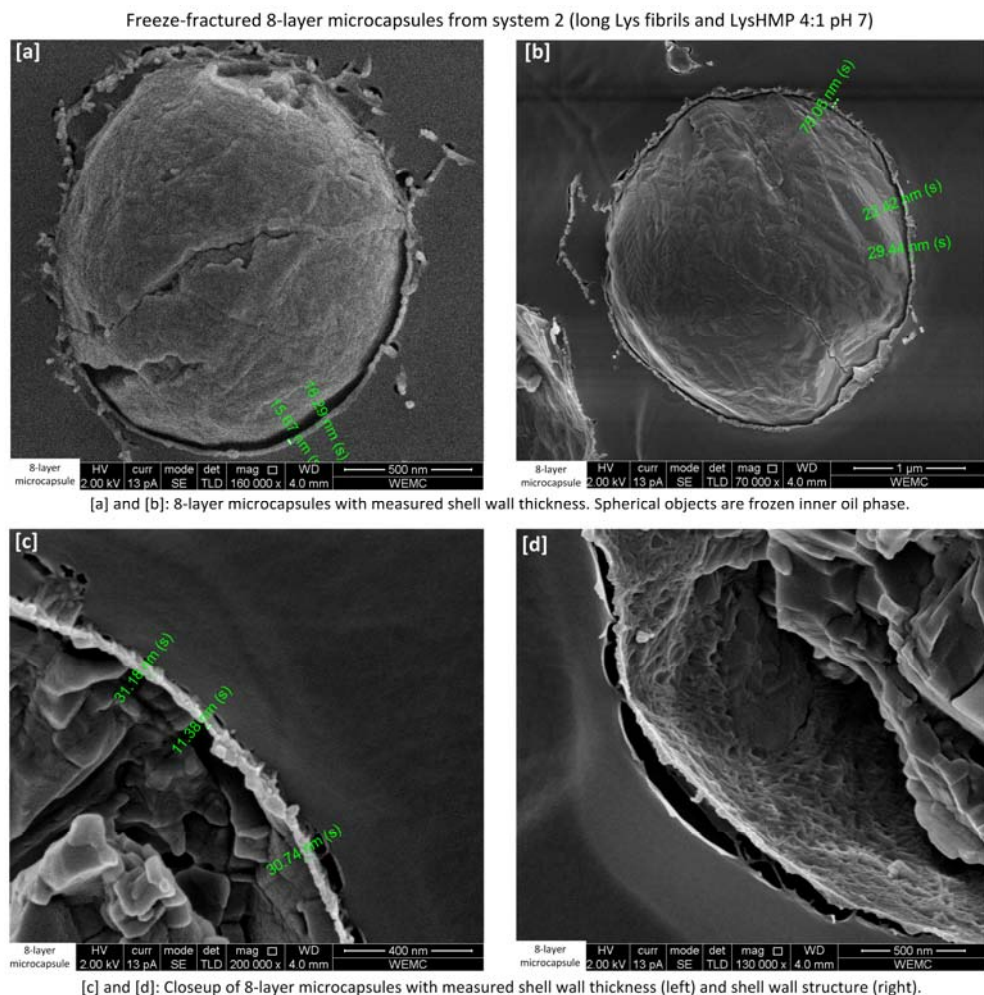
Figure 5.8. Cryo – SEM pictures showing the structure of 8-layer microcapsules prepared from LysHMP 4:1 complexes (odd layers) and long Lys fibrils (even layers). The samples were freeze fractured, after flash freezing in liquid ethane.

The structure of microcapsule shells was also studied with cryo – SEM. In **Figure 5.8(d)** we see that the network structure of the shell in a frozen state is similar to the structure observed in dried microcapsules. This shows that the preparation steps (critical point drying for SEM, and flash freezing for Cryo-SEM) had little effect on the structure of the shell. From panels a – c of **Figure 5.8**, we can obtain an indication of the thickness of the shells of the microcapsules. We see that 8-layer shells have a thickness that varies from less than 20 nm to more than 70 nm, confirming the

inhomogeneity of the microcapsule shells observed in CLSM and SEM pictures of dried microcapsules.

Mechanical stability

In this experiment, we obtained a qualitative measure for the mechanical strength of the capsule shells by exposing them to a high temperature (90 °C) and measuring the time for which the capsules remain spherical, as observed under the microscope. In the SEM experiments, we saw little difference in the structure of the shell of capsules made with either short or long Lys fibrils. These findings are confirmed by the heat stability measurements, where we do not find a significant difference in the dependence of the heat resistance time on the number of layers (**Figure 5.9**).
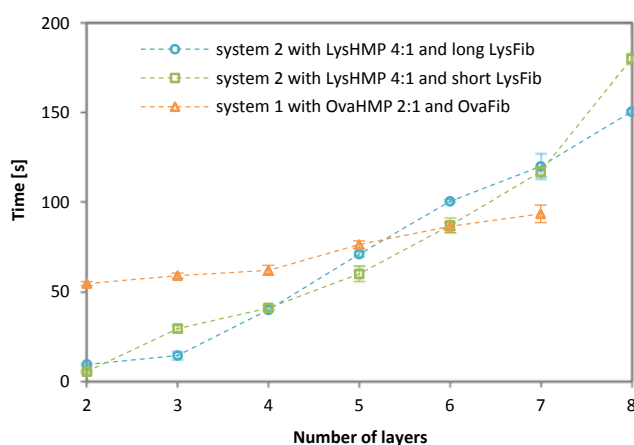
Figure 5.9. Heat resistance time *vs.* number of layers when microcapsules were heated at 90 °C. (Δ): micocapsules from system 1 with OvaHMP 2:1 and Ova fibrils; (o): micocapsules from system 2 with LysHMP 4:1 and long Lys fibrils; and (□): micocapsules from system 2 with LysHMP 4:1 and short Lys fibrils.

From the results of these measurements, it can be seen that microcapsules of system 1 were stronger than those from system 2, for shells with four or fewer layers. The slope of the curves in **Figure 5.9** is, however, considerably steeper for system 2 than for system 1. The short and semi-flexible Ova fibrils, combined with the larger OvaHMP 2:1 complex (a factor 2 larger than LysHMP 4:1 complex), apparently result in a more compact and stretchable shell, whereas the stiffer Lys fibrils result in more inhomogeneous and more brittle shells.

In SEM experiments with dried samples, 3-layer microcapsules from system 1 already remained spherical after drying, while only the 6-layer microcapsules from system 2

could retain their spherical shape. In **Figure 5.9** we see that the 3-layer capsules of system 1 have a heat resistance time similar to that of the 6-layer particles of system 2. These findings show we can tune the mechanical properties of these types of microcapsules by changing the properties of the fibrils.

CONCLUSIONS

In this study we have used the LbL technique to produce microcapsules using food-grade materials and simple operations. In general, the microcapsules are poly-dispersed with a Sauter diameter D(3,2) less than 10 μm. In systems produced with LysHMP complexes and Lys fibrils, no significant difference was observed in mechanical stability between capsules produced with short and rod-like fibrils, and capsules produced with long and semi-flexible. In this system, increasing the number of layers from 2 to 8, increased the heat resistance time (when heating at 90 °C) by more than 15 times. Capsules prepared with semi-flexible Ova fibrils and OvaHMP complexes were stronger than systems based on Lys, for capsules with 4 or fewer layers. But the increase of the heat resistance time with layer number was much smaller for the Ova system (approximately a factor 1.5 in going from 2 to 7 layers). The differences in mechanical strength between these systems were also reflected in the SEM images of critical point dried capsules where 3-layer – capsules prepared with Ova fibrils and OvaHMP remained intact whereas only 6-layer – capsules prepared with Lys fibrils and LysHMP could maintain their spherical shape. Capsules prepared with OvaHMP and semi-flexible Ova fibrils tend to have a more homogeneous and stretchable shell than capsule prepared with LysHMP and more rigid Lys fibrils. These tend to have shells that are more inhomogeneous and brittle. By changing the properties of the fibrils we can clearly tune the mechanical properties of the shell of this type of multilayer capsule.

ACKNOWLEDGEMENTS

REFERENCES

1 Green, B. K. & Schleicher, L. Pressure Responsive Record Materials. 2730456, 2730457 (1956).

2 Madene, A., Jacquot, M., Scher, J. & Desobry, S. Flavour Encapsulation and Controlled Release: A Review. *Int J Food Sci Tech* **41**, 1 – 21 (2006).

3 Dziezak, J. D. Microencapsulation and Encapsulated Ingredients. *Food Technol.* **42**, 136 – 151 (1988).

4 Schrooyen, P. M. M., Meer, R. V. D. & Kruif, C. G. D. Microencapsulation: Its Application In Nutrition. *P Nutr Soc* **60**, 475 – 479 (2001).

5 Jackson, L. S. & Lee, K. Microencapsulation and The Food Industry. *Lebensm Wiss Technol* **24**, 289 – 297 (1991).

6 Shahidi, F. & Han, X.-Q. Encapsulation of Food Ingredients. *Crit Rev Food Sci* **33**, 501 – 547 (1993).

7 F. Gibbs, S. K., Inteaz Alli, Catherine N. Mulligan, Bernard, Encapsulation In The Food Industry: A Review. *Int J Food Sci Tech* 1999, **50,** 213 – 224 (1999)

8 Dewettinck, K. & Huyghebaert, A. Fluidized Bed Coating In Food Technology. *Trends Food Sci Tech* **10**, 163 – 168 (1999).

9 Rosenberg, M. & Sheu, T. Y. Microencapsulation of Volatiles By Spray-Drying In Whey Protein-Based Wall Systems. *Int Dairy J* **6**, 273 – 284 (1996).

10 Decher, G. & Hong, J. D. Buildup of Ultrathin Multilayer Films By A Self-Assembly Process: I. Consecutive Adsorption of Anionic and Cationic Bipolar Amphiphiles. *Makromol. Chem., Macromol. Symp.* **46**, 321 – 327 (1991).

11 Decher, G. & Hong, J. D. Buildup of Ultrathin Multilayer Films By A Self-Assembly Process: Ii. Consecutive Adsorption of Anionic and Cationic Bipolar Amphiphiles and Polyelectrolytes On Charged Surfaces. *Ber. Bunsenges. Phys. Chem.* **95**, 1430 – 1434 (1991).

12 Decher, G., Hong, J. D. & Schmitt, J. Buildup of Ultrathin Multilayer Films By A Self-Assembly Process: Iii. Consecutively Alternating Adsorption of Anionic and Cationic Polyelectrolytes On Charged Surfaces. *Thin Solid Films* **210 – 211**, 831 – 835 (1992).

13 McClements, D. J. Theoretical Analysis of Factors Affecting The Formation and Stability of Multilayered Colloidal Dispersions. *Langmuir* **21**, 9777 – 9785 (2005).

14   Ai, H., Jones, S. A. & Lvov, Y. M. Biomedical Applications of Electrostatic Layer-By-Layer Nano-Assembly of Polymers, Enzymes, and Nanoparticles. *Cell Biochem Biophys* **39**, 23 – 43 (2003).

15   Decher, G. (Eds Gero Decher & Joseph B. Schlenoff) 1 – 46 (Wiley – Vch, 2003).

16   Peyratout, C. S. & Dähne, L. Tailor-Made Polyelectrolyte Microcapsules: From Multilayers To Smart Containers. *Angew Chem Int Edit* **43**, 3762 – 3783 (2004).

17   Sagis, L. M. C. *et al.* Polymer Microcapsules With A Fiber–Reinforced Nanocomposite Shell. *Langmuir* **24**, 1608 – 1612 (2008).

18   Humblet-Hua, K. N. P., Scheltens, G., van der Linden, E. & Sagis, L. M. C. Encapsulation Systems Based On Ovalbumin Fibrils and High Methoxyl Pectin. *Food Hydrocolloid* **25**, 569 – 576 (2011).

19   Mauser, T., Déjugnat, C. & Sukhorukov, G. B. Balance of Hydrophobic and Electrostatic Forces In The pH Response of Weak Polyelectrolyte Capsules. *J Phys Chem B* **110**, 20246 – 20253 (2006).

20   Wang, C. *et al.* Microcapsules For Controlled Release Fabricated Via Layer-By-Layer Self-Assembly of Polyelectrolytes. *J Exp Nanosci* **3**, 133 – 145 (2008).

21   Ye, A. Complexation Between Milk Proteins and Polysaccharides Via Electrostatic Interaction: Principles and Applications – A Review. *Int J Food Sci Tech* **43**, 406 – 415 (2008).

22   Schmitt, C. & Turgeon, S. L. Protein/Polysaccharide Complexes and Coacervates In Food Systems. *Adv Colloid Interfac* **167**, 63 – 70 (2011).

23   Huntington, J. A. & Stein, P. E. Structure and Properties of Ovalbumin. *J Chromatogr B* **756**, 189 – 198 (2001).

24   Imoto, T., Johnson, L. N., North, A. C. T., Phillips, D. C. & Rupley, J. A. In *The Enzymes* Vol. Volume 7 (Ed D. Boyer Paul) 665 – 868 (Academic Press, 1972).

25   Schmidt, I., Cousin, F., Huchon, C., Boué, F. & Axelos, M. A. V. Spatial Structure and Composition of Polysaccharide – Protein Complexes From Small Angle Neutron Scattering. *Biomacromolecules* **10**, 1346 – 1357 (2009).

26   Dalev, P. G. & Simeonova, L. S. Emulsifying Properties of Protein – Pectin Complexes and Their Use In Oil-Containing Foodstuffs. *J Sci Food Agr* **68**, 203 – 206 (1995).

27   Kudryashova, E. V., Visser, A. J. W. G., Van Hoek, A. & De Jongh, H. H. J. Molecular Details of Ovalbumin – Pectin Complexes At The Air/Water Interface: A Spectroscopic Study. *Langmuir* **23**, 7942 – 7950 (2007).

28   Zaleska, H., Mazurkiewicz, J., Tomasik, P. & Ba¸Czkowicz, M. Electrochemical Synthesis of Polysaccharide – Protein Complexes. Part 2. Apple Pectin – Casein Complexes. *Nahrung/Food* **43**, 278 – 283 (1999).

29   Benichou, A., Aserin, A. & Garti, N. Protein – Polysaccharide Interactions For Stabilization of Food Emulsions. *J Disper Sci Technol* **23**, 93 – 123 (2002).

30   Girard, M., Turgeon, S. L. & Gauthier, S. F. Thermodynamic Parameters of β-Lactoglobulin – Pectin Complexes Assessed By Isothermal Titration Calorimetry. *J Agr Food Chem* **51**, 4450 – 4455 (2003).

31   Weinbreck, F., De Vries, R., Schrooyen, P. & De Kruif, C. G. Complex Coacervation of Whey Proteins and Gum Arabic. *Biomacromolecules* **4**, 293 – 303 (2003).

32   Cooper, C. L., Dubin, P. L., Kayitmazer, A. B. & Turksen, S. Polyelectrolyte–Protein Complexes. *Curr Opin Colloid In* **10**, 52 – 78 (2005).

33   Krebs, M. R. H. *et al.* Formation and Seeding of Amyloid Fibrils From Wild-Type Hen Lysozyme and A Peptide Fragment From The A–Domain. *J Mol Biol* **300**, 541 – 549 (2000).

34   Goda, S. *et al.* Amyloid Protofilament Formation of Hen Egg Lysozyme In Highly Concentrated Ethanol Solution. *Protein Sci* **9**, 369 – 375 (2000).

35   Cao, A., Hu, D. & Lai, L. Formation of Amyloid Fibrils From Fully Reduced Hen Egg White Lysozyme. *Protein Sci* **13**, 319 – 324 (2004).

36   Arnaudov, L. N. & De Vries, R. Thermally Induced Fibrillar Aggregation of Hen Egg White Lysozyme. *Biophys. J.* **88**, 515 – 526 (2005).

37   Akkermans, C. *et al.* Shear Pulses Nucleate Fibril Aggregation. *Food Biophys* **1**, 144 – 150 (2006).

38   Veerman, C., De Schiffart, G., Sagis, L. M. C. & van der Linden, E. Irreversible Self-Assembly of Ovalbumin Into Fibrils and The Resulting Network Rheology. *Int J Biol Macromol* **33**, 121 – 127 (2003).

39   Humblet-Hua, N.-P., Sagis, L. M. C. & van der Linden, E. Effects of Flow On Hen Egg White Lysozyme (HEWL) Fibril Formation: Length Distribution, Flexibility, and Kinetics. *J Agr Food Chem* **56**, 11875 – 11882 (2008).

40   Nilsson, M. R. Techniques To Study Amyloid Fibril Formation In Vitro. *Methods* **34**, 151 – 160 (2004).

41   Azakami, H., Mukai, A. & Kato, A. Role of Amyloid Type Cross B – Structure In The Formation of Soluble Aggregate and Gel In Heat-Induced Ovalbumin. *J Agr Food Chem* **53**, 1254 – 1257 (2005).

42   Krebs, M. R. H., Bromley, E. H. C. & Donald, A. M. The Binding of Thioflavin–T To Amyloid Fibrils: Localisation and Implications. *J. Struct. Biol.* **149**, 30 – 37 (2005).

43   Bolder, S. G., Sagis, L. M. C., Venema, P. & van der Linden, E. Thioflavin T and Birefringence Assays To Determine The Conversion of Proteins Into Fibrils. *Langmuir* **23**, 4144 – 4147 (2007).

44   Khodarahmi, R., Soori, H. & Karimi, S. A. Chaperone-Like Activity of Heme Group Against Amyloid-Like Fibril Formation By Hen Egg Ovalbumin: Possible Mechanism of Action. *Int J Biol Macromol* **44**, 98 – 106 (2009).

45   Bromley, E. H. C., Krebs, M. R. H. & Donald, A. M. Aggregation Across The Lengthscales In B-Lactoglobulin. *Faraday Discuss.* **128**, 13 – 27 (2005).

46   Naiki, H., Higuchi, K., Hosokawa, M. & Takeda, T. Fluorometric Determination of Amyloid Fibrils In Vitro Using The Fluorescent Dye, Thioflavine T. *Anal Biochem* **177**, 244 – 249 (1989).

47   Levine Iii, H. & Ronald, W. Quantification of β-Sheet Amyloid Fibril Structures With Thioflavin T *Method Enzymol* **309** 274 – 284 (1999).

48   Nielsen, L. *et al.* Effect of Environmental Factors On The Kinetics of Insulin Fibril Formation: Elucidation of The Molecular Mechanism. *Biochemistry* **40**, 6036 – 6046 (2001).

49   Groenning, M. *et al.* Binding Mode of Thioflavin T In Insulin Amyloid Fibrils. *J Struct Biol* **159**, 483 – 497 (2007).

50   Kroes-Nijboer, A., Lubbersen, Y. S., Venema, P. & van der Linden, E. Thioflavin T Fluorescence Assay For β–Lactoglobulin Fibrils Hindered By Daph. *J Struct Biol* **165**, 140 – 145 (2009).

51   McClements, D. J. Biopolymers In Food Emulsions. In *Modern Biopolymer Science*; Stefan, K., Norton, I. T., Ubbink, J. B., Eds.; Academic Press: New York, **2009**; Chapter 4, Pp 129–166.

52   Schönhoff, M. Layered Polyelectrolyte Complexes: Physics of Formation and Molecular Properties. *J Phys – Condens Mat*, R1781 (2003).

53   Dickinson, E. Mixed Biopolymers At Interfaces: Competitive Adsorption and Multilayer Structures. *Food Hydrocolloid* **25**, 1966 – 1983 (2011).

CHAPTER 6

GENERAL DISCUSSION

The aim of the work described in this thesis was to design novel core-shell encapsulating systems using mesostructures from proteins and polysaccharides. The thesis starts with a discussion of the characterization of the properties of these materials and ends with the mechanical and release properties of the final microcapsules (**Figure 6.1**). We have used the simple and easy to control layer-by-layer (LbL) adsorption technique and standard operations (including mixing and centrifuging) to produce the capsules. The templates of the microcapsules were oil-in-water emulsion droplets that can contain functional ingredients to be encapsulated. The mesostructures used for constructing the shell of the capsules are protein fibrils and protein – polysaccharide complexes from commonly used food-grade components: lysozyme (Lys), ovalbumin (Ova) and high methoxyl pectin (HMP). For Lys, we applied shear during heating to tune the length of the Lys fibrils *(chapter 2).* Ova fibrils were prepared as described in previous studies.[1,2] By mixing proteins (Ova and Lys) with HMP at specific conditions (pH, concentrations and mixing ratios), we could obtain complexes with desired sizes and charges *(chapter 3)*. The differences between these mesostructures led to different rheological properties at the oil – water interface *(chapter 3)*. Using these materials as building blocks for the shell of microcapsules resulted in capsules with tunable mechanical properties *(chapter 4* and *chapter 5)*
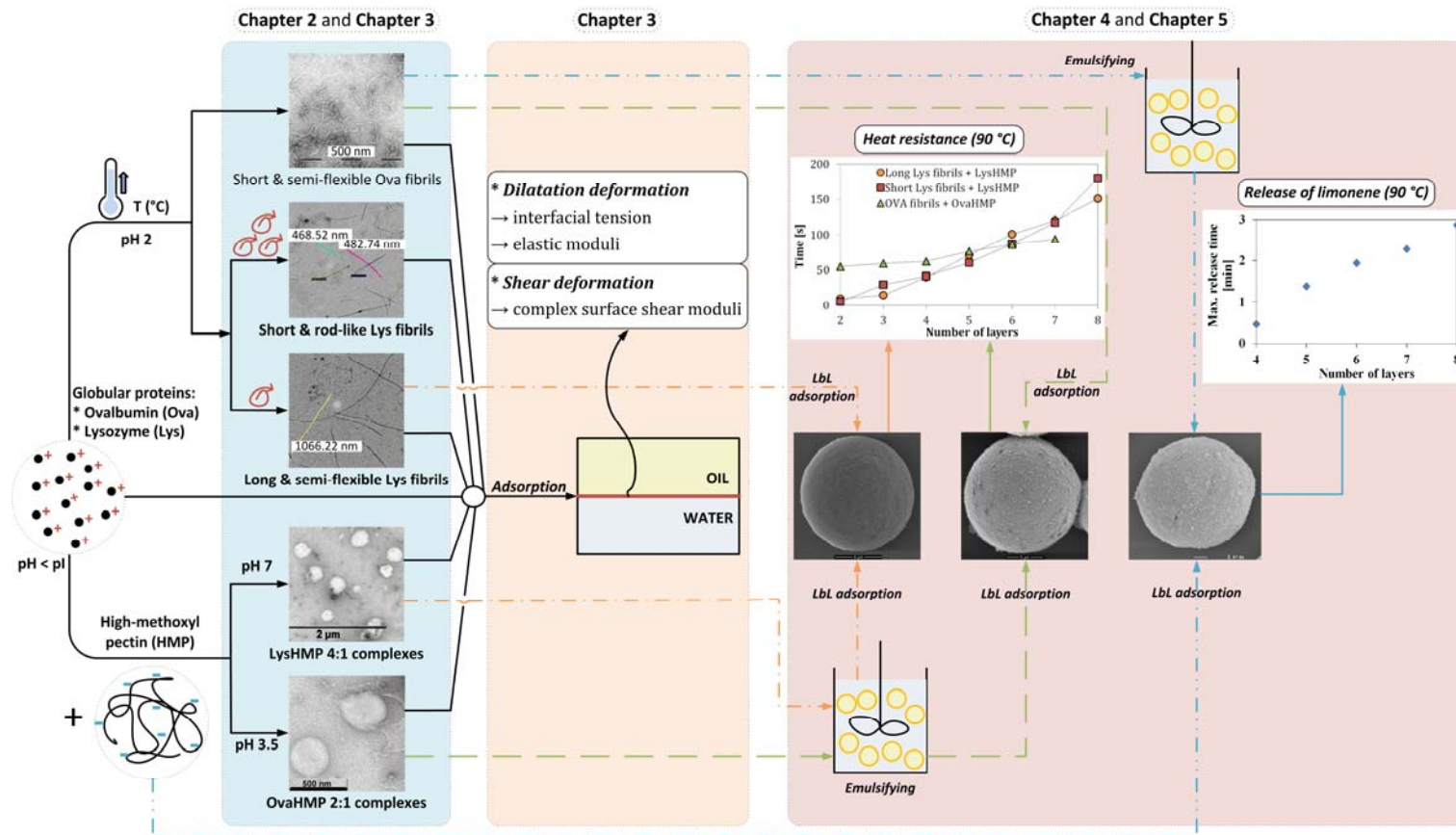
Figure 6.1. Thesis overview

ENCAPSULATING MATERIALS

Protein fibrils

One of the encapsulating materials of interest is fibrils from proteins. Fibril formation is an important example of protein self-assembly.[3–6] It can be controlled by changing the chemical and physical environment of the protein or polypeptide.[7] It was known from previous studies that the formation of fibrils can be induced by elevating temperatures, close to the protein denaturation temperature,[8–10] and/or adding denaturants such as alcohols, salts or metal ions to destabilize the native conformation of the protein.[11] There are two major routes for fibril formation. In one route the proteins are first partially unfolded, and fibrils are formed by inter-strand-alignment of β-sheets. In the other route hydrolysis of the proteins occurs at elevated temperatures, forming peptides. These peptide fragments will then assemble into fibrils.[12–15] For Lys, the inducing conditions will define the formation path.[16–21] A small change in the inducing conditions may consequently change the structure of the fibrils obtained (Jones and Mezzenga[15] and references therein).

We have studied the effects of flows (shear and turbulent) during heating (57 °C) on the length distribution, flexibility and formation rate of fibrils from Lys (*chapter 2*). Applying shear during the fibril formation process has been proved to enhance the rate of fibril formation of β-lactoglobulin.[22,23] The results of our study have shown that flow can also affect the formation rate of Lys fibrils. Both steady shear and turbulent flows increase the conversion rate of Lys proteins into fibrils, similar to what was found in other studies on other proteins.[22–26] Moreover, we have found that flow influences the morphology of the fibrils: higher shearing or stirring rates resulted in shorter fibrils, while at rest or at the lower rates longer semi-flexible fibrils were obtained. In the range of flows applied, a range of sizes (from a few hundreds nanometers to several microns), and flexibilities of the fibrils (from rod-like to semi-flexible) can be obtained. The type of flow also affects the width of the size distribution of the fibrils. In order to obtain fibrils with narrow length distribution, shear flow should be applied since the spatial inhomogeneity of turbulent flows results in fibrils with a wide range of lengths. Those effects of flow were not found for β-lactoglobulin, where the length of the fibrils can be influenced only to a minor extent, and it appears that shear flow results in only slightly shorter fibrils,[23] in spite of the fact that many similarities between the fibril formation of these two proteins were reported in literature.[24] Even the molecular weights of peptide fragments, the secondary structure evolution, and the morphology of the final fibrils are strikingly similar between Lys and β-lactoglobulin.[20,24]

Ova fibrils were obtained by heating Ova monomer solutions at pH 2 at 80 °C. At these conditions, Ova monomers assemble irreversibly into semi-flexible fibrils with a contour length of a few hundred nanometer and effective diameters of a few nanometer.[1]

Protein – polysaccharide complexes

Another type of building blocks used for the shell of the microcapsules was complexes of proteins and polysaccharides. Protein – polysaccharide complexes were shown to have high surface activity, and to have the ability to form thick, gel-like and charged adsorbed layers at fluid – fluid interfaces.[27,28] The mechanical strength of that adsorbed layer, together with the electrostatic and steric repulsion it induces, are the most important factors influencing the kinetic stability of oil-in-water emulsion droplets,[29] and will also affect the stability of emulsion-based microcapsules produced with these complexes. Therefore, protein – polysaccharide complexes can be used as emulsion stabilizers. In fact, one of the most important applications of protein – polysaccharide complexes is forming microcapsules by forming a solid film around emulsion droplets containing encapsulated materials (e.g. aroma compounds) (Benichou *et al.*[30] and references therein). Besides, complexes carry charges that make them suitable for layer-by-layer adsorption based on electrostatic attraction to build up multilayer microcapsules.

The mixing ratios between protein and polysaccharide can influence the characteristics and size of the complexes formed.[31,32] In a mixture with a high proportion of proteins, very large complexes with an excess amount of protein will form.[32] When mixing 0.1 % wt of Ova (pH 3.5) or Lys (pH 7) with HMP at the same concentration and pH, ratios of protein:HMP of 12:1 and 8:1 (wt:wt) resulted in co-precipitate complexes. A ratio of Ova:HMP equal to 2:1 (at pH 3.5) results in spherical complexes with a diameter of about 400 nm and a ξ-potential of about minus (–) 10 mV. A ratio of Lys:HMP equal to 4:1 (at pH 7) results in spherical complexes with a diameter of about 200 nm and a ξ-potential of about minus (–) 20 mV. These complexes maintain their size and charge for at least 4 weeks. Besides mixing ratio, other extrinsic factors determining the characteristics of the complexes are pH, and ionic strength.[28,32,33] Controlling these factors will enable us to tune the characteristics of the complexes formed that in turn will modulate their functional properties such as surface activity.[30]

SURFACE RHEOLOGY

We have designed our microcapsules using emulsion droplets as templates and some of the encapsulating materials were used as emulsifiers and/or emulsion stabilizers

for the template emulsion. Therefore, in *chapter 3* we have studied the rheological properties oil – water interfaces stabilized by the above described structural elements: small and compact spherical structures (Lys or Ova protein), larger spherical and softer structure (their complexes with HMP), and short or long thin structures (fibrils from Ova and Lys) that can be either flexible or stiff. The response of the interface upon expansion and compression deformations gives us information about the stability during emulsifying (and foaming) as well as short-term stability of emulsions and foams.[34] The results of interfacial shear rheology, on the other hand, give us information about the long-term stability of emulsions (and foams).[34] Unlike globular proteins such as Ova and Lys monomer which have been widely used as emulsifiers and stabilizers, the use of fibrils as interfacial agents has just started to gain attention.[2,15] In a study of Jung *et al.*, the authors have found that β-lactoglobulin fibrils were not only able to perform as thickeners and gelatinizers[35–38] but also could be used as stabilizers of air – water and oil – water interfaces.[35]

From the interfacial dilatational rheology measurements, we have found that at two different oil – water interfaces (n-hexadecane – water and MCT – water) and for both proteins, fibrils do not increase the surface pressure as much as the native protein and complexes but they do form viscoelastic films at the interface with significantly higher dilatational moduli.

When comparing the interfacial tension and dilatational modulus of Lys at two pHs: 3.5 and 7, we have observed that after 7h of aging, at the same bulk concentration, interfaces stabilized by native Lys at pH 7 show a lower surface tension and higher dilatational modulus than interfaces stabilized by native Lys at pH 3.5, most likely due to the difference in the molecular net charge. The higher molecular net charge results in higher electrostatic repulsion between the protein molecules. Near the isoelectric point, proteins are therefore thought to be more surface active and form denser films at the interface.[36–38] However, at an aging time of 15 hours, the difference in surface tension and surface dilatational modulus between oil – water interfaces stabilized by native Lys at pH 3.5 or 7 is no longer significant. So it appears that the increased surface charge of the proteins at lower pH merely decreases the rate of the adsorption process, but has only a minor effect on the equilibrium surface properties.

The addition of a charged polysaccharide to existing protein-stabilized interfaces, forming protein – polysaccharide bilayers at the interface, has been studied less often than the direct adsorption of protein – polysaccharide complexes forming mixed adsorbed layers.[39] In a study of Ganzevles *et al.*, a mixed film of β-lactoglobulin – pectin complexes had a lower dilatational modulus at the air – water interface than the pure protein film and the corresponding bilayer film.[39,40] In our study, at MCT – water interfaces, different phenomena were observed: in the case of Lys, mixed layers

are more resistant against compression and expansion than bilayers, and the addition of HMP to the Lys-stabilized interfaces, either simultaneous or sequential, results in higher dilatational modulus than interfaces stabilized by Lys only. OvaHMP complexes form adsorbed layers that are more resistant to dilation than native Ova. The same observations were reported for sodium caseinate and dextran sulphate at the n-tetradecane – water interface.[39] Protein – polysaccharide complexes can form adsorbed layers with higher dilatational moduli than protein alone because they combine the physicochemical and functional properties of the constituting components.[28]

The difference between interfaces stabilized by short and long Lys fibrils was not observed in dilatational measurements but was clearly present in shear surface rheology. Films formed by long fibrils have a complex modulus 10 times higher than films formed by short fibrils. At higher bulk concentration (from 0.01% to 0.1% wt), the complex shear modulus of interfaces stabilized by short and semi-flexible Ova fibrils is of the same order of magnitude as that of interfaces stabilized by long and semi-flexible Lys fibrils.

When comparing the two proteins, results showed that the native proteins Ova and Lys formed adsorbed layers at the MCT – water interface with similar dilatational and shear properties. Complexes from these proteins and HMP have different sizes and surface charge. However, when these complexes are adsorbed onto the MCT – water interface, they form layers with similar dilatational and complex shear moduli, suggesting similar rearrangement of these structural components at the interface.

In conclusion, results of surface rheological experiments have shown that the use of supra-molecular structural building blocks creates a wider range of microstructural features of the interface, and accordingly higher surface shear and dilatational moduli and more complex rheological properties. As mentioned above, the mechanical strength of the adsorbed layer is one of the most important factors influencing the kinetic stability of oil-in-water emulsion droplets.[29] Therefore, these building blocks are ideal not just to produce the shell of microcapsules but also to stabilize the emulsion droplets that serve as templates for producing the microcapsules.

MICROCAPSULES

We have used the LbL technique to produce microcapsules using Ova fibrils, HMP, OvaHMP complexes, Lys fibrils, and LysHMP complexes on oil-in-water emulsion droplet templates. As mentioned above, the application of protein – polysaccharide complexes in microcapsule design has been reported in many studies.[30] Despite that the electrostatic deposition of these polyelectrolytes can be used to design multilayer interfaces in emulsions, in practice, this process has so far been limited to no more

than two or three layers.[41] In this thesis, we have produced microcapsules with up to 8 layers of encapsulating materials.

In *chapter 4* and in *chapter 5*, we presented microcapsules from Ova fibrils and HMP, and two systems of protein complexes and fibrils, respectively. Two different types of Lys fibrils were used but the difference between them was not seen in terms of heat stability, despite their different behavior in interfacial rheology experiments. Apparently, the difference in size and flexibility between these two types of Lys fibrils did not have a significant effect on the structure of the shell of the microcapsules. We will, therefore, only discuss microcapsules from long Lys fibrils and LysHMP complexes as the representative for both of the systems. In general, the microcapsules are polydisperse with a Sauter diameter D(3,2) less than 10 μm. No flocculation of microcapsules during applying of additional layers is observed. In all three systems, the ξ-potentials reverse sign when another layer is applied. The alternating adsorption of the encapsulating materials on the shell of the microcapsules was confirmed by combining the ξ-potential measurements with confocal images of microcapsules prepared with labeled materials.

When applying critical point drying to remove the oil phase, forming dry and hollow microcapsules, the difference between them can be observed. Microcapsules prepared with OvaHMP 2:1 and Ova fibrils were more resistant to the drying process than those prepared with Ova fibrils and HMP, and those prepared with LysHMP 4:1 and Lys fibrils. Microcapsule with 3 layers of OvaHMP and Ova fibrils were found intact while indentation was still observed on 4-layer microcapsules of Ova fibrils and HMP, and 5-layer ones with shells consisting of LysHMP and Lys fibrils. SEM pictures of the microcapsules indicate that shell strength was improved for all systems when the number of layers increased. In other words, the more layers the shell consists of, the more resistant it is against the physical drying process.

The shell structure of all the microcapsules is inhomogeneous. Close-up pictures of the microcapsules of LysHMP complexes and Lys fibrils show that their shells consist of layers of networks of fibrils with relatively large pores, and a considerable number of defects. Increasing the number of layers does seem to decrease the sizes of pores and decrease the number of defects. The presence of large pores and defects can be a disadvantage for encapsulating certain materials, in particular low molecular weight components.

For the microcapsules of Ova fibrils and HMP, the release rate of limonene as encapsulated materials was measured. The time of maximum release from 4-layer to 8-layer microcapsules increases by about a factor 6.

For the microcapsules of protein – HMP complexes and fibrils, the heat stability of microcapsules with limonene as encapsulated material was measured. In systems produced with LysHMP complexes and long Lys fibrils, increasing the number of layers from 2 to 8, increased the heat resistance time (when heating at 90 °C) by more than 15 times. For microcapsules with 5 or fewer layers, microcapsules prepared with semi-flexible Ova fibrils and OvaHMP complexes were stronger than systems based on Lys. But the increase of the heat resistance time with layer number was much smaller for the Ova system (approximately a factor 1.5 in going from 2 to 7 layers). Microcapsules prepared with OvaHMP and semi-flexible Ova fibrils tend to have a more homogeneous and stretchable shell than capsule prepared with LysHMP and more rigid Lys fibrils. These tend to have shells that are more inhomogeneous and brittle. In short, by changing the properties of the fibrils we are able to tune the mechanical properties of the shell of this type of multilayer capsule.

It is interesting to see that there is no significant difference between microcapsules prepared with long (about 1.5 – 2 µm) and short (a few hundred nm) Lys fibrils observed. One may expect that due to curvature effect, long and semi-flexible fibrils would adsorb differently than short and more rod-like ones. Apparently, for a template with a diameter varying from 5 to 10 µm, the difference in length and flexibility between these two types of Lys fibrils is not sufficient to yield capsules with distinguishably different interfacial structures.

For all tested microcapsules, results show that the release properties (as triggered by heating) of the multi-layer microcapsules can be tuned by controlling the number of layers in the shell of the capsules.

In this thesis, more understanding of the physical properties of fibrils and complexes was achieved. Their application as encapsulating materials using the LbL technique results in microcapsules with tunable shell characteristics, controlled release rate and mechanical strength against heat treatment.

OUTLOOK

We have seen that supra-molecular structural building blocks produce a wider range of microstructural features of the interface, and give higher surface shear and dilatational moduli and a more complex dependence on strain rate. In the surface rheological study, we have observed the difference between interfaces stabilized by these structural elements but in order to understand these differences better, detailed knowledge on the interfacial structure of the fibril and complex stabilized interfaces is needed. For fibrils, currently it is still unknown whether they form entangled networks at the interface, or, perhaps, liquid crystalline phases. For the pre-formed protein – polysaccharide complexes (LysHMP and OvaHMP), experimental data

suggest that these complexes of different sizes and charges undergo a similar structural rearrangement upon adsorption at the interface but information about how that happens and how that differs from the sequential adsorption as two individual elements, is not yet available. In general, it will be interesting and beneficial to investigate the morphology and thickness of the adsorbed layers of fibrils and complexes and the fluid – fluid interfaces, at equilibrium and during deformation.

In order to develop 2D structural models that allow for a more satisfactory description of the deformation behavior of interfaces stabilized by those supra-molecular structures, 2D rheo-optics would be a valuable tool because it would allow simultaneous measurement of surface rheological properties and structural changes when a deformation is applied to the interface (either in a surface shear or dilatational rheometer).[42] At this time such methods are only sparsely available, and the field of surface rheology would definitely benefit from the development of such methods.

Furthermore, because the interfacial shear and dilatational properties are not always positively correlated to emulsions stability,[34] it will be interesting to investigate and compare the stability of emulsions using Lys and Ova monomers, complexes with HMP, and fibrils in a more systematic manner. In this thesis we limited ourselves to concentration ranges relevant for the stabilization of the template emulsion. To investigate the suitability of these components as emulsifiers, a wider range of concentrations, pH values, and ionic strengths, as well as the effect of other components (lipids, additional proteins) on emulsion stability should be investigated.

LbL has proved to be an effective method for encapsulation using a wide range of materials. By varying the type of encapsulating materials, their composition, ratios and concentration, and other factors (such as pH, ionic strength of the solvent), tailored microcapsules can be produced for specific purposes. The structure of the shell, consequently, its permeability, can be adjusted by the flexibility, and size of the building blocks. In order to establish more clearly a link between morphology of the fibrils and the shell network characteristics, a more homogenous fibril population (that can be produced by controlled shear flows) could be used to form microcapsules.

This thesis has not yet explored the mechanical strength of the microcapsules and its relation to shell structure in a more quantitative manner (using for example colloidal probe atomic force microscopy). It was difficult to find a suitable technology to determine the mechanical strength of the microcapsules due to their poly-dispersed size distribution and inhomogeneous shell structure. Possible routes to eliminate this problem would be the optimization of the shell structure, reducing the number of defects in the shell, and using mono-disperse solid particles as a template instead of emulsion droplets.

Since there are structural similarities on the mesoscopic length scale between fibrils from Lys and those from β-lactoglobulin, it would also be interesting to compare microcapsules from these two fibrils, to investigate whether the characteristics of the shell are mainly determined by the length and stiffness of the fibrils, or whether these characteristics are also affected by the detailed molecular structure of the fibrils.

In conclusion, the extraordinary properties these building blocks give the interface open new perspectives for the development of multiphase systems such as highly stable foams and emulsions, controlled release systems, and protective coatings.

REFERENCES

1   Veerman, C., De Schiffart, G., Sagis, L. M. C. & van der Linden, E. Irreversible Self-Assembly of Ovalbumin Into Fibrils and The Resulting Network Rheology. *Int J Biol Macromol* **33**, 121 – 127 (2003).

2   Humblet-Hua, K. N. P., Scheltens, G., van der Linden, E. & Sagis, L. M. C. Encapsulation Systems Based On Ovalbumin Fibrils and High Methoxyl Pectin. *Food Hydrocolloid* **25**, 307 – 314 (2011).

3   Dobson, C. M. Protein Misfolding, Evolution and Disease. *Trends Biochem Sci* **24**, 329 – 332 (1999).

4   Dobson, C. M. Protein Folding and Misfolding. *Nature* **426**, 884 – 890 (2003).

5   Dobson, C. M. Principles of Protein Folding, Misfolding and Aggregation. *Semin Cell Dev Biol* **15**, 3 – 16 (2004).

6   Dobson, C. M. Experimental Investigation of Protein Folding and Misfolding. *Methods* **34**, 4 – 14 (2004).

7   Hughes, V. A. & Dunstan, D. E. In *Modern Biopolymer Science* (eds Kasapis, S.; Norton, I. T.; Ubbink, J. B.) 559 – 594 (Academic Press, 2009).

8   Sagis, L. M. C., Veerman, C. & van der Linden, E. Mesoscopic Properties of Semiflexible Amyloid Fibrils. *Langmuir* **20**, 924 – 927 (2004).

9   Veerman, C., Sagis, L. M. C., Heck, J. & van der Linden, E. Mesostructure of Fibrillar Bovine Serum Albumin Gels. *Int J Biol Macromol* **31**, 139 – 146 (2003).

10   Veerman, C., Ruis, H. G. M., Sagis, L. M. C. & van der Linden, E. Effect of Electrostatic Interactions On The Percolation Concentration of Fibrillar Beta-Lactoglobulin Gels. *Biomacromolecules* **3**, 869 – 873 (2002).

11   Schmittschmitt, J. P. & Scholtz, J. M. The Role of Protein Stability, Solubility, and Net Charge In Amyloid Fibril Formation. *Protein Sci* **12**, 2374 – 2378 (2003).

12   Akkermans, C. *et al.* Peptides Are Building Blocks of Heat-Induced Fibrillar Protein Aggregates of ß–Lactoglobulin Formed At pH 2. *Biomacromolecules* **9**, 1474 – 1479 (2008).

13   Lara, C. C., Adamcik, J., Jordens, S. & Mezzenga, R. General Self-Assembly Mechanism Converting Hydrolyzed Globular Proteins Into Giant Multistranded Amyloid Ribbons. *Biomacromolecules* **12**, 1868 – 1875 (2011).

14   Jordens, S., Adamcik, J., Amar-Yuli, I. & Mezzenga, R. Disassembly and Reassembly of Amyloid Fibrils In Water – Ethanol Mixtures. *Biomacromolecules* **12**, 187 – 193 (2011).

15   Jones, O. G. & Mezzenga, R. Inhibiting, Promoting, and Preserving Stability of Functional Protein Fibrils. *Soft Matter* **8**, 876 – 895 (2012).

16   Krebs, M. R. H. *et al.* Formation and Seeding of Amyloid Fibrils From Wild-Type Hen Lysozyme and A Peptide Fragment From The α-Domain. *J Mol Biol* **300**, 541 – 549 (2000).

17   Goda, S. *et al.* Amyloid Protofilament Formation of Hen Egg Lysozyme In Highly Concentrated Ethanol Solution. *Protein Sci* **9**, 369 – 375 (2000).

18   Cao, A., Hu, D. & Lai, L. Formation of Amyloid Fibrils From Fully Reduced Hen Egg White Lysozyme. *Protein Sci* **13**, 319 – 324 (2004).

19   Arnaudov, L. N. & De Vries, R. Thermally Induced Fibrillar Aggregation of Hen Egg White Lysozyme. *Biophys. J.* **88**, 515 – 526 (2005).

20   Mishra, R. *et al.* Lysozyme Amyloidogenesis Is Accelerated By Specific Nicking and Fragmentation But Decelerated By Intact Protein Binding and Conversion. *J Mol Biol* **366**, 1029 – 1044 (2007).

21   Vernaglia, B. A., Huang, J. & Clark, E. D. Guanidine Hydrochloride Can Induce Amyloid Fibril Formation From Hen Egg-White Lysozyme. *Biomacromolecules* **5**, 1362 – 1370 (2004).

22   Hill, E. K., Krebs, B., Goodall, D. G., Howlett, G. J. & Dunstan, D. E. Shear Flow Induces Amyloid Fibril Formation. *Biomacromolecules* **7**, 10 – 13 (2006).

23   Akkermans, C., van der Goot, A. J., Venema, P., van der Linden, E. & Boom, R. M. Formation of Fibrillar Whey Protein Aggregates: Influence of Heat and Shear Treatment, and Resulting Rheology. *Food Hydrocolloid* **22**, 1315 – 1325 (2008).

24   Lara, C., Usov, I., Adamcik, J. & Mezzenga, R. Sub-Persistence-Length Complex Scaling Behavior In Lysozyme Amyloid Fibrils. *Phys. Rev. Lett.* **107**, 238101 (2011).

25   Akkermans, C. *et al.* Shear Pulses Nucleate Fibril Aggregation. *Food Biophys* **1**, 144 – 150 (2006).

26   Dunstan, D. E., Hamilton-Brown, P., Asimakis, P., Ducker, W. & Bertolini, J. Shear-Induced Structure and Mechanics of β-Lactoglobulin Amyloid Fibrils. *Soft Matter* **5**, 5020 – 5028 (2009).

27   Ye, A. Complexation Between Milk Proteins and Polysaccharides Via Electrostatic Interaction: Principles and Applications – A Review. *Int J Food Sci Tech* **43**, 406 – 415 (2008).

28   Schmitt, C. & Turgeon, S. L. Protein/Polysaccharide Complexes and Coacervates In Food Systems. *Adv Colloid Interfac* **167**, 63 – 70 (2011).

29   McClements, D. J. Theoretical Analysis of Factors Affecting The Formation and Stability of Multilayered Colloidal Dispersions. *Langmuir* **21**, 9777 – 9785 (2005).

30   Benichou, A., Aserin, A. & Garti, N. Protein – Polysaccharide Interactions For Stabilization of Food Emulsions. *J Disper Sci Technol* **23**, 93 – 123 (2002).

31   Weinbreck, F., Nieuwenhuijse, H., Robijn, G. W. & De Kruif, C. G. Complexation of Whey Proteins With Carrageenan. *J Agr Food Chem* **52**, 3550 – 3555 (2004).

32   Turgeon, S. L.; Laneuville, S. I. Chapter 11 - Protein + Polysaccharide Coacervates and Complexes: From Scientific Background to their Application as Functional Ingredients in Food Products. In *Modern Biopolymer Science* (eds Kasapis, S.; Norton, I. T.; Ubbink, J. B.) 327-363 (Academic Press: San Diego, 2009).

33   Turgeon, S. L., Schmitt, C. & Sanchez, C. Protein – Polysaccharide Complexes and Coacervates. *Curr Opin Colloid In* **12**, 166 – 178 (2007).

34   Bos, M. A. & Van Vliet, T. Interfacial Rheological Properties of Adsorbed Protein Layers and Surfactants: A Review. *Adv Colloid Interfac* **91**, 437 – 471 (2001).

35   Bolder, S. G., Hendrickx, H., Sagis, L. M. C. & van der Linden, E. Ca^{2+}-Induced Cold-Set Gelation of Whey Protein Isolate Fibrils. *Appl Rheol* **16**, 258 – 264 (2006).

36   Bolder, S. G., Hendrickx, H., Sagis, L. M. C. & van der Linden, E. Fibril Assemblies In Aqueous Whey Protein Mixtures. *J Agr Food Chem* **54**, 4229 – 4234 (2006).

37   Kroes-Nijboer, A., Venema, P., Baptist, H. & van der Linden, E. Fracture of Protein Fibrils As Induced By Elongational Flow. *Langmuir* **26**, 13097 – 13101 (2010).

38   Veerman, C., Sagis, L. M. C. & van der Linden, E. Gels At Extremely Low Weight Fractions (0.07%) Formed By Irreversible Self-Assembly of Proteins. *Macromol Biosci* **3**, 243 – 247 (2003).

39   Jung, J.-M. & Mezzenga, R. Liquid Crystalline Phase Behavior of Protein Fibers In Water: Experiments Versus Theory. *Langmuir* **26**, 504 – 514 (2009).

40   Dickinson, E. Milk Protein Interfacial Layers and The Relationship To Emulsion Stability and Rheology. *Colloid Surface B* **20**, 197 – 210 (2001).

41   Lu, J. R., Su, T. J. & Howlin, B. J. The Effect of Solution pH On The Structural Conformation of Lysozyme Layers Adsorbed On The Surface of Water. *The J Phys Chem B* **103**, 5903 – 5909 (1999).

42   Magdassi, S. & Kamyshnu, A. Ch. 1. In *Surface Activity of Proteins : Chemical and Physicochemical Modifications* (Ed Shlomo Magdassi) 1 – 38 (Dekker, 1996).

43   Jourdain, L. S., Schmitt, C., Leser, M. E., Murray, B. S. & Dickinson, E. Mixed Layers of Sodium Caseinate + Dextran Sulfate: Influence of Order of Addition To Oil – Water Interface. *Langmuir* **25**, 10026 – 10037 (2009).

44   Ganzevles, R. A., Cohen-Stuart, M. A., Van Vliet, T. & De Jongh, H. H. J. Use of Polysaccharides To Control Protein Adsorption To The Air – Water Interface. *Food Hydrocolloid* **20**, 872 – 878 (2006).

45   Dickinson, E. Mixed Biopolymers At Interfaces: Competitive Adsorption and Multilayer Structures. *Food Hydrocolloid* **25**, 1966 – 1983 (2011).

46   van der Linden, E., Sagis, L. M. C. & Venema, P. Rheo-Optics and Food Systems. *Curr Opin Colloid In* **8**, 349 – 358 (2003).

SUMMARY

This thesis describes the design of encapsulation systems using mesostructures from proteins and polysaccharides. The thesis can be divided into two main parts: in part 1 (*chapter 2* and *chapter 3*), the physical properties of the encapsulating materials (protein fibrils and protein – polysaccharide complexes) are investigated. In part 2 (*chapter 4* and *chapter 5*), microcapsules with tunable release rate and mechanical strength are discussed.

In *chapter 2*, the effect of steady shear and turbulent flow on the formation of amyloid fibrils from hen egg white lysozyme (Lys) was studied. We determined the conversion and size distribution of fibrils obtained by heating Lys solutions at pH 2. The formation of fibrils was quantified using flow-induced birefringence. The size distribution was fitted using decay of birefringence measurements and Transmission Electron Microscopy (TEM). The morphology of Lys fibrils and kinetics of their formation varied considerably depending on the flow applied. With increasing shear or stirring rate, more rod-like and shorter fibrils were obtained, and the conversion into fibrils was increased. The size distribution and final fibril concentration were significantly different from those obtained in the same heat treatment at rest. The width of the length distribution of fibrils was influenced by the homogeneity of the flow.

In *chapter 3* we have investigated the surface rheological properties of oil – water interfaces stabilized by fibrils from lysozyme (long and semi-flexible, and short and rigid ones), fibrils from ovalbumin (short and semi-flexible), lysozyme – pectin complexes, or ovalbumin – pectin complexes. We have compared these properties with those of interfaces stabilized by the native proteins. The surface dilatational and surface shear moduli were determined using an automated drop tensiometer, and a stress controlled rheometer with biconical disk geometry. Results show that interfaces stabilized by complexes of these proteins with high methoxyl pectin have higher surface shear and dilatational moduli than interfaces stabilized by the native proteins only. The interfaces stabilized by ovalbumin and lysozyme complexes have comparable shear and dilatational moduli though ovalbumin – pectin complexes are twice as large in radius as lysozyme – pectin complexes. At most of the experimental conditions, interfaces stabilized by fibrils have the highest surface rheological moduli. The difference between long semi-flexible lysozyme fibrils or short rigid lysozyme fibrils is not pronounced in interfacial dilation rheology but significant in interfacial shear rheology. The complex surface shear moduli of interfaces stabilized by long semi-flexible fibrils are about 10 times higher than those of interfaces stabilized by short rigid fibrils, over a range of bulk concentrations. Interfaces stabilized by short

and more flexible ovalbumin fibrils have a significantly higher surface shear modulus than those stabilized by the somewhat longer and more rigid short lysozyme fibrils. This study has shown that the use of such supra-molecular structural building blocks creates a wider range of microstructural features of the interface, with higher surface shear and dilatational moduli, and a more complex dependence on strain (rate).

In the second part of this thesis (*chapter 4* and *chapter 5*), encapsulation systems are developed using layer-by-layer adsorption of food-grade polyelectrolytes on an emulsion droplet template. The formation of the capsules involves merely standard operations that can easily be scaled up to industrial production.

The encapsulation system presented in *chapter 4* was built with alternating layers of ovalbumin fibrils and high methoxyl pectin. By varying the number of layers, the release of active ingredients can be controlled: increasing the number of layers of the shell from 4 to 8, decreases the release rate by a factor 6.

In *chapter 5*, we compared the mechanical stability of microcapsules with shells consisting of alternating layers of ovalbumin – high methoxyl pectin complexes (OvaHMP) and flexible ovalbumin fibrils (OvaFib) (average contour length $L_c \sim 200nm$), with microcapsules built of alternating layers of lysozyme – high methoxyl pectin complexes (LysHMP) and lysozyme fibrils (LysFib). Two types of lysozyme fibrils were used: short and rod-like ($L_c \sim 500$ nm), and long and semi-flexible ($L_c = 1.2 – 1.5$ μm). At low number of layers (≤ 4), microcapsules from ovalbumin complexes and fibrils were stronger than microcapsules prepared from lysozyme complexes and fibrils. Increasing the number of layers, the mechanical stability of microcapsules from LysHMP – LysFib increased significantly, and capsules were stronger than those prepared from OvaHMP – OvaFib with the same number of layers. The contour length of the Lys fibrils did not have a significant effect on mechanical stability of the LysHMP – LysFib capsules. The stiffer lysozyme fibrils produce capsules with a hard but more brittle shell, whereas the semi-flexible ovalbumin fibrils produce capsules with a softer but more stretchable shell. These results show that mechanical properties of this type of capsule can be tuned by varying the flexibility of the protein fibrils.

In *chapter 6*, we have discussed the results obtained from previous chapters and several topics for further research are identified. An important issue that arises from this work is that in order to interpret the highly nonlinear surface rheological behavior of interfaces stabilized by supra-molecular structures, detailed knowledge on the interfacial morphology and structural changes of these interfaces upon deformation is essential. The field of surface rheology would benefit substantially from the development of surface rheo-optical methods, which allow for simultaneous probing of stress-deformation behavior and surface structure.

For microcapsules with shells consisting of supra-molecular structures, a more quantitative characterization of the mechanical strength of the microcapsules would be desirable. To characterize these capsules with techniques such as colloidal probe AFM, the structure of the shell needs to be optimized, to reduce the number of defects.

SAMENVATTING

Dit proefschrift beschrijft het ontwerp van encapsulatiesystemen met behulp van mesostructuren van eiwitten en polysachariden. Het proefschrift kan worden onderverdeeld in twee delen: Het eerste deel (*hoofdstuk 2* en *hoofdstuk 3*) behelst de fysische eigenschappen van de encapsulatiematerialen (eiwitfibrillen en eiwit-polysacharide complexen). Het tweede deel (*hoofdstuk 4* en *hoofdstuk 5*) gaat over microcapsules met variabele afgiftesnelheid en mechanische sterkte.

In *hoofdstuk 2* werd het effect van afschuif- en turbulente stroming op de vorming van amyloïde fibrillen van het kippeneiwit lysozyme (Lys) besproken. We bepaalden de omzetting en grootteverdeling van fibrillen, verkregen door verhitting van Lys-oplossingen bij pH 2. De vorming van fibrillen werd gekwantificeerd met behulp van metingen van stromingsgeïnduceerde dubbele breking. De grootteverdeling werd bevestigd met vervalmetingen van dubbele breking en transmissie-elektronenmicroscopie (TEM). De morfologie van Lys-fibrillen en kinetiek van hun vorming varieerden aanzienlijk afhankelijk van de aangebrachte stroming. Met toenemende afschuifstroming of roersnelheid werden meer staafvormige en kortere vezels verkregen, en werd de omzetting in fibrillen verhoogd. De grootteverdeling en fibrilconcentratie waren significant verschillend van die verkregen in hetzelfde verhittingsproces uitgevoerd in rust. De breedte van de lengteverdeling van fibrillen werd beïnvloed door de homogeniteit van de stroming.

In *hoofdstuk 3* hebben we onderzoek gedaan naar de reologische eigenschappen van olie-water grensvlakken gestabiliseerd door fibrillen van lysozyme (lange en semi-flexibele fibrillen, en korte en stijve fibrillen), fibrillen van ovalbumine (kort en semi-flexibel), lysozyme-pectinecomplexen, of ovalbumine-pectinecomplexen. We hebben deze eigenschappen vergeleken met die van grensvlakken gestabiliseerd door de natieve eiwitten. De oppervlaktedilatatie- en oppervlakte-afschuifmodulus werden bepaald met behulp van een geautomatiseerde druppel-tensiometer en een stress-gecontroleerde reometer met een biconische geometrie. Resultaten tonen aan dat grensvlakken die gestabiliseerd zijn door complexen van de eiwitten met HM-pectine (HMP), een hogere oppervlakte-afschuif- en dilatatiemodulus hebben dan grensvlakken die zijn gestabiliseerd door alleen natieve eiwitten. De grensvlakken die gestabiliseerd zijn door ovalbumine- en lysozymecomplexen hebben een vergelijkbare afschuif- en dilatatiemodulus, al hebben ovalbumine-pectine complexen een twee keer zo grote straal als lysozyme-pectine complexen. Bij de meeste experimentele omstandigheden hebben grensvlakken gestabiliseerd door fibrillen de hoogste oppervlakte-reologische moduli. Het verschil tussen de lange semi-flexibele lysozyme-fibrillen en korte stijve lysozyme-fibrillen is niet erg uitgesproken in de dilatatie-

eigenschappen, maar is wel significant voor de afschuifeigenschappen. De complexe afschuifmodulus van grensvlakken die zijn gestabiliseerd door lange semi-flexibele vezels is ongeveer 10 maal hoger dan die van grensvlakken gestabiliseerd door korte stijve vezels, over een bereik van bulkconcentraties. Grensvlakken die werden gestabiliseerd door korte en flexibelere ovalbuminefibrillen hebben een significant hogere afschuifmodulus dan grensvlakken die werden gestabiliseerd door de iets langere en stijvere korte lysozyme-fibrillen. Dit onderzoek heeft aangetoond dat het gebruik van dergelijke supramoleculaire structurele bouwstenen een breder scala aan microstructurele kenmerken van het grensvlak creëert, met hogere afschuif- en dilatatiemoduli en een complexere afhankelijkheid van de deformatie(snelheid).

In het tweede deel van dit proefschrift (*hoofdstuk 4* en *hoofdstuk 5*), zijn encapsulatiesystemen ontwikkeld met behulp van laag-voor-laagadsorptie van voedselveilige polyelektrolyten op een emulsiedruppel. De vorming van de capsules behelst louter standaard bewerkingen die gemakkelijk kunnen worden opgeschaald naar industriële productie. Het inkapselingssysteem dat werd gepresenteerd in *hoofdstuk 4* werd gemaakt met afwisselende lagen van ovalbumine-fibrillen (OvaFib) en HMP. Door het aantal lagen te variëren, kan de afgifte van werkzame bestanddelen worden gecontroleerd: Door het aantal lagen van de schil van 4 tot 8 te verhogen, vermindert de afgiftesnelheid met een factor 6.

In *hoofdstuk 5* vergeleken we de mechanische stabiliteit van microcapsules met omhulsels bestaande uit afwisselende lagen van ovalbumine-HM-pectinecomplexen (OvaHMP) en flexibele ovalbumine-fibrillen (gemiddelde contour lengte Lc ~ 200nm), met microcapsules opgebouwd uit afwisselende lagen van lysozyme-HM-pectinecomplexen (LysHMP) en lysozyme-fibrillen (LysFib). Daarvoor werden twee soorten lysozyme-fibrillen gebruikt: korte staafvormige (L_c~500 nm) en lange semi-flexibele (L_c = 1,2 tot 1,5 um). Bij lage aantallen lagen (≤ 4), waren microcapsules uit ovalbumine-complexen en fibrillen sterker dan microcapsules bereid uit lysozyme-complexen en fibrillen. Verhoging van het aantal lagen liet de mechanische stabiliteit van microcapsules van LysHMP – LysFib aanzienlijk toenemen en capsules waren daardoor sterker dan die bereid uit OvaHMP – OvaFib met hetzelfde aantal lagen. De contourlengte van de lysozyme-fibrillen had geen significant effect op de mechanische stabiliteit van de LysHMP – LysFib capsules. De stijvere lysozyme-fibrillen produceerden capsules met een harder, maar brosser omhulsel, terwijl de semi-flexibele ovalbumine-fibrillen capsules produceerden met een zachter, maar rekbaarder omhulsel. Deze resultaten tonen aan dat de mechanische eigenschappen van dergelijke capsules kan worden geregeld door het variëren van de flexibiliteit van de eiwitfibrillen.

In *hoofdstuk 6* hebben we gesproken over de resultaten van de vorige hoofdstukken en een aantal onderwerpen voor verder onderzoek geïdentificeerd. Een belangrijk punt dat in dit werk naar voren is gekomen is, dat om het sterk niet-lineair oppervlakte-reologisch gedrag van grensvlakken gestabiliseerd door supramoleculaire structuren te interpreteren, gedetailleerde kennis over de grensvlakmorfologie en de structurele veranderingen die deze grensvlakken bij vervorming ondergaan, essentieel is. Het vakgebied van oppervlakte-reologie zou veel baat hebben bij de ontwikkeling van reo-optische methoden, die het mogelijk maken om reologisch gedrag en oppervlaktestructuren simultaan te bepalen.

Voor microcapsules met omhulsels bestaande uit supramoleculaire structuren is een kwantitatieve karakterisering van de mechanische sterkte van de microcapsules gewenst. Om deze capsules te kunnen karakteriseren met technieken zoals colloidal probe AFM, dient de structuur van de capsule te worden geoptimaliseerd, om het aantal defecten te reduceren.

DANKWOORD

Een thesis schrijf je niet alleen, luidt het cliché. Het nare van de meeste clichés is dat ze zo verschrikkellijk waar zijn. Dat geldt ook voor deze. Ik wil hier graag de mensen bedanken die een bijdrage hebben geleverd aan mijn proefschrift, al zal de lijst vast niet volledig zijn.

Ten eerste wil ik mijn promotor Erik bedanken voor zijn enthousiasme en inspiratie. Na onze gesprekken was ik altijd weer gemotiveerd. Leonard, een betere begeleider had ik me simpelweg niet kunnen wensen. Ik ben niet erg makkelijk maar jij wist me zo te begeleiden dat ik al die jaren met plezier aan mijn project heb gewerkt.

Ook mijn collega's waren van onschatbare waarde. Ardy, door de enorme positiviteit die jij uitstraalt, wist ik iedere keer alles weer te relativeren. Dilek, je bent een fantastische vriendin en je wist het altijd weer gezellig te maken in kamer 306. Fijn ook dat je mijn paranimf wil zijn. Elisabete, thanks for our nice time together and for being my paranymph even though you are so very busy.

Paul, bedankt voor jouw hulp met de reo-optica en gezelligheid. Els, jij maakte het verschil omdat je zoveel meer deed dan alleen je werk. Harry, bedankt voor je ontelbare reparaties aan de apparaten die ik iedere keer weer professioneel sloopte, en natuurlijk voor de vele metingen die je voor me hebt verricht.

Gerben, bedankt voor jouw assistentie en het was jammer dat je me niet tot het eind toe kon helpen.

Silvia, Jerome, Elke en Yul, jullie gaven de tijd bij FPH kleur en de AIO-reis was een mooie evaring. Alev, it was short but nice being your colleague. Diana, gracias por las lecciones de español.

Linlin Fan, Liya Yi, Sha Liu, Maarten Stolk, Hong Guo and Hisfazilah Saari, I enjoyed supervising you guys, and thanks for your contributions.

Tijs Rovers, Ruud Spruijt en Rob Koehorst: bedankt voor jullie bijdrage aan het project. Adriaan van Aelst, Henk Kieft en Norbert de Ruijter, bedankt voor de foto's!

Christopher, danke sehr für deine hilfe mit reo-optica. Remco Fokkink, bedankt voor je hulp met de ellipsometer en reflectometer. Martin Neubauer, thanks for the AFM measurements. Michiel Postema, bedankt voor de ultrasoundmetingen.

I also would like to thank my colleagues from the project partners SIK, ETH, Unilever and TUM for the fine co-operation and great project meetings.

Peter en Riet, bedankt voor jullie liefde en geduld met de "monsters". Het is mijn geluk om jullie als schoonouders te hebben.

Ba mẹ yêu quý, con biết ơn ba mẹ đã luôn tin tưởng và yêu thương con. Ba mẹ luôn là chỗ dựa tinh thần vô giá của con để mỗi khi con gặp khó khăn, con biết mình luôn có chỗ để quay về.

Chị Hai thật may mắn đã có bé Mai bên cạnh suốt hai năm vừa rồi. Chị Hai cảm ơn sự giúp đỡ, hỗ trợ và tình yêu thương bé Mai dành cho chị Hai.

Nyah và Amelie, các con là nguồn năng lượng vô tận của mẹ. Nhờ các con, những ngày dài làm việc của mẹ trở nên nhẹ nhàng hơn. Nhờ các con, mẹ giữ được cân bằng trong cuộc sống. Cảm ơn hai tình yêu bé bỏng của mẹ!

Martijn, niets is fijner dan geliefd en verliefd te mogen zijn. Mijn promotieproject is afgelopen maar ons life-project moet nog heel lang duren. Sterkte! ☺

PUBLICATIONS

Humblet-Hua, N.-P., Sagis, L. M. C. & van der Linden, E. Effects of Flow on Hen Egg White Lysozyme (HEWL) Fibril Formation: Length Distribution, Flexibility, and Kinetics. *J Agr Food Chem* **56**, 11875 – 11882 (2008).

Humblet-Hua, K. N. P., Scheltens, G., van der Linden, E. & Sagis, L. M. C. Encapsulation systems based on ovalbumin fibrils and high methoxyl pectin. *Food Hydrocolloid* **25**, 569 – 576 (2011).

Humblet-Hua, N.-P. K.; van der Linden, E.; Sagis, L. M. C., Microcapsules with Protein Fibril Reinforced Shells: Effect of Fibril Properties on Mechanical Strength of the Shell. *J Agr Food Chem60* **37**, 9502-9511 (2012).

Humblet-Hua, N.-P. K.; van der Linden, E.; Sagis, L. M. C., Surface rheological properties of liquid – liquid interfaces stabilized by protein fibrillar aggregates and protein – polysaccharide complexes, *submitted*.

Proceedings

N.P. Humblet-Hua, L.M.C. Sagis, E. van der Linden, "Encapsulation systems based on proteins, polysaccharides, and protein – polysaccharide complexes", The International Symposium on Food Rheology and Structure (ISFRS), 2009, Zürich

OVERVIEW OF COMPLETED TRAINING ACTIVITIES

	ECTS
Discipline specific activities	
Courses	
Polysaccharides as food colloids and Biomaterials: Fundamentals and applications, VLAG, 2007	1.0
12th European School on Rheology, Leuven, 2009	1.5
Meetings	
XVI International Conference on Bioencapsulation, Dublin, 2008	0.9
Liquids & Interfaces, NWO meeting, Lunteren, 2009	1.6
The International Symposium on Food Rheology and Structure – ISFRS, Zurich, 2009	2.1
Delivery of Functionality in complex food systems, Wageningen, 2009	2.1
Food Colloids, Granada, 2010	2.1
The International Symposium on Food Rheology and Structure – ISFRS, Zurich, 2010	2.1
The XVIth International Congress on Rheology, Lisbon, 2012	2.4
STREP, Vlaardingen, Gothenburg, Otterlo, Vals, 2007 – 2010,	6.7
General courses	
VLAG PhD week, 2007	1.5
Techniques for writing and presenting a scientific paper, Wageningen Graduate Schools, 2008	1.2
Advance course guide to scientific artwork, Wageningen University, 2008	0.6
Starting with the client: New approaches to effective health promotion, VLAG, Wageningen, 2009	0.6
Career assessment, Wageningen Graduate Schools, 2010	0.3
Optionals	
Preparation PhD research proposal	4.0
PhD trip Food Physics Group to Japan, 2010	2.3
Science meetings Food Physics Group, 2007 – 2011	3.0
Total	**36.0**

CURRICULUM VITAE

Hứa Kiều Nam Phương (K.N.P. Humblet-Hua) was born in Ho Chi Minh City, Vietnam on the 23rd of October, 1978. She went to Ho Chi Minh City University of Technology, where she received her BEng in Food and Chemical Technology in 2001. In the same year she received her BA in Foreign Language Teacher Education from Ho Chi Minh City University of Pedagogy.

In 2004 she started studying Food Technology at Wageningen University, specializing in Product Functionality. After her internship at TNO, she graduated in 2006. In that year she started working for Nestlé Nederland B.V. in Nunspeet. In 2007 she became a PhD student at Physics and Physical Chemistry of Foods (Food Physics) group, Wageningen University.